HUNGARIAN

Journal of

INDUSTRIAL CHEMISTRY

Edited by

the Hungarian Oil & Gas Research Institute (MÁFKI),
the Research Institute for Heavy Chemical Industries (NEVIKI),
the Research Institute for Technical Chemistry of the
Hungarian Academy of Sciences (MÜKKI),
the Veszprém University of Chemical Engineering (VVE).
Veszprém (Hungary)

Volume 13. 1985. Number 1.

HU ISSN: 0133—0276
CODEN: HJICAI

The "Hungarian Journal of Industrial Chemistry" is a joint publication of the Veszprém scientific institutions of the chemical industry that deals with the results of applied and fundamental research in the field of chemical processes, unit operations and chemical engineering. The papers are published in four numbers at irregular intervals in one annual volume, in the English, Russian, French and German languages

Editorial Office:
Veszprémi Vegyipari Egyetem
"Hungarian Journal of Industrial Chemistry"
H–8201 Veszprém, P.O. Box: 158.
Hungary

Distributor for Albania, Bulgaria, China, Cuba, Czechoslovakia, German Democratic Republic, Korean People's Republic, Mongolia, Poland, Rumania, USSR, Viet-Nam and Yugoslavia:
KULTURA Foreign Trading Co. H-1389, BUDAPEST, P.O. Box 149. Hungary
For all other countries:
VNU Science Press P.O. Box 2073 3500 GB UTRECHT The Netherlands

FELELŐS SZERKESZTŐ: DR. BODOR ENDRE
KIADJA A LAPKIADÓ VÁLLALAT, 1073 Bp. VII., LENIN KRT. 9–11.
TELEFON: 221-285. LEVÉLCÍM: 1906 BP. PF. 223.
FELELŐS KIADÓ: SIKLÓSI NORBERT VEZÉRIGAZGATÓ

HUNGARIAN JOURNAL
OF INDUSTRIAL CHEMISTRY
VESZPRÉM
Vol. 13. pp. 1–10 (1985)

EXAMINATION OF CHANGES IN PHASE AND CHEMICAL COMPOSITION OF PYROPHYLLITE-1Tc ON CHLORINATION

I. VASSÁNYI, S. SZABÓ, MRS. ZS. CSIKÓS, and R. JELINKÓ*

(Department of Mineralogy, Veszprém University of Chemical Engineering, Veszprém, Hungary, and *Research Institute of Technical Chemistry of the Hungarian Academy of Sciecnce, Veszprém, Hungary)

Received: April 20, 1984.

Phase and chemical changes of pyrophyllite-1Tc resulting from heat treatments at 873, 973, 1123 and 1273 K in a CO/Cl_2 atmosphere were determined. Three models were established for the structures of the solid chlorination residues. According to the most likely models, the chlorination residues of pyrophyllite-1Tc are mixtures of dehydroxylated pyrophyllite having vacancies and amorphous SiO_2.

Introduction

Since our knowledge about the kaolinite-chlorine reaction has in effect increased [1, 2] the examination of other minerals with layer silicate structure has become necessary. This paper deals with the chlorination of pyrophyllite [$Si_4Al_2O_{10}(OH)_2$] of the layer silicates.

Description of sample

Pyrophyllite used in the experiments was from a Hungarian deposit at Pázmánd. The material originally contained a major amount of contamination from haematite (α-Fe_2O_3), geothite (α-FeOOH), alunite [$KAl_3(OH)_6(SO_4)_2$] quartz (α-quartz, SiO_2) and rutile (TiO_2), and a minor amount of anatase (TiO_2). After decomposition much of the quartz, haematite, goethite and almost all the titanium dioxide had been removed. Residue of quartz had been dissolved with HF, the alunite with NaOH and the ferrous phases with HCl. The pyrophyllite so cleaned contained only a very small amount of alunite.

Triclinic and monoclinic pyrophyllite is known [3, 4, 5, 6]. On the basis of *X*-ray diffraction examinations *(Figure 1)* the pyrophyllite from Pázmánd has proved to be triclinic-1Tc. Its chemical composition *(Table 2)* and the stoichiometric formula calculated from it [7] allow the assumption to be made of an almost ideal pyrophyllite structure.

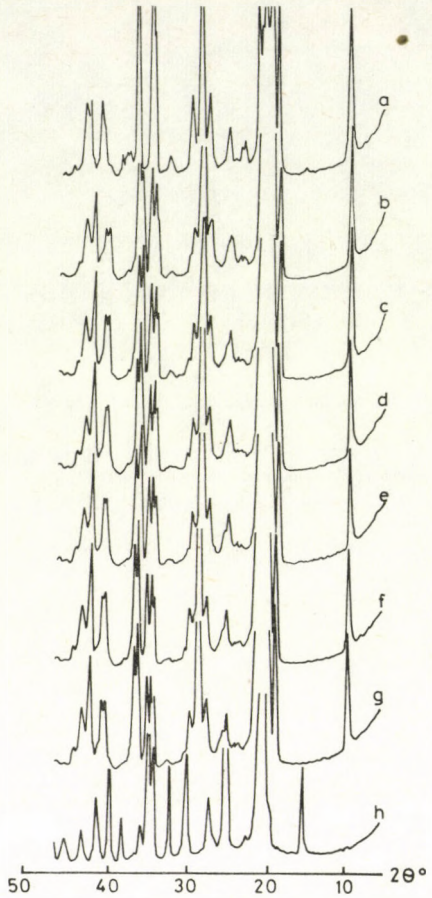

Figure 1
X-ray diffractograms of original pyrophyllite samples and of those subjected to heat treatments at different temperatures and reaction time
a: original; *b:* 873 K, 1 hour; *c:* 973 K, 1 hour; *d:* 1123 K, 1 hour; *e:* 1273 K, 1 hour; *f:* 1273 K, 2 hours; *g:* 1273 K, 3 hours; *h:* 1773 K, DTA examination residue

Experimental

The chlorination of the material was carried out in a quartz tube reactor [8]. The flow rates V_{Cl_2} and V_{CO} of the chlorinating gas mixture were maintained at 12 l/h and 8 l/h, respectively. The phase analytical examinations were made with a Philips *X*-ray diffractometer using CuKα radiation and a crystall monochromator. To determine the chemical composition, a Philips PW 1540/10 fluorescent *X*-ray spectrometer and the double dilution technique [9] were used.

Mass Losses of Heating and Chlorinating Experiments

Samples were heated and chlorinated at 873, 973, 1123 and 1273 K, always taking a new sample. Since the material proved to be very resistant against chlorination, experiments of not only 1 hour, but of 2 or 3 hours as well were

made in order to achieve more significant chlorination losses. The mass losses occurring during the treatments are summarized in *Table 1.*

Losses in Column 2 of *Table 1* may also result from dehydroxylation and chlorination of the pyrophyllite. The solid chlorination residue heated at 1273 K for 1 hour is certainly dehydroxylated and the volatile chlorides that may have condensed, were also removed. The sum of Columns 2 and 3 is thus the sum of the mass losses resulting from removing all hydroxyl groups and from the chlorination itself. Deducting the mass loss given by hydroxyl

Table 1.

Mass losses of pyrophyllite from Pázmánd occurring due to different treatments (w %).

Treatment temperature, reaction time	Losses				
	1.	2.	3.	4.	5.
	heating (in air)	gross chlorinat.	chlorinat. residue at 1273 K, 1 h heating	columns 2+3	net chlorination column 4.–5.3%
873 K, 1 h	4.00	4.12	1.18	5.30	0.00
973 K, 1 h	5.01	6.21	0.27	6.48	1.18
1123 K, 1 h	5.30	7.41	0.00	7.41	2.11
1273 K, 1 h	5.30	13.28	1.33	14.61	9.31
1273 K, 2 h	5.30	23.13	0.43	23.56	18.26
1273 K, 3 h	5.30	27.08	0.00	27.08	21.78

groups removal from the values of Column 4 in *Table 1*—which in the case of Pázmánd pyrophyllite was 5.30% — the net chlorination loss is obtained.

Phase Composition of Solid Residues from Chlorination and Heating Experiments

X-ray diffractograms of original pyrophyllite samples and those subjected to heating in air, are shown in *Figure 1.* The material converts to dehydroxylated pyrophyllite structure due to heat effects as early as 873 K, though the whole quantity of hydroxyl groups is not yet removed completely at this temperature (Column 1 in *Table 1*). The heat treatments with increasing temperature in the temperature range of *Table 1* fail to change the structure of dehydroxylated pyrophyllite, and cause only minor *d* values shifts and changes in reflection intensities. The residue from the DTA examination at 1773 K, however, is already mullite and cristobalite.

The *X*-ray diffractograms of solid residues from chlorination experiments *(Figure 2)* fail to indicate changes, beside the value *d* and intensity shifts, the solid chlorination residue—even that subjected to 3 hours, chlorination at 1273 K—is of dehydroxylated pyrophyllite structure. The dehydroxylated pyrophyllite structure proved to be more stable than that of γ-Al_2O_3 and iron oxides [10, 11, 12].

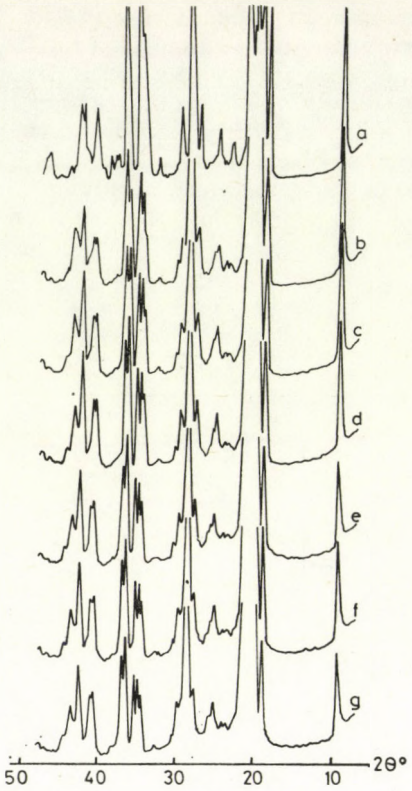

Figure 2

X-ray diffractograms of original Pázmánd pyrophyllite samples and of those subjected to chlorination at different temperature and reaction time

a: original; *b:* 873 K, 1 hour; *c:* 973 K, 1 hour; *d:* 1123 K, 1 hour; *e:* 1273 K, 1 hour; *f:* 1273 K, 2 hours; *g:* 1273 K, 3 hours

Chemical Composition of Solid Chlorination Residues

Chemical composition of original pyrophyllite and solid chlorination residues concerning the state heated at 1273 K, are shown in *Table 2.*

Table 2.

Chemical composition of original and chlorinated Pázmánd pyrophyllites samples, concerning state heated at 1273 K (w %).

Chlorination temps. and reaction time	SiO_2	TiO_2	Al_2O_3	Fe_2O_3	Total
original	68.52	0.20	30.97	0.21	99.90
873 K, 1 hour	68.65	0.20	30.94	0.23	100.02
973 K, 1 hour	68.53	0.05	30.91	0.23	99.72
1123 K, 1 hour	69.14	0.05	31.04	0.21	100.44
1273 K, 1 hour	70.21	0.07	29.33	0.20	99.81
1273 K, 2 hours	72.33	0.06	27.12	0.20	99.71
1273 K, 3 hours	72.97	0.03	25.67	0.16	98.83

The chemical changes occurring due to chlorination are not evident from *Table 2*, so the net chlorination weight loss values given in Column 5 of *Table 1* should also be considered *(Table 3)*. This can be done because the sum of Ca and Mg content of original pyrophyllite appeared lower than 0.1%. *Table 3* gives four figures for each chemical component. The first one *(r)* considers that mass percent values in *Table 2* refer to the chlorination residue of smaller mass rather than to the original material. Thus if mass percentage values referring to the original material 100% are to be calculated, then the mass

Table 3.

Compositions of original and chlorinated Pázmánd pyrophyllite samples, related to material heated at 1273 K. The chlorinated sample data are calculated considering net chlorination loss.

Chlorination temperatures, reaction time		SiO_2	TiO_2	Al_2O_3	Fe_2O_3	SiO_2/Al_2O_3
Original		68.52	0.20	30.97	0.21	2.212
873 K	*r*	68.65	0.20	30.94	0.21	2.219
1 hour	*r*%	—	—	—	—	
	l	—	—	—	—	—
	l%	—	— o	—	—	
973	*r*	67.72	0.05	30.55	0.23	2.217
1 hour	*r*%	98.83	25.00	98.64	—	
	l	0,80	0,15	0,42	—	1.905
	l%	1.17	75.00	1.36	—	
1123 K	*r*	67.68	0.05	30.39	0.21	2.227
1 hour	*r*%	98.77	25.00	98.18	—	
	l	0.84	0.15	0.58	—	1.448
	l%	1.23	75.00	1.87	—	
1273 K	*r*	63.67	0.06	26.60	0.18	2.394
1 hour	*r*%	92.92	30.00	85.84	85.72	
	l	4.85	0.14	4.37	0.03	1.110
	l%	7.08	70.00	14.11	14.28	
1273 K	*r*	59.12	0.05	22.17	0.16	2.667
2 hours	*r*%	86.28	25.00	71.59	76.19	
	l	9.40	0.15	8.80	0.05	1.068
	l%	13.72	75.00	28.41	23.81	
1273 K	*r*	57.08	0.02	20.08	0.13	2.843
3 hours	*r*%	83.30	10.00	64.84	61.90	
	l	11.44	0.18	10.89	0.08	1.051
	l%	16.70	90.00	35.16	38.10	

r = chlorination residue considering net chlorination loss
r% = *r* in percentage relating to the original value
l = chlorination loss considering the net chlorination loss
l% = *l* in percentage relating to the original value

percentage values in *Table 2* should be multiplied by (100 — net chlorination loss)/100. For example SiO_2 content of sample chlorinated at 1273 K for 3 hours, regarding the original material, is:

$$72.97(100-21.78)/100=57.08 \text{ (w \%)}.$$

The second figure (r%) indicates what percentage the mass percent value so calculated represents compared to the original value. With the cited example:

$$57.08/0.6852=83.30(\%).$$

The third figure *(l)* is the difference between the mass percentage value for each component of the original Pázmánd pyrophyllite and the value calculated by considering the net chlorination loss (68.52 − 57.08 = 11.44 w%), that is the material leaving the gas phase during chlorination indicates the extent of loss.

The fourth figure (l%) shows what percentage of each component for the original Pázmánd pyrophyllite the loss means (11.44/0.6852 = 16.70% and 100 − 83.30 = 16.70%). *Table 3* also indicates the alteration of the ratio SiO_2/ /Al_2O_3 in the solid chlorination residue or in the material removed. Data of *Table 3* are graphically shown in *Figures 3* and *4*. In these Figures, changes in quantity of the two main components, SiO_2 and Al_2O_3 are illustrated. For subsequent calculations, TiO_2 and Fe_2O_3 contents due to their small amounts

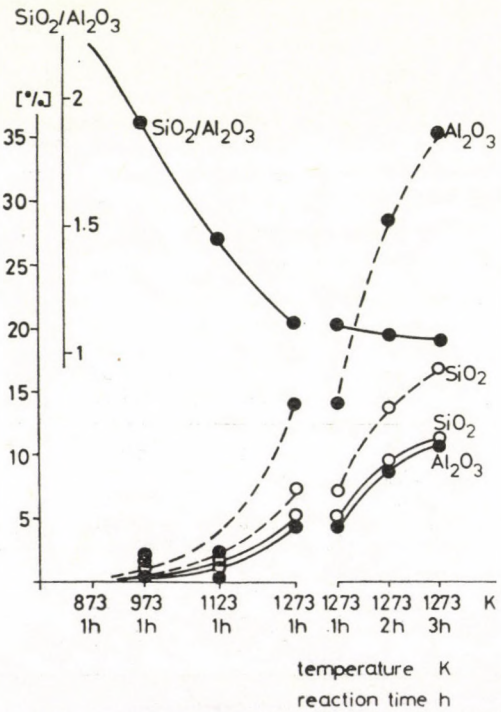

Figure 3

SiO_2 and Al_2O_3 losses of chlorinated Pázmánd pyrophyllite samples; ——— l and — — — l% values in *Table 3*. The SiO_2/Al_2O_3 ratios in the material removed

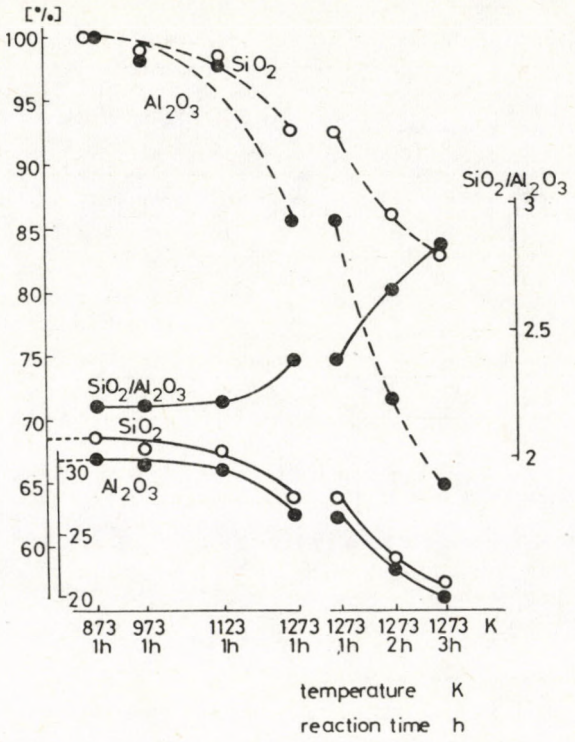

Figure 4
SiO_2 and Al_2O_3 content of chlorinated residues for chlorinated Pázmánd pyrophyllites samples; ———r, — — —r% values in *Table 3*. The SiO_2/Al_2O_3 ratios in the chlorinated residues

and to the fact that they in all probability are residues of contaminating materials, were not taken into consideration.

Quantity of SiO_2 and Al_2O_3 in the material removed during chlorination *(Figure 3)* is nearly the same. With a similar running the percentage values concerning the original material as 100% show that with rising temperature and duration of chlorination, Al becomes increasingly chlorinated, so for example after 3 hours' chlorination at 1273 K 35% of the Al_2O_3 content of the original material is removed, while only 17% of the SiO_2 content. The formation of ratio SiO_2/Al_2O_3 in the material removed also indicates this.

In chlorination residues both SiO_2 and Al_2O_3 content decreases *(Figure 4)*, but Al content to a much greater extent. Consequently the ratio SiO_2/Al_2O_3 of the chlorination residues significantly increases.

Discussion

Data obtained from chlorination experiments of pyrophyllite from Pázmánd allow two basic statements to be made:

1. chlorination residues contain a single crystalline component, dehydroxylated pyrophyllite,

Table 4.

Models for chlorination residues of Pázmánd pyrophyllite

Chlorination temperatures, reaction time	Chlorination residue as dehydroxylated pyrophyllite type compound *A*	Chlorination residue as dehydroxylated pyrophyllite *B*	+SiO_2	Chlorination residue as dehydroxylated pyrophyllite with vacancies *C*
873 K, 1 hour	$(Si_{3.93}Al_{0.07})^{IV}Al^{VI}_{2.02}O_{11}$	$(Si_{3.93}Al_{0.07})^{IV}Al^{VI}_{2.02}O_{11}$	—	$(Si_{3.93}Al_{0.07})^{IV}Al^{VI}_{2.02}O_{11}$
973 K, 1 hour	$(Si_{3.93}Al_{0.07})^{IV}Al^{VI}_{2.02}O_{11}$	$(Si_{3.93}Al_{0.07})^{IV}Al^{VI}_{2.02}O_{11}$	0.14	$Si_{3.88}Al_{2.06}O_{10.85}$
1123 K, 1 hour	$(Si_{3.94}Al_{0.06})^{IV}Al^{VI}_{2.02}O_{11}$	$(Si_{3.93}Al_{0.07})^{IV}Al^{VI}_{2.02}O_{11}$	0.46	$Si_{3.88}Al_{2.05}O_{10.84}$
1273 K, 1 hour	$(Si_{4.02}Al_{1.98}O_{11})$	$(Si_{3.93}Al_{0.07})^{IV}Al^{VI}_{2.02}O_{11}$	5.23	$Si_{3.65}Al_{1.79}O_{9.99}$
1273 K, 2 hours	$(Si_{4.13}Al_{1.87}O_{11})$	$(Si_{3.93}Al_{0.07})^{IV}Al^{VI}_{2.02}O_{11}$	12.25	$Si_{3.39}Al_{1.50}O_{9.03}$
1273 K, 3 hours	$(Si_{4.20}Al_{1.74}O_{11})$	$(Si_{3.93}Al_{0.07})^{IV}Al^{2.02}_{VI}O_{11}$	16.18	$Si_{3.27}Al_{1.34}O_{8.55}$

2. in the chlorination residues, the amount of Si is greater and Al content is smaller, compared to the original material.

The two statements seemingly contradict each other since if the chemical composition of the chlorination residues fails to equal that of the original material, then the question is, how chlorination residues can keep the phase composition corresponding to the chemical composition, of the original material?

For this, a rough answer is given by establishing three partly differring models. Statement 1 is the initial one for all three models, but they differ in the way they satisfy Statement 2. The required data are contained in Table 4.

Model *A:* it is assumed that the actual analytical data given for chlorination residues in *Table 2* represent the chemical composition of a dehydroxylated crystalline compound with pyrophyllite structure (Statement 1.) Given the analysis data the stoichiometric formula of the chlorination, residues can be calculated (Column *A* in *Table 4*). It can be seen that as chlorination proceeds, the coefficients change due to change in SiO_2/Al_2O_3 ratio; for example, in the case of silicon it increases from a level of 3.93 corresponding to an hour chlorination at 873 K, to 4.20. Model *A* allows for a chlorination residue of uniform chemical composition which contains Si and Al in proportions corresponding to the instantaneous chlorination state in a dehydroxylated pyrophyllite type structure and by this formally meets Statement 2. However, it represents only a formal solution, because the number of tetrahedral positions is at most 4 compared to 4.20 Si mentioned above. The other difficulty in accepting the model is that it requires re-organisation in time, even during chlorination at a single temperature and not only at points attacked by the chlorinating gas mixture, but in the whole mass of the sample. Thus Model *A* can be disregarded.

Model *B:* similarly to Model *A* dehydroxylated crystalline material with pyrophyllite structure is also accepted in the case of Model *B* in the chlorination residues, according to Statement 1, but this is regarded as having unchanged stoichiometric composition throughout the chlorination. Accordingly, the chlorination residue richer in silicon compared to the original pyrophyllite (Statement 2), is a mixture of the dehydroxylated pyrophyllite with the

original composition and the silica obtained through greater chlorination of the aluminium. The reason for the change in the ratio SiO_2/Al_2O_3 in the chlorination residues is free SiO_2 built up at the attacked points, while the dehydroxylated pyrophyllite structure at other positions remains unchanged. The amount of the free SiO_2 can be calculated from analysis data *(Table 2)*, the total chlorination residue as a percentage is shown is Column *B* of *Table 4*. For example, the residue of chlorination experiment at 1273 K for 3 hours should have according to Model *B*, 16% of SiO_2 which is high enough for a safe *X*-ray diffractional phase analysis. However, there is no SiO_2 as crystalline component in the chlorination residue, but it may be present as an *X*-ray amorphous phase, a fact that is made probable by a slight rise in the base line, observed in the relevant *X*-ray diffractograms.

Model *C:* according to this model Si and Al positions removed during chlorination remain vacant, that is a dehydroxylated pyrophyllite structure with vacancies is assumed. The number of positions left vacant increases with the chlorination loss. In the residue of a chlorination experiment at 1273 K for 3 hours, it reaches almost one fourth of the originally filled cation positions. Continuing this process theoretically, for example by extending the duration of chlorination, the number of missing points should increase. Provided that SiO_2/Al_2O_3 ratio in the removed material *(Figure 3)* is unchanged at the same temperature, a state should be reached when there is no Al left in the dehydroxylated pyrophyllite structure. Then only two tetrahedral layers are left in the three layered pyrophyllite structure, with many cations also missing, and this obviously leads to the collapse of the lattice. The model's range of validity seemingly depends on how many vacancies the dehydroxylated pyrophyllite structure can tolerate, however the limit value of this is not known.

Conclusions

During the chlorination of Pázmánd pyrophyllite, Models *B* and/or *C* indicate the probability in such a way that while the pyrophyllite structure can tolerate the build up of vacant positions, Model *C* is predominant. Reaching a certain value, any further increase in the number of vacancies leads to the collapse of the lattice and following this a quantitatively decreasing dehydroxylated pyrophyllite structure of the limit value and an amorphous SiO_2 increase in quantity, are in coexistence.

Acknowledgements

The authors wish to express their thanks to prof. E. Nemecz and A. Ujhidy for their valuable advise and guidance.

SYMBOLS

V_{Cl_2} flow rate of Cl_2 (l/h)
V_{CO} flow rate of CO (l/h)
CuKα Kα characteristic *X*-ray radiation of copper, CuK$\alpha = 0.154$ nm
d interplanar spacing, nm
2Θ angle between the incident and reflected *X*-ray beams, °

REFERENCES

1. LANDSBERG, A.: Met. Trans. B., *1977*, 8 B, 435–441.
2. NEMECZ, E., VASSÁNYI, I. és SZABÓ S.: Építőanyag, *1981*, 23, 241–243.
3. ZVYAGIN, B. B., MISHCHENKO, K. S. and SOBOLOVA, S. V.: Sov. Phys.-Cryst., *1969*, 13, 511–515.
4. BRINDLEY, G. W. and WARDLE, R.: Am. Miner., *1970*, 55, 1259–1272.
5. WARDLE, R. and BRINDLEY, G. W.: Am. Miner., *1972*, 57, 732–750.
6. LEE, J. H. and GUGGENHEIM, S.: Am. Miner., *1981*, 66, 350–357.
7. ROSS, C. S. and HENDRICKS, S. B.: Prof. Pap. U.S. Geol. Surv., *1945*, 205 B, 23–79.
8. POLINSZKY, K., UJHIDY, A. and SZÉPVÖLGYI, J.: Hung. J. Ind. Chem., *1977*, 5, 97–108.
9. TERTIAN, R.: Chim. Ana., *1969*, 51, 525–536.
10. SZABÓ, L., VASSÁNYI, I. and SZABÓ, S.: Sprechsaal, *1981*, 114 (6), 437–440.
11. FRAU SZABÓ-SIPOS, L., UJHIDY, A. and VASSÁNYI, I.: Hung. J. Ind. Chem., *1983*, 11, 91–96.
12. UJHIDY, A., S. SZABÓ, L. MRS.: Proceedings of the 4th Conference on Applied Chemistry, August 30–September 1, *1983*, Veszprém, Hungary, Pap. No.: 2.1.3.3.

РЕЗЮМЕ

Авторы изучали фазовые и химические изменения пирофиллита ITc термообработанного при температурах 873, 973, 1123 и 1223 K в атмосфере содержащего окись углерода и хлора. Разработали три различных моделей для описания структуры хлористых остатков. Наиболее вероятным для остатки пирофиллита 1Tc структура дехидроксиллированного пирофиллита в которой можно найти аморфный SiO_2 и места аномалий.

HUNGARIAN JOURNAL
OF INDUSTRIAL CHEMISTRY
VESZPRÉM
Vol. 51. pp. 11–17 (1985)

ELECTROCHEMICAL TREATMENT OF SULPHUR KOMPOUNDS AND ORGANICS CONTAINING WASTE WATERS

B. Kovács, P. Mészáros and I. Ország*

(Institute for Inorganic Chemical Technology, and *Department of Physical Chenistry
University of Chemical Engineering, Veszprém, Hungary)

Received: May 15, 1984

A self-circulating electrochemical cell, developed for the treatment of sodium dithionite-containing waste waters [1, 2], was used for the treatment of sodium sulphite, sodium thiosulphate and phenol-containing waste waters, and the oxidation efficiency with respect to the sulphur compounds, phenol and organics were determined. The effects of the sodium chloride concentration upon the rate of oxidation of sodium sulphite and phenol were determined. All three materials studied could be oxidized in the auto-circulating electrochemical cell. Increased salt concentration improved the current efficiency and decreased the specific power consumption. The relative power consumption was higher than that obtained for sodium dithionite, because no aeration was used.

Introduction

In two previous papers [1, 2] the cell design, the results of laboratory experiments and the pilot-plant-scale unit developed for the electrochemical oxidation of sodium chloride and sodium dithionite-containing waste water were described. This paper deals with the electrochemical treatment of other waste waters, which contain various sulphur compounds and organics. Tomilov et al. [3], studying the electrochemical treatment of sulphur-containing waste waters, found that in the absence of chloride ions, at a current density of 2 A/dm^2 applied for 8 hours, a 24.2 g O_2/l COD could be decreased to 2.2 g O_2/l COD, and in the presence of 50 g/l NaCl a 180 g O_2/l COD could be decreased to 0.4 g O_2/l.

Osadeshenko et al. [4] studied the oxidation of sulphites in the presence and absence of chloride ions. They found that the current efficiency of sulphite oxidation in the absence of chloride was 50%, while in its presence it was 94–98%.

Harlamova and Tedoradze [5] reported the efficient use of electrochemical treatment for the removal of phenol, oil and cyanides from waste waters. They found that for efficient treatment in the 250 mg/l to 30 g/l phenol

concentration range the concentration of chloride ions should be at least 80 g Cl^-/g phenol. The optimum temperature range was 70–80 °C, and the specific power consumption was 30–90 kWh/kg phenol.

This paper describes the laboratory experiments carried out with the auto-circulating cell described in [1], without aeration, for the treatment of sodium sulphite, sodium thiosulphate and phenol-containing model solutions, and for the treatment of the organics-containing waste water of the Nitrokemia Works at Fűzfőgyártelep, Hungary.

Experimental

Reagent grade sodium sulphite, sodium thiosulphate and phenol (Reanal) were used to prepare 5 l volumes each of 38 ± 2 g/l sodium sulphite, 41 ± 2 g/l sodium thiosulphate and 0.25, 1 and 2.5 g/l phenol model solutions. The waste water sample, obtained from the Nitrokemia Works had a COD value of 3780 mg O_2/l. Solution pH was set to 7.5–8, by the addition of NaOH. External cooling was used to maintain the temperature of the solutions during electrolysis at 58 ± 2 °C. In the case of phenol solutions, the temperature did not rise above 40 ± 1 °C, consequently no external cooling was applied and the experiments were carried out at that temperature. In our opinion, this difference does not lead to a significant error, because, as shown in [1], above 40 °C the potential drop across the cell does not vary largely with the temperature. The sodium chloride concentration of the solution was maintained at 280 ± 5 g/l. In the case of sodium sulphite, further measurements were carried out in the absence of salt, and also at salt concentrations of 70 and 140 g/l. The concentration of sodium chloride was varied in the case of the phenol solutions as well, because 90 g salt was introduced into the system with each gramme of phenol. The current density varied in the 30 to 70 A/dm^2 range. Tests were carried out in the auto-circulating cell, with a perforated graphite anode and scaly stainless steel (KO 37) cathode, without aeration. During electrolysis, samples were taken at regular intervals and were analyzed by iodometric titration (for sulphur) and by the potassium bichromate method (MSZ 260/16–67 Hungarian Industrial Standard) for COD. After completion of the electrolysis, the sulphate content of the solutions was determined gravimetrically. It was found that at the end, sulphur was present as sulphate.

Results and discussion

a) *Oxidation of Sodium Sulphite and Sodium Thiosulphate*

The concentration of sodium sulphite and sodium thiosulphate as a function of time is plotted in *Fig. 1* and *2*, respectively, for various current densities. The rate of oxidation increases in both cases with the current density, i.e. the time-requirement of electrolysis decreases. The specific power consumption value, the most important economic criterion in electrochemical waste treatment, and current efficiency, both calculated from the measured values are listed in *Table 1*. In the case of sodium sulphite and sodium thiosulphate, at a current density of 50 A/cm^2, the specific power consumption is approxi-

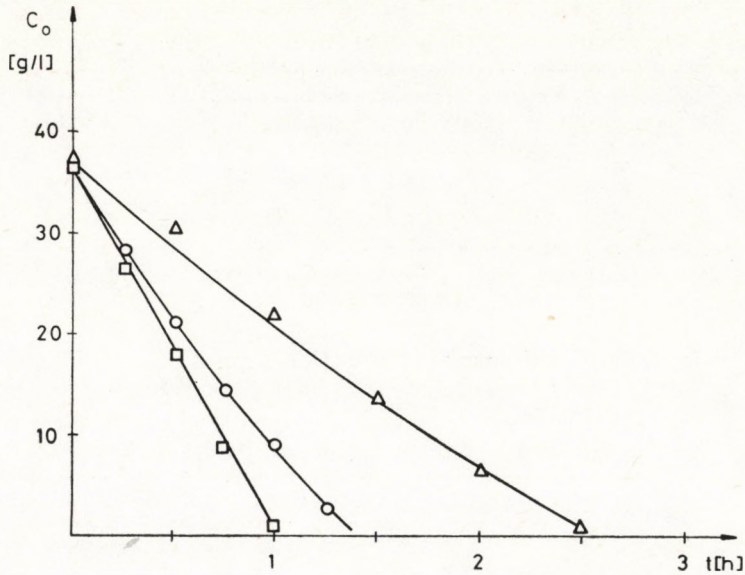

Fig. 1
Concentration of sodium sulphite as a function of time at various current densities.
△ — 30 A/dm²; ○ — 50 A/dm²; □ — 70 A/dm²

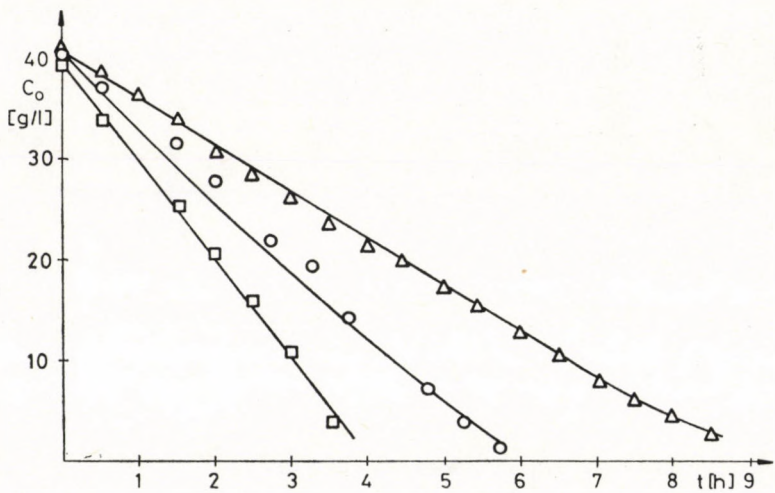

Fig. 2
Concentration of sodium thiosulphate as a function of time at various current densites
△ — 30 A/dm²; ○ — 50 A/dm²; □ — 70 A/dm²

mately proportional to the change of the degree of oxidation. It was shown in [1] that at a current density of 50 A/dm² and aeration rate of 12–13 l/A h, the specific power consumption of sodium dithionite oxidation was 4.5–5 kW h/kg reducing material. If one assumes that the specific power con-

Table 1.

Current efficiency (η) and specific power consumption (E) values of electrolysis

Solution	D A/dm²	C_{NaCl} g/l	$C_{initial}$ g/l	E kWh/kg	η %
Sodium sulphite	30	280	38.21	1.899	97.3
	50	280	36.10	2.212	99.2
	70	280	37.85	2.638	99.2
Sodium thiosulphate	30	280	41.27	6.251	94.1
	50	280	42.36	8.211	92.2
	70	280	39.61	8.560	91.2
Sodium sulphite	50	—	37.49	7.070	31.6
	50	70	38.98	6.715	39.0
	50	140	37.85	4.370	55.0
	50	280	36.10	2.212	99.2

sumption is also proportional to the change of the degree of oxidation in the case of sodium dithionite, it can be concluded that aeration decreases the specific power consumption by 20–25%.

The relationship between the rate of oxidation and salt concentration at a current density of 50 A/dm² is shown in *Fig. 3*. At identical initial sodium sulphite concentrations, the addition of sodium chloride increases the current efficiency and decreases the length of the electrolysis time. Specific power consumption and current efficiencies are plotted in *Fig. 4*. At a salt concentration of 280 g/l, the current efficiency is almost 100% and the specific power consumption is only 2.21 kWh/kg, compared to the 7.07 kWh/kg value observed in the absence of salt.

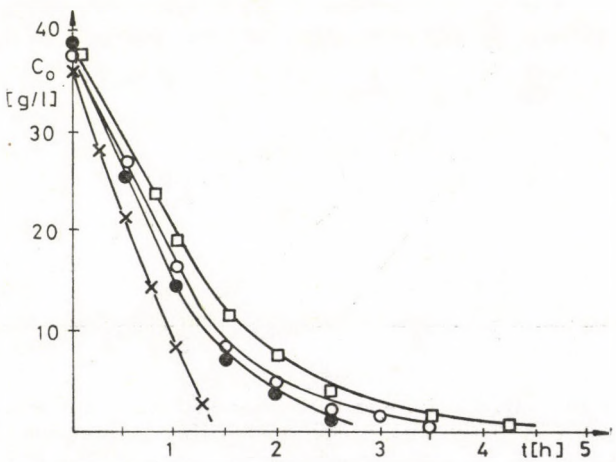

Fig. 3

Concentration of sodium sulphite as a function of time in solutions of varying salt concentration

$D = 50$ A/dm²

X — 280 g NaCl/l; ● — 140 g NaCl/l; ○ — 70 g NaCl/l; □ — 0 g NaCl/l

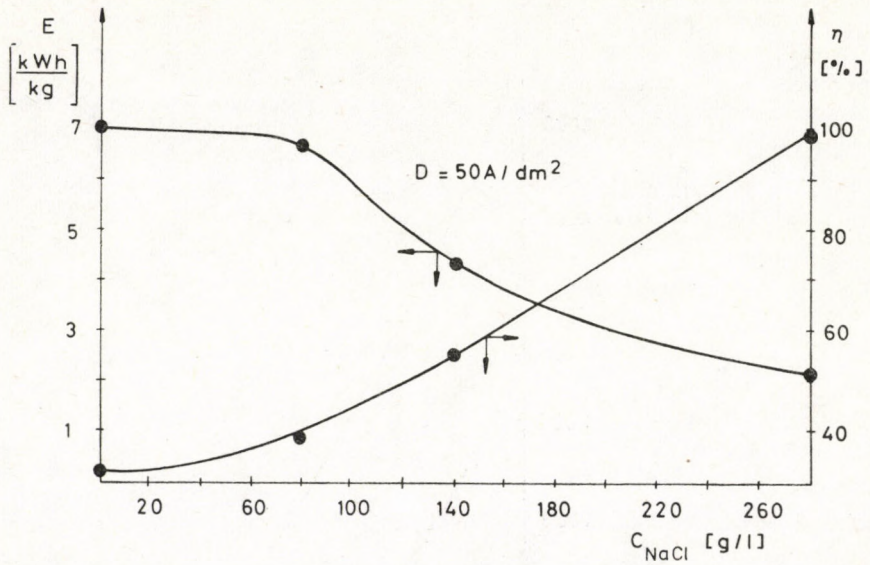

Fig. 4
Relationship between the apparent current efficiency and salt concentration, and the specific power consumption and salt concentration
$D = 50$ A/dm²

b) *Oxidation of Phenol*

Phenols and phenol derivatives, present in waste waters, can be relatively simply oxidized. When reacted with chlorine, some phenol derivatives are oxidized to carbon dioxide or to nontoxic, biologically degradable products. Some researchers [6] believe that phenol-containing waste waters are best processed electrochemically. Electrolysis is carried out between graphite anodes and perforated steel cathodes, in the presence of sodium chloride.

A 50 A/dm² current density was maintained in the phenol oxidation experiments. At first, a 40 g NaCl/g phenol salt concentration was used, but phenol could not be oxidized, in agreement with [5] which maintains that a minimum 80 g NaCl/g phenol is required for successful oxidation. Therefore, a 90 g NaCl/g phenol concentration was used in the following experiments. The chemical oxygen demand (COD) is plotted against the oxidation time in *Fig. 5*. The effects of salt concentration are also apparent in *Fig. 5:* an increase in NaCl concentration from 22.5 g/l to 225 g/l decreased the oxidation time by a factor of two. Since the exact pathway of electrochemical oxidation of phenol is not known, an apparent current efficiency was calculated as the ratio of the mass of oxygen calculated from the change of COD, and the mass of oxygen that can be produced by the current passing the cell. The apparent current efficiencies at various phenol concentrations were as follows: 0.25 g/l phenol: 26.32%, 1.0 g/l: 57.97%, 2.5 g/l: 64.36%. The specific power consumption is large, except for the 2.5 g phenol/l solution when it decreased to 90 kWh/kg.

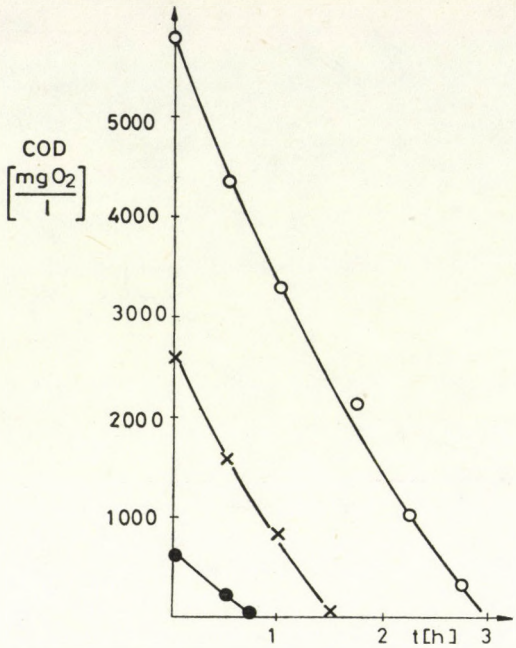

Fig. 5
COD of the phenol solution as a function of time at various initial phenol concentrations $D = 50$ A/dm². Initial phenol concentrations:
● — 0.25 g/l; X — 1.00 g/l; ○ — 2.5 g/l

c) *Oxidation of Organics-Containing Industrial Waste Water*

Process waste waters of the Nitrokemia Works are united in a buffer lagoon, neutralized and are further processed biologically. This neutralized waste water, with an initial COD of 3780 mg O_2/l was processed at 50 A/dm² for 4 hours, yielding a water with a COD of 22 mg O_2/l. The apparent current efficiency, calculated as in the case of phenol, was 31.47%, the specific power consumption was 0.27 kWh/l.

In conclusion it can be stated that the sulphur compounds tested can be oxidized efficiently, under the same conditions as sodium dithionite, though the specific power consumption is higher, because of the lack of aeration. Increasing salt concentration improves both the rate of oxidation and the specific power consumption. Waste water, containing phenol and organic pollutants, can also be treated in the auto-circulating cell, but the apparent current efficiency of oxidation is much lower and the specific power consumption is almost an order of magnitude larger than in the case of the inorganic sulphur compounds. At identical salt concentrations, the apparent current efficiency obtained for phenol is almost twice as large as that obtained for the organic pollutants.

REFERENCES

1. Mészáros, P., Ország, I., Kovács, B. and Kovács Z.: Hung. J. Ind. Chem., *1984*, 12, 151.
2. Mészáros, P., Ország, I., Kovács, B., Kovács Z. and Maloveczky Gy.: Hung. J. Ind. Chem., *1984*, 12, 163.
3. Tomilov, A. P., Osadeshenko, I. M. and Fuks, N. S.: Khim. Prom. *1972*, 48, 267.
4. Osadeshenko, I., M., Tomilov, A. P. and Rublev, V. V.: Zh. obsh. Khim. *1973*. *1973*, 43, 1654.
5. Harmalova, T. A. and Redoradze, G. A.: Khim. Prom. *1981*, 58, 85.
6. Pini, G.: Chemie Technik. *1975*, 4, 257.

РЕЗЮМЕ

В ходе экспериментов авторы использовали ранее опубликованную в 1,2 саморециркуляционную електражзер пригодную для оксидирования сточных вод, для очистки модельных растворов содержащих тиосульфат натрия и фенола и также для очистки сточной воды содержащей органические вещества с целью определения эффективности оксидации единичных серистых соединений фенола и органического вещества в саморециркуляционной камере. Для растворов содержащих сульфит натрия и фенол, изучали влияние концентрации хлорида натрия на скорость оксидации. Установили, что все вышеотмеченные вещества можно оксидировать в саморециркуляционной камере электролиза; увеличение концентрации соли увеличивает выход по токуи и уменшает удельный расход электроэнергии. У изученных серистых соединений относительный удельный расход электроэнергии больше, чем у дитионита натрия, так как настоящую серию экспериментов проводили без продувки воздуха.

HUNGARIAN JOURNAL
OF INDUSTRIAL CHEMISTRY
VESZPRÉM
Vol. 13. pp. 19–37 (1985)

AN EFFECTIVE FLASH ALGORITHM FOR PROCESS SIMULATORS USING CUBIC EQUATIONS OF STATE

L. Timár and J. Siklós

(Hungarian Oil and Gas Research Institute, Veszprém)

Received: June 29, 1984

An effective algorithm is proposed to solve isothermal flash problems in process simulation using cubic equation of state for the calculation of vapour-liquid equilibria. In accordance with the increased importance of time and storage savings in flowsheet programmes compared to a stand-alone flash calculation, the main aspect was to develop a reliable and fast converging algorithm of moderate storage demand, that also made medium size computer implementations possible. Furthermore, the trivial x = y solution, as an unfortunate peculiarity of the equation of state approach, is attempted to avoid by a properly chosen calculation strategy, rather than by any forcing technique. The applicability of the algorithm is demonstrated by some sample problems known as difficult examples from a numerical aspect.

Introduction

Isotherm flash modules constitutes one of the most frequently encountered operation units of the modularly structured process simulators. Accordingly, much has been done on the development of reliable and fast converging algorithms for the calculation task consisting of the separation of a material stream at a given pressure and temperature into vapour and liquid streams that are in equilibrium with each other. Nevertheless, while the flash calculations can be considered more or less easy problems for the activity coefficient approach (e.g. Wilson, NRTL, and UNIQUAC), the same flash modules may often fail if using any equation of state (e.g. [1], [2]) for the calculation of the vapour-liquid equilibrium. The computation difficulties manifest themselves by the slow convergence and/or the problem referred to as trivial solution ($x_i = y_i$, $i = 1, 2, \ldots, c$), close to the critical point. In case of poor initial guesses for the iteration variables x, y, the trivial solution may be attained even for moderate pressures. Despite the use of equations of state for some decades, until recently little attention was paid to this aspect. In addition, the number of publications, that did also consider the special claims made by flowsheet programmes, is rather small. In the last 5–10 years, on the other hand, attempts

were made to scrutinize the problem and to suggest some procedures for the avoidance of the trivial solution (e.g. [3], [4], [5], [6], [7]).

All authors agree that the trivial solution is accounted for by the poor initial phase compositions in the early iterations, that resulted in a vapour-like (liquid-like) fugacity coefficient, instead of a desired liquid-like (vapour-like) one. As for the prevention of the trivial solution, there are two different approaches to the problem. Some authors ([4], [5]) focussed their attention on the diagnosis and correction of the undesired root of the equation of state, assuming that this forcing technique is required only throughout a few iterations. They are not specific about the choice of the calculation strategy and the initialization method. Others ([3], [7]), on the other hand, consider the appropriate choice of the calculation strategy and initialization method to be the decisive factor in the avoidance of the trivial solution.

Following the latter strategy-oriented concept, we developed an efficient algorithm for isothermal flash calculations. While not all the features presented in the next sections are brand-new, taken together they make a complete, easy-to-programme procedure that exhibits a reliable and fast convergence in a wide pressure and temperature range, they involve a reliable and fast phase detection procedure and have simple and efficient selfstarting and restart capabilities (initialization).

Formulation of the Problem

The calculation of vapour-liquid equilibrium separators, often called flash process *(Fig. 1)* means the solution of the following types of equations:

total mass balance:

$$F = V + L \tag{1}$$

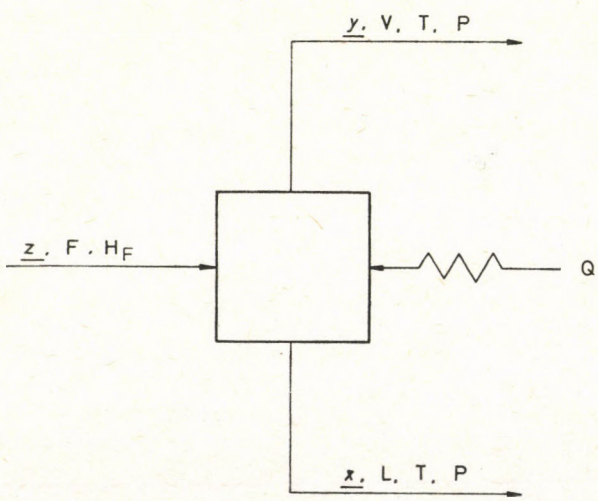

Fig. 1
Schematic diagram of isotherm flash

component balances:

$$F_i z_i = V_i y_i + L_i x_i \qquad i = 1, 2, \ldots, c \tag{2}$$

vapour-liquid relationship:

$$y_i = K_i(T, P, \mathbf{x}, \mathbf{y}) x_i \tag{3}$$

mole fraction restrictions:

$$\sum_{i=1}^{c} y_i = 1 \tag{4a}$$

or

$$\sum_{i=1}^{c} x_i = 1 \tag{4b}$$

or

$$\sum_{i=1}^{c} y_i - \sum_{i=1}^{c} x_i = 0 \tag{4c}$$

heat balance:

$$Q = H_F F - H_L L - H_V V \tag{5}$$

In the isotherm case, F $\mathbf{z}$ P T and H are specified and V, L, $\mathbf{x}$, $\mathbf{y}$ and Q have to be calculated.

The concrete form of the K_i function depends on the equilibrium model applied. For an equation of state approach, the K_i equilibrium ratios are given by the ratios of the fugacity coefficients of the liquid and vapour phases, respectively:

$$K_i = \bar{\varphi}_i^{L} / \bar{\varphi}_i^{V} \qquad i = 1, 2, \ldots, c \tag{6}$$

The fugacity coefficients are estimated with the same equation of state for both phases, choosing the corresponding Z compressibility root for the phase in question, after the solution of the cubic equation of state:

$$f(Z) = Z^3 - Z^2 + AZ - B \tag{7}$$

The calculation of A and B constants and further details of the determination of the fugacity coefficients by means of the compressibility factor can be taken from any of the original articles [1], [2].

Substituting Eq. (3) into Eq. (2) and Eq. (4c), and introducing the $a = V/F$ notation for the vaporization ratio, we gain the well-known formulation of the isotherm flash problem (for simplicity, the heat balance is omitted because it can be solved for Q separately):

$$g_i(\mathbf{x}, \mathbf{y}, a) = x_i - \frac{z_i}{a(K_i - 1) + 1} = 0 \tag{8}$$

$$g_{i+c}(\mathbf{x}, \mathbf{y}, a) = y_i - \frac{K_i z_i}{a(K_i - 1) + 1} = 0 \tag{9}$$

$$g_{2c+1}(\mathbf{x}, \mathbf{y}, a) = \sum_{i=1}^{c} \frac{(K_i - 1) z_i}{a(K_i - 1) + 1} = 0 \tag{10}$$

This is a nonlinear equation set made up of equations with $2c+1$ variables to be calculated iteratively. So, the general form of the problem can be written as:

$$\mathbf{g}(\mathbf{u}) = \mathbf{0} \tag{11}$$

where:

$$\mathbf{u} = [\mathbf{x}, \mathbf{y}, a]$$

Choice of the Calculation Strategy

Considering the complex dependence of K_i values of **x** and **y**, a general NEWTON–RAPHSON procedure solving all equations (8–10) simultaneiusly, seems to be the correct method. In spite of this evidence, such robust algorithms have been proposed only for some years (e.g. [3], [8]). This delay and reluctance can be explained by the expensive Jacobian evaluation for Eq. (11):

$$J_{ij} \cong \frac{g_i(u_j + \Delta u_j, \mathbf{u}_{i \neq j}) - g_i(u_j, \mathbf{u}_{i \neq j})}{\Delta u_j} \tag{12}$$

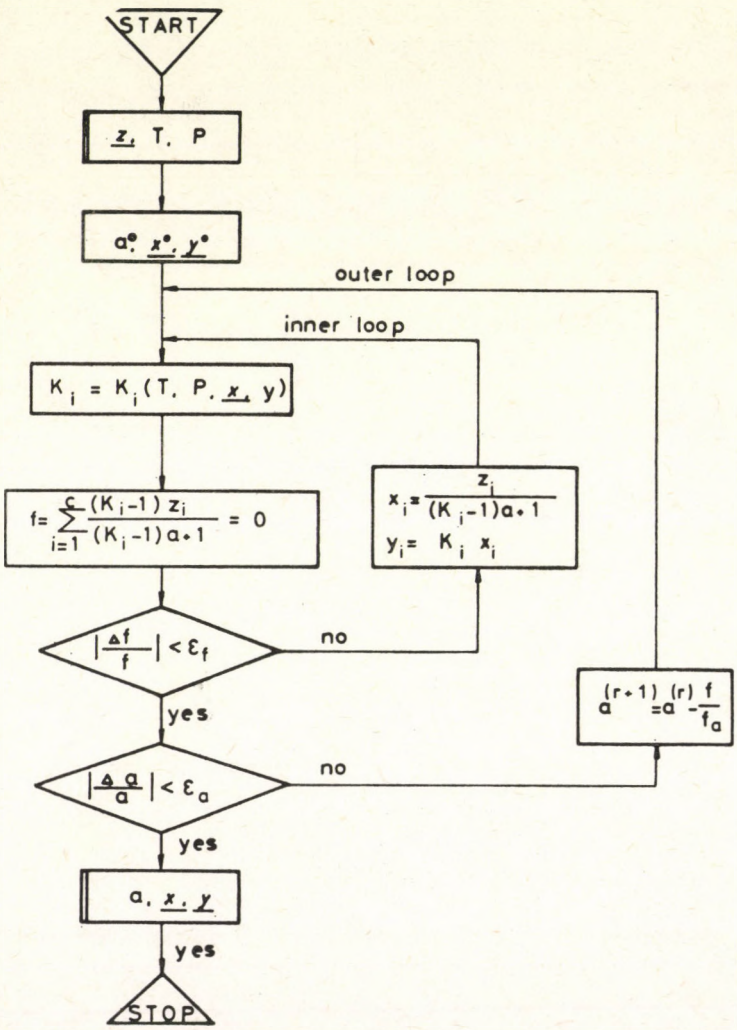

Fig. 2
Version 1 of two-loop strategy

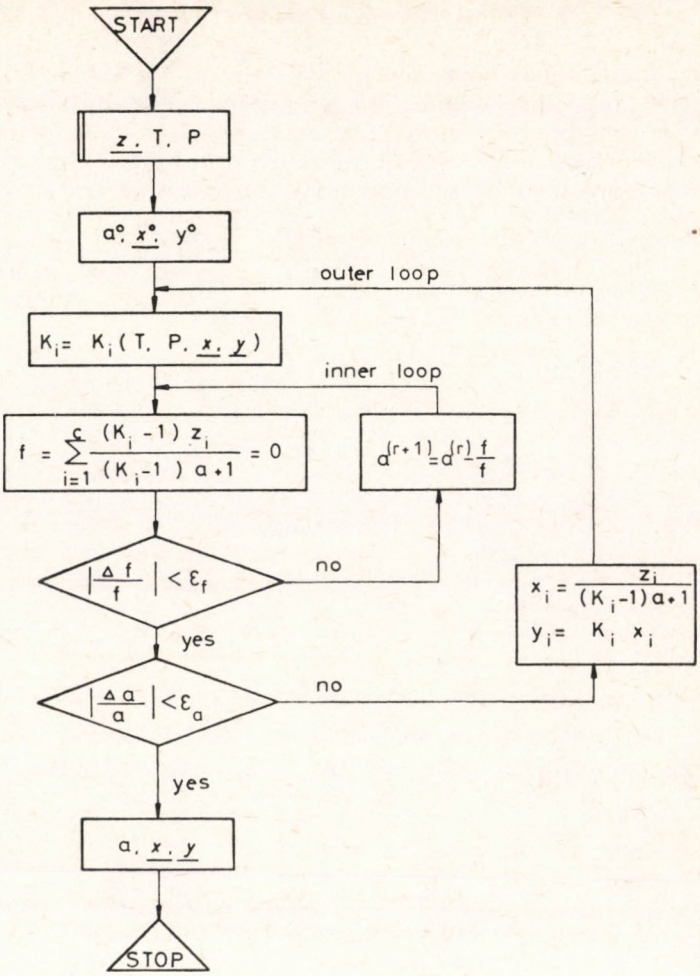

Fig. 3
Version 2 of two-loop strategy

So, the procedure would require $(2c+1)^2$ partial derivatives per iterations-involving $2c+1$ evaluations of the thermodynamic functions K_i per iterations.

Since the computation time is more or less proportional to the number of K_i evaluations, this method may be very expensive, even if it converges in relatively few iterations.

The propagators of the NEWTON–RAPHSON strategy are correct that the derivatives can also be produced analytically for most of the equation of state models, which would reduce the time consumption associated with the K_i evaluations. However, this method for applications in flowsheet programmes is usually impossible, because the thermodynamic property packages do not include the corresponding derivative routines. This is evident, since analy-

tical derivation would require a considerable enlargement of the property routines. (Among others, each K routine would necessitate additional derivative routines for the $\delta K/\delta x$, $\delta K/\delta y$ derivatives.) Fortunately, Equations (8)–(10) can also be solved separately, decoupling the equations in an appropriate manner. Namely, Eq. (10) can be solved for $a = V/F$ (e.g. with NEWTON–RAPHSON), considering K_i constant throughout the iteration. On the other hand, Equations (8) and (9) can be used for the correction of x and y values in order to recalculate the K_i values. Let us call this approach the two-loop strategy. Depending on the concrete form of the variable-to-loop coupling, there may be two different versions, each having an inner and an outer loop. *Version 1 (Fig. 2)* uses an outer loop for solving Eq. (10) to correct a, while the x and y values are corrected in an inner loop by repeated application of Equations (8) and (9).

Essentially, the inner loop serves the function evaluations required by the NEWTON procedure in the outer loop. This calculation pattern can be considered as an extension of the traditional approach, developed for an ideal vapour-liquid equilibrium case, to nonideal cases, inasmuch as the composition dependence of the K_i values is being taken into account by a few inner loop calculations of the function (10) at constant a, while iterating x and y to a prescribed convergence. Recently, a reversed application of the loops was proposed [6], [9]. The *version 2 (Fig. 3)* solves Eq. (10) for a at given K_i (i.e. x and y values), in the inner loop. The iterative correction of x and y takes place in the outer loop. Without any testing, it is obvious that the number of K_i evaluations per iteration is smaller for the two-loop approach than for the NEWTON–RAPHSON one. In addition, using the two-loop approach, version 2 is more advantageous than version 1, in this respect. Considering the aspects associated with the implementation in flowsheet programmes (relatively few K_i evaluations, no need for K_i derivatives with respect to the composition, and moderate storage requirement), the decision was made on the version 2 of the two-loop approach.

Convergence Acceleration in the outer Loop

Approaching the critical pressure of the mixture (e.g. under criogenic conditions), the convergence speed becomes very slow. The slow converging variables are the compositions that are iterated in the outer loop with direct substitution, using Equations (8) and (9). Observations have shown that the relationship between the composition values in two subsequent iterations becomes more or less linear after reaching a "slowing" point:

$$\mathbf{u}^{(r+1)} \cong \mathbf{A}\mathbf{u}^{(r)} + \mathbf{b} \tag{13}$$

where:

$$\mathbf{u} = [\mathbf{x}, \mathbf{y}]^{\cdot}$$

Consequently, the dominant eigen value method (DEM) [10] is expected to accelerate the convergence:

$$\hat{u}_i^{(r+1)} = u_i^{(r)} + \frac{1}{1-\lambda}\left(u_i^{(r+1)} - u_i^{(r)}\right) \qquad i = 1, 2, \ldots, c \tag{14}$$

where:

$$\lambda \cong \frac{\|\mathbf{u}^{(r+1)} - \mathbf{u}^{(r)}\|}{\|\mathbf{u}^{(r)} - \mathbf{u}^{(r-1)}\|}$$

A similar linear relationship was also observed for the values of function (10):

$$f^{(r+1)} \cong af^{(r)} + b \tag{15}$$

which would suggest that the following estimation for λ should be used:

$$\lambda \cong \frac{f^{(r+1)} - f^{(r)}}{f^{(r)} - f^{(r-1)}} \tag{16}$$

Due to the strong interaction between the variables (x, y) the (14) relationship, using the eucledian norms of u, was preferred in our algorithm.
The criterion of the intervention by DEM was chosen as:

$$\Delta\lambda = \frac{|\lambda^{(r)} - \lambda^{(r-1)}|}{|\lambda^{(r)}|} < 0.05 \tag{17}$$

In addition a bound of 0.98 for λ was applied to avoid overestimations due to round-off failures when approaching the accuracy limit of the computer. The latter case often occurs near the critical point of the mixture.

Initialization

Irrespective of the chosen strategy (NEWTON–RAPHSON, or version 1 or 2 of the two-loop approach), a good initialization, i.e. a consistent estimate for $a = V/F$, x and y proved to be of more decisive importance in the case of an equation of a state equilibrium model than for the activity coefficient approaches (e.g. WILSON, NRTL, and UNIQUAC). Especially near to the critical point, poor initial guesses may easily lead to the trivial $x = y$ solution. The term consistent estimate means that the iteration variable a, x and y should be of the same source or calculated with the same method. In addition, the initialization method should be simple with ignorable time-consumption compared to the total computation time of the flash calculation. Accordingly, the equilibrium ratios are usually estimated from Raoult's law:

$$K_i = P_i^s/P \qquad i = 1, 2, \ldots, c \tag{18}$$

where the vapour pressure is calculated with one of the available methods [11]. For this purpose, we found RIEDEL's correlation successful to perform most of the problems encountered:

$$P_i^s = \exp[\alpha_c \ln T_r - 0.0838 \times (\alpha_c - 3.75) \times (36/T_r - 35 - T_r^6 + 42 \times \ln T_r)] \times P_c \tag{19}$$

where the α_c constant can be calculated if Eq. (19) is written for the normal boiling point and solved for α_c. In the case of supercritical components ($T > T_{ci}$), the K_i obtained with Eq. (19) was limited to 10,000, to reduce overestimations. We also investigated the method proposed by ASSELINEAU et al. [3]. In this, the vapour pressures are estimated from the critical data and normal boiling point by linear interpolation or extrapolation:

$$\frac{\ln P_i^s - \ln P_{bi}}{\ln P_{ci} - \ln P_{bi}} = \frac{1/T - 1/T_{bi}}{1/T_{ci} - 1/T_{bi}} \tag{20}$$

This simple method was also found to be efficient for most of the problems, except for systems with a high CO_2 content (70–80 mole per cent) and near the critical pressure. Further benefits can be gained when the flash calculation is restarted from a previously converged solution, but with different values of z or/and T or/and P. This situation often happens in process simulation when the change in z is due to the changes in the recycle flows. In such cases, the convergence for the somewhat new condition is achieved in a few (2–3) iterations. Experiences have shown that more sophisticated methods to initialization (eg. CANFIELD [12]), do not result in a significant improvement, but often considerably raise the computation effort.

Detection of Single Phase Region

Flash calculations in single phase regions very often lead to a trivial solution. This phenomen is not surprising, since far below the bubble point there is no equilibrium vapour phase. Consequently, there is no vapour-like root for Z of Eq. (7). Similarly, the disappearence of the liquid-like root above the dew point can also be justified. Accordingly, for the prevention of this situation, the determination of the bubble and dew point seems to be the sure and correct way. Nevertheless, the calculation of the bubble and dew points takes a significant percentage of the total time requirement of the flash calculation. In flowsheeting, where the same flash unit should be computed more times due to the recycles, this correct method of phase detection may be very expensive.

There is another argumentation against the application of bubble and dew point calculations, as phase indicators. This is the increased danger of gaining a trivial solution, compared to that of the flash calculation. Experiences have shown [7] that the initial guess for the temperature must be close enough to the true value to avoid the trivial solution. Besides, in the case of retrograde phenomen on the mixture has no bubble or dew point at all.

In the flash modules of classic simulators, the phase detection is usually evaded by using the sums of $K_i \cdot z_i$ and z_i/K_i at the given pressure and temperature, as phase indicators in the following sense:

If $\Sigma K_i z_i \leq 1$, then liquid,
if $\Sigma z_i/K_i \geq 1$, then vapour phase

is stated. This way is very efficient for $K_i - s$ that do not strongly depend on the phase compositions. In case of composition-dependence, however, the summation must be repeated at the given temperature, until the changes in K_i values are less than a prescribed ε. For equations of state, however, this procedure may give rise to a trivial solution, resulting in false phase detection. Say, a vapour phase is diagnosed instead of liquid (a typical example is the subcooled absorption oil in hydrocarbon processing).

Keeping in view the aspects of the time-saving requirement of simulation programmes, a simple, but useful phase detection procedure was developed, the essence of which is the extension of the interpretation of the function $f(a) = \Sigma y - \Sigma x$ to $a = V/F$ less than 0 and greater than 1 values. So, the solution is searched for in the region of:

$$a_L < a < a_U,$$

where a_L and a_U are reasonably chosen lower and upper limits below 0 and above 1, respectively. The term "reasonable" means those experimentally chosen points where the given phase is considered to "disappear". In our experience, $a_L = -1$ and $a_U = 2$ are reasonable limits for most of the problems. Accordingly, the iteration for a is carried out in the region $-1 < a < 2$.

The convergence to any $-1 < a < 0$ or $1 < a < 2$ means a single liquid or vapour phase. Besides, the user can obtain useful information about "how much" the given phase is liquid or vapour. For instance, the phase with $a = -0.5$ is "more subcooled" than with $a = -0.1$, for the same mixture. In addition, this information might be useful, if a is prescribed and the corresponding temperature has to be calculated by solving the following design specification problem in a flowsheet:

$$g(T) = a(T) - a_s = 0 \tag{21}$$

It is evident that the $g'(a)$ derivative would always be zero below the bubble or above the dew point region if a were set to 0 or 1 for $a < 0$ or $a > 1$, in accordance with the conventional interpretation. Outside the experimentally given a_L, a_U bounds, the iteration is arbitrary broken in the outer loop when the decrease or increase in a after 3 subsequent outer loop steps becomes monotonic. Thus, if:

$$a^{(r)} < -1 \wedge a^{(r)} < a^{(r-1)} < a^{(r-2)}$$

then liquid, if:

$$a^{(r)} > 1 \wedge a^{(r)} > a^{(r-1)} > a^{(r-2)} \tag{22}$$

then the vapour phase is stated.

These relationships have performed successfully even for K_i values approaching to 1, since the iteration is always broken at the right moment, usually after 3–4 iterations. In order to ensure it, a maximum stepsize of 0.2 and a maximum number of iterations of 10 are allowed for the inner-loop.

Of course, the **y** and **x** values are calculated with setting a to 0 and 1 for $a < 0$ and $a > 1$, respectively, in order to obtain correct physical properties (e.g. enthalpy and entropy).

The Applicability of Forcing Techniques to Avoid Trivial Solutions

GUNDERSEN [4] proposed a mathematical manipulation which is based on appropriate shifting of the Z compressibility curve to accept the maximum or minimum value of the Z-function as a root, instead of the true ones, depending on the type of the phase in questions. Since the applicability of this procedure is limited to low and moderate pressures (the curve has no local extrema at higher pressures), it cannot be considered a general treatment of the problem. Nevertheless, we have not met any problem, which could not also be solved without this mathematical trick. Even the 8-component example presented by the author was easily solved without any intervention. Moreover, in the single phase region continuous intervention is usually required that sometimes leads to false values of a.

POLING et al. [5] suggest the use of the thermodynamic function of the isothermal compressibility to diagnose the spurious Z-roots. Moreover, they give

a procedure to remove the false root byappropriate adjustement of the pressure or composition to produce the desired vapour (liquid) phase. Though their method of diagnosis is thermodynamically exact, the experimental bounds providing the basis for the decision on the type of the given phase, have proved too strict in some cases. In other words, the intervention according to the bounds proposed by the authors resulted in a false diagnosis and unnecessary forcing. Consequently, the problem in question could be solved only without the diagnosis and intervention. In spite of these failures, the latter method seems to be promising, because of its thermodynamically well-founded derivation. To find a reliable (experimental) way for a better estimation of the bounds depending on the pressure (or other parameters), would we think be a significant step for the liquidation of the trivial solution problem.

Algorithm Proposed for Flowsheeting

The details described in the previous sections were put together to gain an efficient algorithm, whose schematic diagramme is illustrated in *Fig. 4.* The *inner loop* is devoted to the full convergence of the NEWTON–iteration for $a = V/F$. For success near to the arctical point, it is also advisable to converge the iteration up to a strict accuracy limit, way

$$|f| < 1E-9.$$

Though this condition may be too strict for low or moderate pressures, the iteration surplus of 1–2 means only an ignorable computation effort compared to the time consumption of the K_i evaluation in the outer loop. The *outer loop* serves to converge the x and y values, using acceleration by DEM, if necessary.

The two-loop procedure is ended if:

$$|f^{(r)}| < \varepsilon_f \wedge |a^{(r)} - a^{(r-1)}| < \varepsilon_a \tag{23}$$

criterion holds. It should be noted that $f^{(r)}$ refers here to the preiteration value of function (10), when entering into the inner loop with the new K_i constants.

Observations have indicated that the f values may decrease with some order of magnitude over the whole range of $0 < a < 1$ when approaching the critical point. Accordingly, the ε_f ought to be a dynamical bound rather than a fixed prescription. We found that the ratio of the minimum of $K_i > 1$ values to the maximum of $K_i < 1$ values provides a satisfactory measure for the distance from the critical point:

$$\alpha = K_{min}/K_{max}$$

Based on experiences, the following dynamical bounds for ε_f were given, in the function of α:

$$\varepsilon_f = 1E-5 \quad 1.5 < \alpha$$

$$\varepsilon_f = 1E-6 \quad 1.1 < \alpha < 1.5$$

$$\varepsilon_f = 1E-7 \quad \alpha < 1.1$$

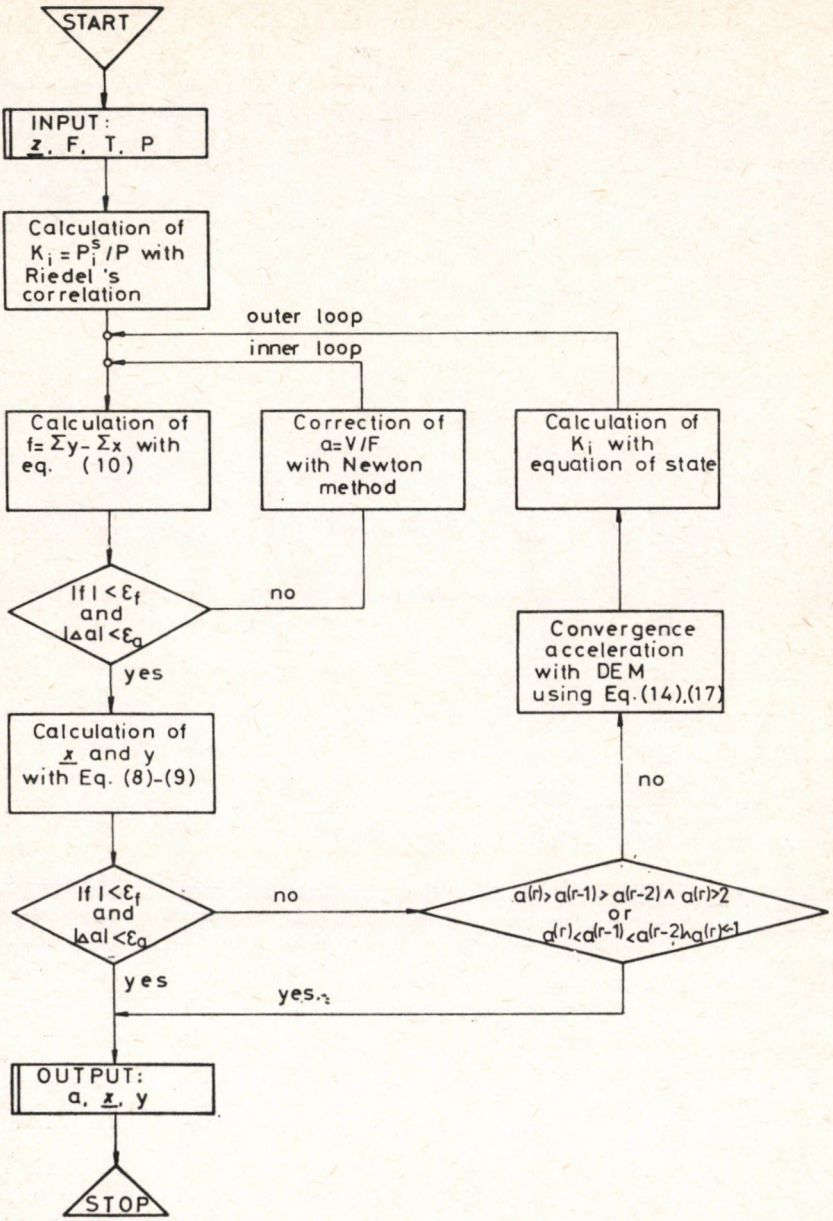

Fig. 4
Schematic diagram of the algorithm

For $\alpha \leqq 1.05$, we often had to face roundoff difficulties associated with the accuracy limit of the computer. Similarly, ε_a was also given in the function of α:

$$\varepsilon_a = 5E-5 \qquad 1.1 < \alpha$$
$$\varepsilon_a = 1E-5 \qquad \alpha < 1.1$$

Programme Implementations

The FORTRAN programme of the algorithm was inserted into the PROPAC property calculation package [14] and is being used by the IFLASH module of the MASTEP flowsheeting programme that can be accessed on a SIEMENS 7000 time-sharing computer system (BS 2000 operating system) [13].

In addition, a stand-alone BASIC version on a Hewlett–Packard desktop computer (HP 9845, HP 9835, HP 9830) was also elaborated, for drawing up the complete phase envelope of mixtures of given composition.

Sample Problems and Discussion

From the examples tested, four representative mixtures were selected. Examples 1–3, taken from literature on flash calculation, are considered difficult from the point of view of convergence behaviour and example 4 was encountered in our industrial practice. The composition of the mixtures with the corresponding references is given in *Table 1*. While the interaction coefficients of the RKS equation of state were all set to zero for examples 1–3, the example 4 was run with realistic values according to *Table 2*.

To illustrate the advantage of version 2 over version 1 of the two-loop strategy, the results of *example 1* are compared in *Table 3*, for both versions.

Table 1

Sample problems

Component	Mole fractions of example			
	1	2	3	4
Nitrogen	0.0064		0.0450	0.0190
Methane	0.7280		0.7000	0.1547
Ethane	0.0546	0.4000	0.1171	0.0103
Carbon Dioxide				0.8096
Hydrogen Sulfide				0.0030
Propane	0.0302	0.4000	0.0497	0.0020
n-Butane	0.0307	0.2000	0.0277	0.0009
n-Pentane	0.0688		0.0150	0.0004
n-Hexane	0.0438		0.0098	0.0001
n-Heptane	0.0375			
n-Octane				
n-Nonane			0.0357	
Source	GUNDERSEN [4]	COWARD [15]	ASSELINEAU [3]	own practice
Eq. of state	REDLICH–KWONG–SOAVE			

Table 2

Interaction coefficients
(example 4)

Component	N_2	C_1	C_2	CO_2	H_2S	C_3	C_4	C_5	C_6
N_2	—	0.0278	0.0407	−0.0315	0.1696	0.0763	0.0700	0.0878	0.1496
C_1		—	−0.0078	0.0933	0.0000	0.0090	0.0056	0.0190	0.0307
C_2			—	0.1363	0.0852	−0.0022	0.0067	0.0056	0.0041
CO_2				—	0.0000	0.1289	0.1430	0.1311	0.1100
H_2S					—	0.0885	0.0511	0.0689	0.0700
C_3						—	0.0000	0.0233	0.0041
C_4							—	0.0204	−0.0004
C_5								—	0.0019
C_6									—

Table 3

Comparison of version 1 and 2 of the two-loop approach
(example 1)

P [MPa]	T [K]	$a = V/F$	CPU	
			version 1	version 2
12.8	250	0.0243	3.4	2.3
	320	0.6489	3.1	2.1
	400	vapour	2.1	0.9
16.0	270	0.0965	4.2	2.7
	280	0.2695	4.7	2.6
	320	0.5562	4.7	2.4
	360	0.7696	5.0	2.4
	375	0.9058	6.0	2.3
17.2	300	0.0609	6.1	2.8
	320	0.3443	5.8	2.6
	340	0.6259	5.8	2.6
	400	vapour	1.9	1.8

It can be seen that the computation effort (CPU-time) is much smaller for version 2, due to the fewer K_i evaluations in the outer loop. In addition it should be noted that no forcing intervention suggested by GUNDERSEN [4] was necessary to avoid trivial solutions. In all probability, we had better initialization or calculation strategy.

Example 2 is a seemingly simple, narrow boiling mixture (C_2, C_3, C_4) that was created as a deterrent for the users of equation of state equilibrium

Table 4

Performance of version 2 with extended range for $a = V/F$ (example 2)

P [MPa]	T [K]	$a = V/F$	Iterations
5.0	354	−1.00	14
	356	−0.55	14
	358	−0,25	14
	360	−0.11	13
	362	−0.02	13
	364	0.2107	13
	366	0.5356	13
	368	0.9160	13
	370	1.08	6
5.1	362	−0.11	5
	364	−0.04	9
	366	0.1975	16
	368	0.9130	19
	368.5	1.10	18
5.13	366.5	−0.0011	39
	367.0	0.2196	37
	367.5	0.6165	13
	367.55	1.0062	32

models in flash calculations. Using our algorithm, however, no computational problem was encountered even in the closeness of the critical point, as illustrated in *Table 4*. The data also illustrates the extension of the interpretation of the meaning of the vapourization ratios. Moreover, it should be noted that at a pressure of 5 MPa and at a temperature of 368 K, the phase diagnosis

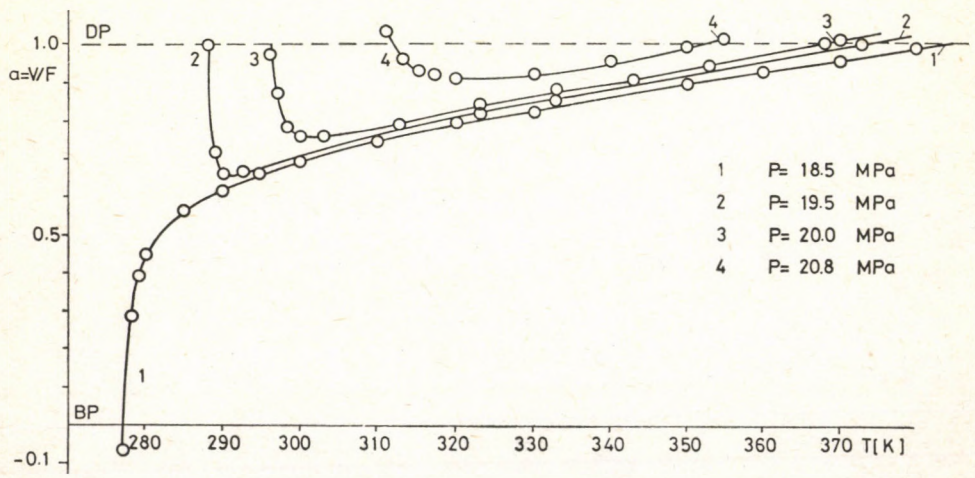

Fig. 5
Retrograde phenomena for example 3

Table 5

Set of $a = V/F$ values for different T and P (example 3)

Pressure, MPa	Temperature, K	Vaporization ratio, $a = V/F$
15.00	249.00	−0.0563 23
	250.00	0.0702 22
	253.00	0.2572 20
	255.00	0.3249 19
	260.00	0.4337 22
	265.00	0.5042 16
	270.00	0.5570 17
	280.00	0.6352 14
	300.00	0.7382 12
	320.00	0.8061 12
	340.00	0.8567 9
	360.00	0.8985 11
	380.00	0.9382 6
	400.00	0.9807 9
	420.00	1.0356 9
18.00	272.50	−0.3000 58
	273.00	0.1430 51
	274.00	0.3026 45
	275.00	0.3740 40
	276.00	0.4160 34
	278.00	0.4757 29
	283.00	0.5604 22
	293.00	0.6541 18
	313.00	0.7624 16
	353.00	0.8935 13
	373.00	0.9499 13
	378.00	0.9836 13
	383.00	1.0060 13
18.50	277.00	−0.0775 32
	278.00	0.2805 47
	279.00	0.3954 39
	280.00	0.4479 31
	285.00	0.5613 12
	290.00	0.6191 18
	295.00	0.6611 17
	300.00	0.6947 16
	310.00	0.7487 13
	320.00	0.7910 13
	330.00	0.8270 13
	350.00	0.8940 13
	360.00	0.9216 10
	370.00	0.9500 13
	390.00	1.0211 13
19.00	282.00	0.2517 50
	283.00	0.4302 51
	284.00	0.4937 43
	285.00	0.5282 36
	290.00	0.6100 22
	295.00	0.6575 18
19.00	300.00	0.6935 17
	310.00	0.7500 16
	320.00	0.7951 13
	330.00	0.8328 13
	340.00	0.8723 9
	350.00	0.8993 13
	360.00	0.9313 13
	370.00	0.9646 13
	380.00	1.0012 10
19.50	288.00	0.9925 50
	289.00	0.7222 49
	290.00	0.6605 15
	291.00	0.6534 15
	293.00	0.6579 24
	323.00	0.8268 14
	333.00	0.8533 21
	343.00	0.8800 15
	373.00	0.9951 10
20.00	295.50	1.3000 49
	296.00	0.9700 50
	297.00	0.8776 27
	298.00	0.7820 22
	300.00	0.7599 24
	303.00	0.7593 17
	323.00	0.8313 17
	333.00	0.8691 16
	343.00	0.9061 15
	353.00	0.9432 10
	370.00	1.0107 14
20.70	308.00	1.1116 50
	310.00	0.9660 26
	312.00	0.9219 20
	314.00	0.9040 17
	315.00	0.8962 21
	325.00	0.8987 17
	330.00	0.9087 17
	340.00	0.9411 17
	345.00	0.9595 17
	350.00	0.9790 16
	360.00	1.0231 14
20.80	311.00	1.0386 32
	315.00	0.9350 17
	317.00	0.9215 18
	320.00	0.9100 21
	330.00	0.9219 17
	340.00	0.9519 18
	355.00	1.0115 14

and adjustment proposed by POLING et al. [5] proved to be unjustified. Only the change in the bound of the isothermal compressibility from 0.03 to 0.07 could overcome the convergence difficulty associated with the continual performance of the forcing procedure.

Example 3 proved to be the most difficult case, which is also demonstrated by the relatively large number of iterations *(Table 5)*. Calculations of such wide-boiling mixtures having very light components, together with relatively nonvolatile components and lacking components of intermediate volatility, are usually difficult to converge. This can be explained by the fact that close-boiling components have more linear objective functions than wide boiling mixtures. Moreover, the accuracy limit of the computer gives rise to larger round-off errors.

The a vs. T curves for various pressures, drawn up in *Fig. 5*, also illustrate the applicability of the algorithm in the case of retrograde condensation (two dew points at the same pressure).

Example 4 is a hydrocarbon mixture with high CO_2 content. The task was to draw up the phase envelope from the pressure of 7.0 MPa, *Table 6* involves the necessary a vs. T values, calculated at increasing pressures for reasonably chosen temperature steps. From these data, the a vs. T curves for various

Table 6.

Set of $a = V/F$ values for different T and P (example 4)

Pressure, MPa	Temperature, K	Vaporization ratio. $A = V/F$	Pressure, MPa	Temperature, K	Vaporization ratio, $A = V/F$
7.00	269.00	0.0004	8.20	288.00	0.2579
	272.00	0.0600		289.00	0.4187
	276.00	0.1685		290.00	0.6667
	279.00	0.2843		291.00	1.2675
	282.00	0.4466			
	287.00	0.9000	8.25	287.00	0.0727
	288.00	1.0300		288.00	0.1825
				289.00	0.3449
7.50	270.00	−0.1100		290.00	0.6182
	276.00	0.0132		290.30	0.7718
	280.00	0.1495		290.50	0.9114
	284.00	0.3702		290.60	0.9976
	288.00	0.7562			
	289.00	0.9000	8.30	287.00	−0.0167
	290.00	1.0603		288.00	0.0800
				289.00	0.2316
8.00	280.00	−0.0847		290.00	0.5661
	282.00	−0.0081		290.10	0.6463
	283.00	0.0396		290.20	0.7899
	286.00	0.2405		290.30	1.1700
	288.00	0.4551			
	290.00	0.7939	8.32	287.70	−0.0032
	291.00	1.0496		288.00	0.0277
				288.50	0.0849
8.20	285.00	−0.0156		289.00	0.1571
	286.00	0.0545		290.00	0.5150
	287.00	0.1432			

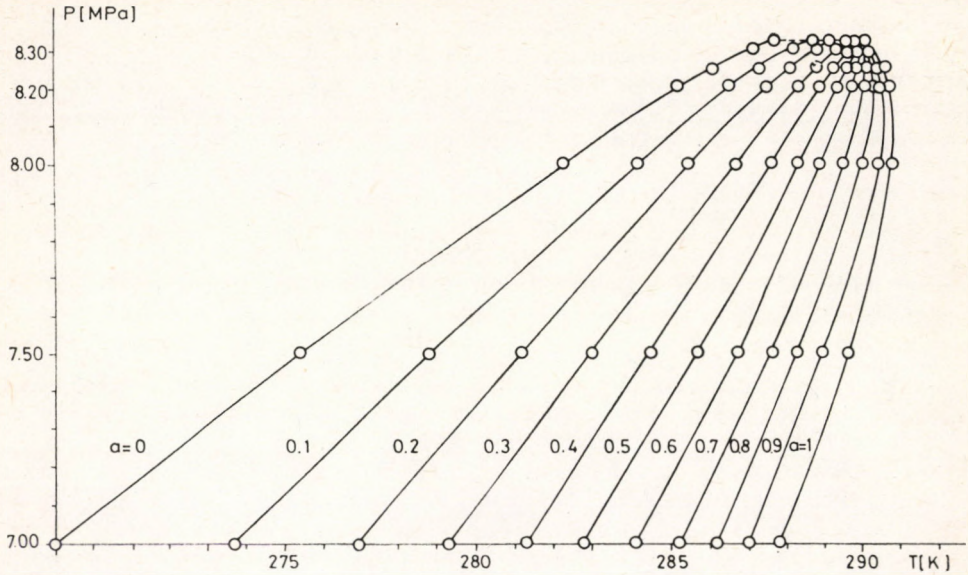

Fig. 7
Phase diagram for example 4

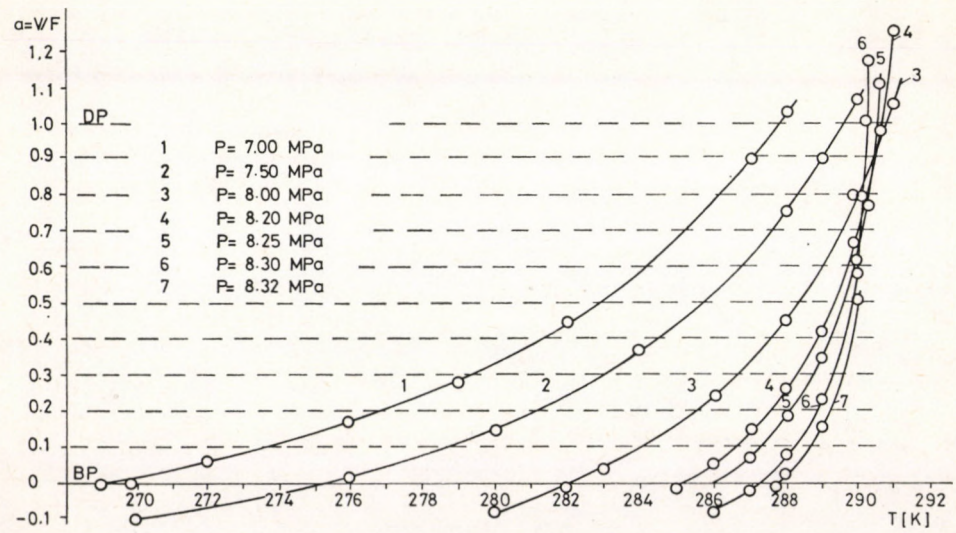

Fig. 6
Auxiliary curves to phase diagram for example 4

pressures were constructed *(Fig. 6)*. Then, based on the obtained curves, the $P-T$ points of the phase envelope, corresponding to a given $a=V/F$ point of the a vs. T curve, were drawn up, yielding the phase diagram shown in *Fig. 7*. Of course, the above outlined procedure could also be automated by writing an appropriate programme that carries out the flash calculations and the curve fitting and drawing (this work is under way).

Conclusion and Significance

An efficient algorithm was developed for flash calculations in simulation programmes, using a cubic equation of a state approach to vapour liquid equilibrium estimation.

- The algorithm exhibits a reliable and fast convergence in a wide range of state variables, up to 95–98 per cent of the critical pressure (below or above, in the case of retrograde behaviour).
- The convergence acceleration with DEM in the outer loop provides a considerable decrease in the total number of the time-consuming K_i evaluations.
- The extension of $a=V/F$ outside the physically interpretable range of 0—1, made the single phase detection fast and reliable, eliminating the need for the time-consuming bubble and dew point calculations. Moreover, a useful and visual measure of subcooled and superheated conditions is also provided for the user of the flowsheeting programme.
- The measuring of the distance from the critical point with K_{max}/K_{min} makes a dynamical prescription of the iteration ending possible.
- The algorithm is selfstarting, i.e. the user is not required to specify initial estimates for the phase compositions. The application of Riedel's correlation together with Rault's law proved to be a successful method for most of the problems. As for the restarting capability in process simulation, the previously converged solution serves as a very good initialization for the new conditions arising from the iterative change in the recycle streams.
- For computers of moderate memory size, the relatively small storage requirement of the algorithm can be an additional advantage in the implementation.

SYMBOLS

a vapour-to-feed ratio, $(a=V/F)$
c number of components in the mixture
H_F feed molar enthalpy, J/kmole
H_L liquid phase molar enthalpy, J/kmole
H_V vapour phase molar enthalpy, J/kmole
K vapour-liquid equilibrium ratio
L total liquid phase rate, kmole/h
P pressure, Pa
P_c critical pressure, Pa
P^s vapour pressure, Pa
Q heat input, J/h
T temperature, K
T_b normal boiling point, K
T_c critical temperature, K
T_r reduced temperature

u vector composed of **x**, **y** and **a**
V total vapour phase rate, kmole/h
z feed mole fraction
Z compressibility
x liquid mole fraction
x vector of liquid mole fractions
y vapour mole fraction
y vector of vapour mole fractions

greek letters

α measure of distance from the critical point ($\alpha = K_{max}/K_{min}$)
α_c Riedel's constant
$\bar{\varphi}$ fugacity coefficient in the mixture

indices

i component index
r iteration index

REFERENCES

1. Soave, G.: Chem. Eng. Sci. *1972*, 27, 1197.
2. Peng, D. Y. and Robinson, D. B.: Ind. Eng. Chem. Fundam. *1976*, 15 (1), 59.
3. Asselineau, L., Bogdanic, G. and Vidal, J.: Fluid Phase Equilibrium, *1979*, 3, 273.
4. Gundersen, T.: Comp. and Chem. Eng. *1982*, 6, 245.
5. Poling, B. E., Grens, E. A. and Prausnitz, J. M.: Ind. Eng. Chem. Proc. Des. Dev. *1981*, 20, 127.
6. Sandler, S. I.: Foundations of Computer-Aided Chemical Process Design, Vol. 2., p. 83., Engineering Foundation, New York, 1981.
7. Veeranna, P. and Rihani, D.: Fluid Phase Equilibrium, *1984*, 16, 41.
8. Hirose, Y., Kawase, Y. and Kudih, M.: J. Chem. Eng. Japan, *1978*, 11, 150.
9. Prausnitz, J. M., Anderson, T. F., Grens, E. A., Eckert, C. A., Hsieh, R. and O'Connell, J.: Computer Calculations for Multicomponent Vapour-Liquid and Liquid-Liquid Equilibria. Prentice-Hall, Englewood Cliffs, 1980. p. 124.
10. Orbach, O. and Crowe, C. M.: Canad. J. Chem. Eng. *1971*, 49, 509.
11. Reid, R. C., Prausnitz, J. M. and Sherwood, Th. K.: The Properties of Gases and Liquids. McGraw-Hill, New York, 1977. p. 181.
12. Canfield, F. B.: Hydrocarbon Proc. *1971*, 50 (4), 137.
13. Timár L., Simon, F., Csermely, Z., Siklós, J. and Bácskai S.: MASTEP — Sequential and Simultaneous Modular Algorithms in a Flowsheeting Programme. Proc. of CHEMPLANT '80 EFCE Symposium (EFCE Publ. Ser. No. 10) 1980, Hévíz, Hungary, p. 115.
14. Simon F., Siklós J., Timár, L. and Bácskai, S.: An Interactive System Approach for Estimation of Physical and Thermodynamic Properties. Proc. of CHEMPLANT '80 EFCE Symposium (EFCE Publ. Ser. No. 10) 1980. Hévíz, Hungary, p. 1133.
15. Coward, I., Gale, S. E. and Webb, D. R.: Trans. Inst. Chem. Eng. *1978*, 56, 19

РЕЗЮМЕ

В настоящей стати изложена характеристика эффективного алгоритма для расчета изотермических паро-жидкостных сепараторов сложных химико-технологических схем (СХТС) с использованием кубических уравнений состояния к описанию фазового равновесия.

Учитывая особенное значение экономии времени и хранения при расчете СХТС по сравнению с случаем отдельно стоящего сепаратора, главным аспектом развития была разработка такого алгоритма, который обеспечивает надежную и скору сходимость при использовании памяти небольшего объема.

Наряду с этим для предотвращения тривиального x=y решения (специфичность уравнений состояния) предпочитается настоящая стратегия к различным „форсирующим" процедурам.

Для демонстрации преимуществ алгоритма приведены некоторые трудные с точки зрения сходимости задачи.

HUNGARIAN JOURNAL
OF INDUSTRIAL CHEMISTRY
VESZPRÉM
Vol. 13. pp. 39–46 (1985)

RESIDENCE TIME DISTRIBUTION IN A BAFFLE PLATE TYPE TUBULAR LIQUID-LIQUID TWO-PHASE REACTOR

A. Aranyi*, M. Bakos, J. Kreidl* and B. Stefkó*

(Veszprém University of Chemical Engineering. Department of Chemical Process Engineering, Veszprém, Hungary
* Chemical Works of G. Richter Ltd., Budapest, Hungary)

Received: July 18, 1984

Residence time distributions were measured in a two-phase reacting system containing *i*-amyl-acetate as dispersed phase and 0.1 mol/l NaOH-solution as continuous phase in a baffle-plate type reactor. The mean residence times, the equivalent numbers of reactors in series and the axial dispersion coefficients were calculated in the usual way. Experiments were also performed in a single-phase system for comparison.

Experimental

Apparatus

The experiments were carried out in a baffle-plate type tubular reactor consisting 24 baffle-plates and surrounded by a water jacket for constant temperature circulating system. It is shown schematically in *Fig. 1.* The length of the reactor section is 1,126 mm, the inner diameter of the tube 50 mm, the plate spacing 41.6 mm. The reactor is equipped with 9 magnetic valves for removing samples at spacing of 125 mm.

The schematic diagram of the experimental set up is shown in *Fig. 2.* The NaOH solution and the *i*-amyl-acetate are pumped from the reservoire (1 and 2) by centrifugal pumps (3 and 4) through a preheater (7) and ultrathermostats (8 and 9) to the reactor (11). Their volumetric flow rates are determined by rotameters (5 and 6). The reactor (11) is thermostated through a constant temperature circulating system operated by ultrathermostat (10).

By varying the flow rate and the ratio of dispersed phase to the total feed, a wide range of conditions could be studied [1].

Method

Residence time distribution of the continuous phase were measured in a two-phase reacting system containing *i*-amyl-acetate as dispersed phase and 0.1 mol/l NaOH-solution as continuous phase. Bromphenol blue dissolved in

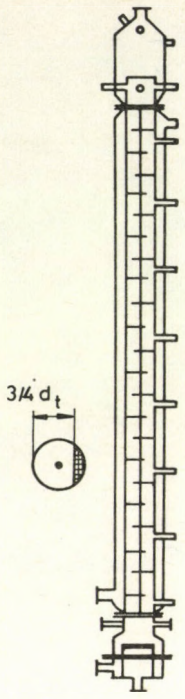

Fig. 1
Schematic of the reactor

0.1 mol/l NaOH-solution was used as a tracer. (It does not dissolve in the *i*-amyl-acetate.) The concentration of tracer was measured at the top of the reactor by colorimetric method.

The experiments were also performed in a 0.1 mol/l NaOH-solution single-phase system for comparison.

The moment method was used for the determination of the mean residence time of the continuous phase ($\bar{t}_C$), the axial dispersion coefficient (D_{ax}) and the equivalent number of reactors in series (n_e), respectively [2].

The BODENSTEIN number (Bo) and the equivalent number of reactors in series (n_e) were determined from the second central moment by:

$$\sigma^2 = \frac{2}{\mathrm{Bo}^2}(\mathrm{Bo} - 1 + e^{-\mathrm{Bo}}) = \frac{1}{n_e} \tag{1}$$

The axial dispersion coefficient (D_{ax}) was calculated from the BODENSTEIN number:

$$\mathrm{Bo} = \frac{vL}{D_{ax}} \tag{2}$$

The mean residence time of the dispersed phase was estimated by:

$$\bar{t}_D = \frac{L}{v_D} = \frac{\varepsilon AL}{B_D} \tag{3}$$

Table 1.

Experimental conditions ($T = 20$ °C)

Run code	$B \cdot 10^6$ m³/s	φ —	$B_C \cdot 10^6$ m³/s	$A \cdot 10^4$ m²	$v_C \cdot 10^3$ m/s	Re_C —
1.1	8.3	0.12	7.4	9.72	8.05	268
1.2	7.4	—	7.4	10.10	7.42	265
2.1	27.9	0.10	25.1	9.67	26.8	931
2.2	25.2	—	25.2	10.10	25.2	895
3.1	27.8	0.14	23.9	9.64	26.6	879
3.2	24.2	—	24.2	10.10	24.2	859
4.1	27.8	0.25	20.8	9.50	26.2	778
4.2	21.4	—	21.4	10.10	21.4	755
5.1	27.9	0.50	14.0	9.25	25.6	534
5.2	14.4	—	14.4	10.10	14.4	512
6.1	38.9	0.50	19.4	9.01	34.8	743
6.2	19.7	—	19.7	10.10	19.7	702
7.1	16.9	0.49	8.6	9.36	15.7	350
7.2	9.44	—	9.4	10.10	9.44	338
8.1	10.0	0.50	5.0	9.60	9.53	182
8.2	5.0	—	5.0	10.10	5.00	178

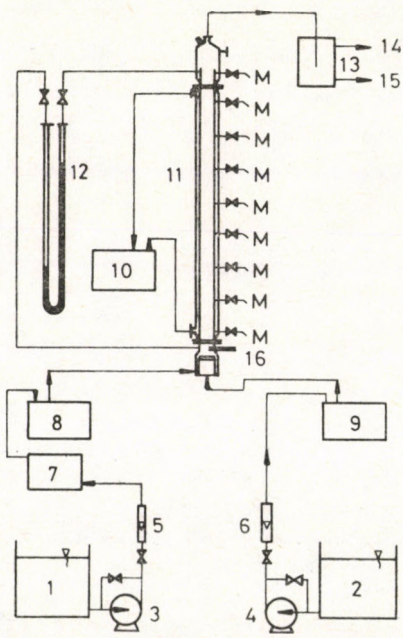

Fig. 2

Schematic diagram of the experimental set up. *1* — NaOH solution reservoir; *2* — *i*-amyl-acetate reservoir; *3*, *4* — centrifugal pumps; *5*, *6* — rotameters; *7* — preheater; *8*, *9*, *10* — ultrathermostats; *11* — reactor; *12* — manometer; *13* — separator; *14* — organic phase outlet; *15* — aqueous phase outlet; *16* — thermometer; *M* — magnetic valves

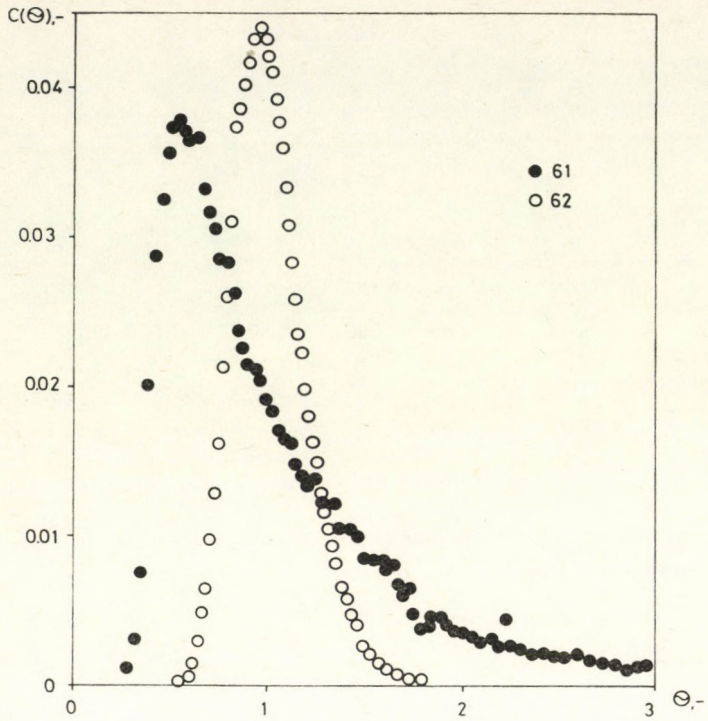

Fig. 3
An example of residence time distributions. ● — two-phase flow (run 6.1), ○ — single-phase flow (run 6.2)

Results

The experimental conditions are listed in *Table 1.* An example of residence time distributions is shown in *Fig. 3.*

The effect of the continuous phase REYNOLDS number (Re_C) on the axial dispersion coefficient (D_{ax}) in both single-phase and two-phase flow is shown in *Fig. 4.* The curves marked with the sign △ represent the single-phase flow, the curves with ○ the two-phase flow in all the Figures. The single phase curve represents the experimental data with the same feed as the feed of the continuous phase in the two-phase flow *(see Table 1).*

The effect of the ratio of the dispersed phase to the total feed (φ) on the axial dispersion coefficient (D_{ax}) is shown in *Fig. 5.*

The effects of Re_C and φ respectively, on the equivalent number of reactors in series (n_e) are shown in *Fig. 6* and *7.*

The effects of Re_C and φ, respectively on the mean residence time of the continuous phase ($\bar{t}_C$) are shown in *Fig. 8* and *9.*

The mean residence times of the dispersed phase ($\bar{t}_D$) estimated from Eq. (3) are plotted against the Re_C and φ, respectively, in *Fig. 10* and *11.*

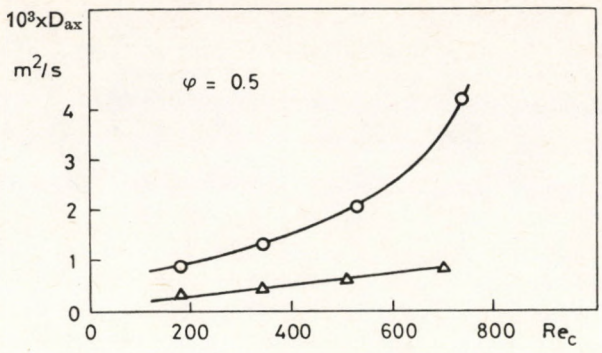

Fig. 4
D_{ax} as a function of Re_C at constant φ ratio

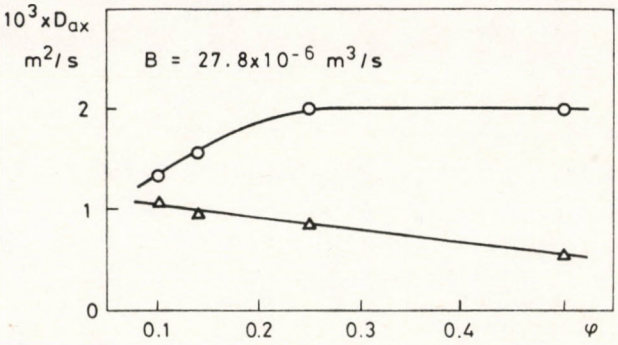

Fig. 5
D_{ax} as a function of the φ ratio at constant total feed

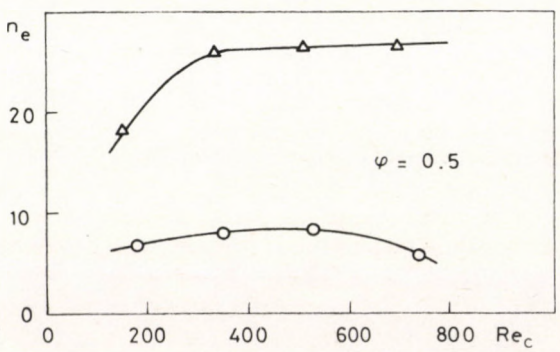

Fig. 6
n_e as a function of Re_C at constant φ ratio

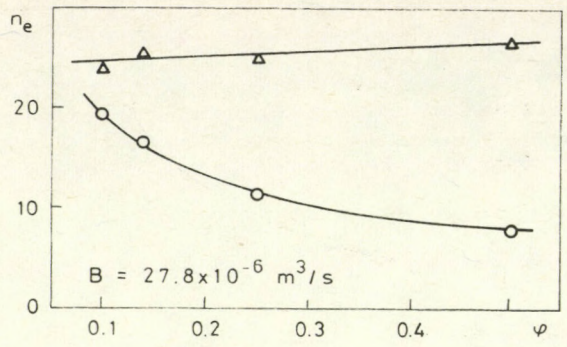

Fig. 7
n_e as a function of the φ ratio at constant total feed

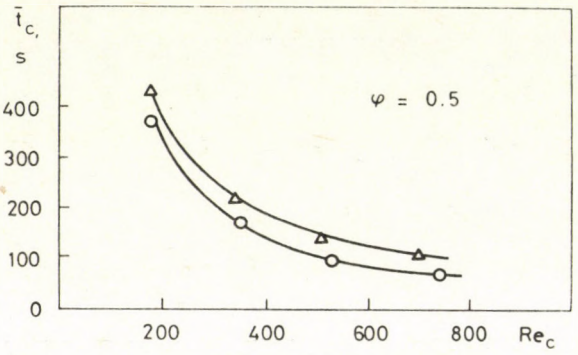

Fig. 8
Mean residence time of the continuous phase as a function of Re_C at constant φ ratio

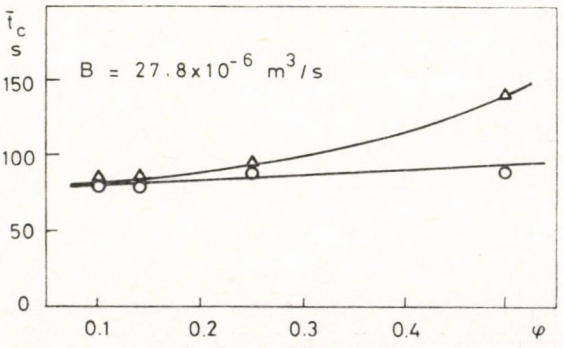

Fig. 9
Mean residence time of the continuous phase as a function of the φ ratio at constant total feed

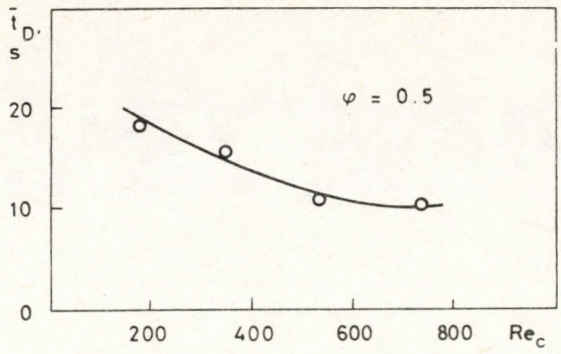

Fig. 10
Mean residence time of the dispersed phase as a function of Re_C at constant φ ratio

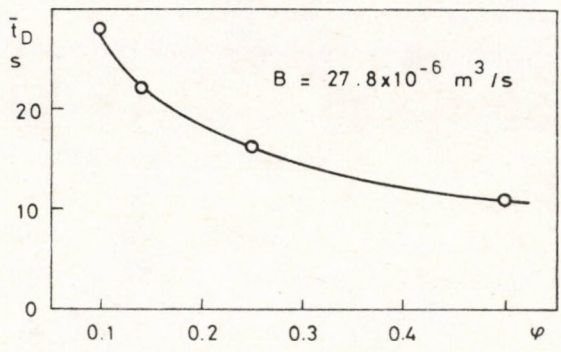

Fig. 11
Mean residence time of the dispersed phase as a function of the φ ratio at constant total feed

Conclusions

The axial dispersion coefficient in two-phase flow is higher than in single-phase flow and increases faster with the increasing REYNOLDS number *(Fig. 4)*.

Accordingly, the equivalent number of reactors in series in two-phase flow is much lower than in single-phase flow and shows very small dependency on the REYNOLDS number *(Fig. 6)*.

In the case of a high φ ratio, the axial dispersion coefficient is much higher in two-phase flow than in the adequate single-phase flow. For low φ ratio, nearly the same values appear *(Fig.5)*.

Accordingly, the equivalent number of reactors in series in two-phase flow is much lower than in the adequate single-phase flow. With decreasing φ, it increases significantly *(Fig. 7)*.

The estimated mean residence time of the dispersed phase decreases, of course, with increasing REYNOLDS number *(Fig. 10)*. It is remarkable that at constant total feeds, it decreases significantly with the increasing φ ratio *(Fig. 11)*.

SYMBOLS

A mean cross-section of flow, m^2
B total feed, m^3/s
B_C feed of continuous phase, m^3/s
B_D feed of dispersed phase, m^3/s
Bo Bodenstein number, dimensionless
C normalized concentration, dimensionless
D_{ax} axial dispersion coefficent, m^2/s
d_t inner diameter of reactor, m
L mean flow path in the reactor, m
n_e equivalent number of reactors in series, dimensionless
Re_C Reynolds number of continuous phase, dimensionless
$\bar{t}_C$ mean residence time of continuous phase, s
$\bar{t}_D$ mean residence time of dispersed phase, s
v_C real velocity of continuous phase, m/s
v_D real velocity of dispersed phase, m/s
ε hold-up of dispersed phase, dimensionless
Θ normalized time, dimensionless
σ^2 second central moment, dimensionless
φ ratio of the dispersed phase to the total feed, B_D/B, dimensionless

REFERENCES

1. ARANYI, A.: Dissertation. Veszprém Univ. of Chem. Engng., Veszprém 1983.
2. LEVENSPIEL, O.: Chemical Reaction Engineering. John Wiley and Sons. Inc., New York–London 1965.

РЕЗЮМЕ

Авторы изучали распределение времени пребывания в двухфазном реакторе оснащенного с отражательными перегородками, в котором дисперсной фазой является *i*-амилацетат, а основной фазой раствор концентрацией 0.1 моль/л NaOH (непрерывеая фаза). Для расчёта среднего времени пребывания, эквивалентного числа реакторов подключенных в ряд и коэффициентов осевой дисперсии использовали известные методы. С целью сопоставления данных проводили эксперименты и в однофазной системе.

HUNGARIAN JOURNAL
OF INDUSTRIAL CHEMISTRY
VESZPRÉM
Vol. 13. pp. 47–67 (1985)

ON THE DETERMINATION OF THERMOSTATIC EQUATIONS OF STATE. II.

GY. FÁY and R. TŐRÖS

(Research Institute for Technical Chemistry of the Hungarian Academy of Sciences, Veszprém, Hungary)

Received: August 8, 1984.

The present paper shows the determination of equations of state of homogeneous thermodynamic systems with two degrees of freedom with help of thermodynamical characteristics. In previous papers [1], [2] the interdependence of characteristic quantities were shown. Part I of the present paper [3] consists of simplified cases where the accidental choice of variables made the equations easy to solve. The present paper reduces the determination of the equations of state to the integration of the stability matrix of the internal energy function of the system and discusses the criteria of existence of solution.

Introduction

There are different methods to determine the equation of state [4, 5, 6]. The present paper defines a list of characteristic quantities and shows the general method of determining the equations of state from them.

Let us consider the following eight thermodynamic characteristic quantities:

$$c_p = T\left(\frac{\partial S}{\partial T}\right)_p \quad \text{isobar} \qquad \left.\begin{matrix}\\ \\ \\ \\ \end{matrix}\right\} \text{specific heat} \qquad (1)$$

$$c_v = T\left(\frac{\partial S}{\partial T}\right)_v \quad \text{isochore} \qquad (2)$$

$$x_T = -\frac{1}{V}\left(\frac{\partial V}{\partial P}\right)_T \quad \text{isoterm} \qquad \left.\begin{matrix}\\ \\ \\ \\ \end{matrix}\right\} \text{compressibility factor} \qquad (3)$$

$$x_S = -\frac{1}{V}\left(\frac{\partial V}{\partial P}\right)_S \quad \text{adiabatic} \qquad (4)$$

$$\beta_v = \frac{1}{P}\left(\frac{\partial P}{\partial T}\right)_v \quad \text{isochore} \qquad \left.\begin{matrix}\\ \\ \\ \\ \end{matrix}\right\} \begin{matrix}\text{coefficient of} \\ \text{pressure variation} \\ \text{with temperature}\end{matrix} \qquad (5)$$

$$\beta_S = \frac{1}{P}\left(\frac{\partial P}{\partial T}\right)_S \quad \text{adiabatic} \qquad (6)$$

$$\alpha_P = \frac{1}{V}\left(\frac{\partial V}{\partial T}\right)_P \quad \text{isobar} \qquad (7)$$

$$\alpha_S = -\frac{1}{V}\left(\frac{\partial V}{\partial T}\right)_S \quad \text{adiabatic} \qquad (8)$$

} coefficient of thermal expansion

There are more quantities often measured [7]–[12], the connections of (1)–(8) with them are listed below:

$$z = \frac{PV}{RT} \qquad x_T = \frac{1}{P} - \left(\frac{\partial \ln z}{\partial P}\right)_T \qquad (9)$$

$$\mu_S = \left(\frac{\partial T}{\partial P}\right)_S \qquad \beta_S = \frac{1}{P\mu_S} \qquad (10)$$

$$l_T = T\left(\frac{\partial S}{\partial V}\right)_T \qquad \beta_V = \frac{l_T}{PT} \qquad (11)$$

$$\gamma = \frac{1}{P_0}\left(\frac{\partial P}{\partial T}\right)_V \qquad \beta_V = \frac{P_0}{P}\gamma \qquad (12)$$

$$\sigma = \frac{1}{P_0}\left(\frac{\partial T}{\partial P}\right)_V \qquad \beta_V = \frac{P_0}{P}\sigma \qquad (13)$$

$$\varepsilon = \frac{1}{V_0}\left(\frac{\partial V}{\partial P}\right)_T \qquad x_T = -\frac{V_0}{V}\varepsilon \qquad (14)$$

$$\alpha = \frac{1}{V_0}\left(\frac{\partial V}{\partial T}\right)_P \qquad \alpha_P = \frac{V_0}{V}\alpha \qquad (15)$$

$$\mu = \frac{T\left(\frac{\partial V}{\partial T}\right)_P - V}{c_p} \qquad \alpha_P = \frac{\mu c_p + V}{TV} \qquad (16)$$

(10) is often called the differential Joule–Thomson coefficient [12]. The determination of the reduction of (1)–(8) from (9)–(16) seems to be very simple, so our efforts were restricted to determining the equations of state from three quantities arbitrarily chosen from (1)–(8).

I.
Determination of Stability Matrix and Interdependence of Characteristics

Let us consider a homogeneous thermodynamic system with two degrees of freedom. The caloric equation of state is denoted:

$$E(S, V) \qquad (17)$$

On the base of the second law of thermodynamics:

$$\left(\frac{\partial E}{\partial S}\right)_V = T; \qquad \left(\frac{\partial E}{\partial V}\right)_S = -P \tag{18}$$

the matrix consisting of second derivatives is called the stability matrix and its elements are denoted by the symbols of irreversible thermodynamics i.e. g_{ik}; $i, k = 1, 2$

$$\begin{pmatrix} g_{11} & g_{12} \\ g_{21} & g_{22} \end{pmatrix} = \begin{pmatrix} \left(\frac{\partial T}{\partial S}\right)_V & \left(\frac{\partial T}{\partial V}\right)_S \\ \left(\frac{\partial(-P)}{\partial S}\right)_V & \left(\frac{\partial(-P)}{\partial V}\right)_S \end{pmatrix} \tag{19}$$

and $g_{12} = g_{21}$ which is the simplified form of the Maxwell-relationship [13]:

All the calculations in this paper were reduced to the determination of (19) with the help of (1)–(8) characteristics.

It is easy to verify that the following formulas are valid:
Where $D = g_{11}g_{22} - g_{12}^2$ is the determinant of (19). The next step is to form inverse formulas of three chosen equations from the equations in Table 1.

Table 1.

Characteristics	Unit	Characteristics	Unit
$c_P = \frac{T}{D} g_{22}$	$\frac{J}{\text{molK}}$	$c_V = \frac{T}{g_{11}}$	$\frac{J}{\text{molK}}$
$\varkappa_T = \frac{1}{V} \frac{g_{11}}{D}$	$\frac{1}{\text{Pa}}$	$\varkappa_S = \frac{1}{V} \frac{1}{g_{22}}$	$\frac{1}{\text{Pa}}$
$\beta_V = -\frac{1}{P} \frac{g_{12}}{g_{11}}$	$\frac{1}{\text{K}}$	$\beta_S = -\frac{1}{P} \frac{g_{22}}{g_{12}}$	$\frac{1}{\text{K}}$
$\alpha_P = -\frac{1}{V} \frac{g_{12}}{D}$	$\frac{1}{\text{K}}$	$\alpha_S = -\frac{1}{V} \frac{1}{g_{11}}$	$\frac{1}{\text{K}}$

This is always possible with the exception of the following group of three characteristics:

$$c_p,\ \alpha_p,\ \beta_S$$
$$c_V,\ \alpha_S,\ \beta_V$$
$$\alpha_p,\ \beta_V,\ \varkappa_T$$
$$\alpha_S,\ \beta_S,\ \varkappa_S$$

It was shown [3] that the relationships:

$$c_p = PVT\alpha_p\beta_S$$
$$c_V = PVT\alpha_S\beta_V$$
$$\alpha_p = P\beta_V\varkappa_T$$
$$\alpha_S = P\beta_S\varkappa_S$$

do not make the inversions possible. In other cases, the inversion was carried out. The following scheme explains the formulas:

Table 2.

$$\begin{matrix} N_1 & N_2 \\ \begin{pmatrix} g_{11} & g_{12} \\ g_{21} & g_{22} \end{pmatrix} \\ N_3 & N_4 \end{matrix} \tag{20}$$

The numbers $(N_1 \ldots N_4)$ show the list number between those matrices, where the comparison was carried out to control the validity of the calculation with results in [1], [2]. All the matrices are equal to each other, thus if those matrices are equalised where only one characteristic is different (for example in 1 and 3) then the interdependence of these characteristics may be obtained. These formulas were calculated by us [1], [2] another way too, therefore these verifications seem to be convincing beside the necessary (but not sufficient) analysis of the dimensions. The following list shows the matrices. *(Table 3.)*

Table 3.

1. $$g_{ik}(c_p, c_v, \alpha_p) = \begin{pmatrix} & 5 \\ \frac{T}{c_v}; & \frac{1}{\alpha_p V}\left(\frac{c_v - c_p}{c_v}\right) \\ \frac{1}{\alpha_p V}\left(\frac{c_v - c_p}{c_v}\right); & \frac{c_p}{\alpha_p^2 V^2 T}\left(\frac{c_p - c_v}{c_v}\right) \\ 5 & 5 \end{pmatrix}$$

2. $$g_{ik}(c_p, c_v, \alpha_s) = \begin{pmatrix} & 12 \\ \frac{T}{c_v}; & -\frac{1}{V}\frac{1}{\alpha_s} \\ -\frac{1}{V}\frac{1}{\alpha_s}; & \frac{1}{TV^2\alpha_s^2}\frac{c_p c_v}{c_p - c_v} \\ 12 & 12 \end{pmatrix}$$

3. $$g_{ik}(c_p, c_v, \beta_v) = \begin{pmatrix} & 4 \\ \frac{T}{c_v}; & -p\beta_v\frac{T}{c_v} \\ -p\beta_v\frac{T}{c_v}; & \frac{T}{c_v^2}\beta_v^2 p^2\frac{c_p c_v}{c_p - c_v} \\ 2 & \end{pmatrix}$$

Table 3 (contiued),

4. $g_{ik}(c_p, c_v, \beta_s) = \begin{pmatrix} & 3 \\ \frac{T}{c_v}; & Tp\beta_s\left(\frac{1}{c_p}-\frac{1}{c_v}\right) \\ T_p\beta_s\left(\frac{1}{c_p}-\frac{1}{c_v}\right); & -\beta_s^2 p^2 T\left(\frac{1}{c_p}-\frac{1}{c_v}\right) \\ 3 & 3 \end{pmatrix}$

5. $g_{ik}(c_p, c_v, \varkappa_T) = \begin{pmatrix} & 1 \\ \frac{T}{c_v}; & -\sqrt{\frac{c_p-c_v}{c_v}\cdot\frac{T}{c_v\varkappa_T V}} \\ -\sqrt{\frac{c_p-c_v}{c_v}\cdot\frac{T}{c_v\varkappa_T V}}; & \frac{c_p}{c_v\varkappa_T V} \\ 1 & 1 \end{pmatrix}$

6. $g_{ik}(c_p, c_v, \varkappa_s) = \begin{pmatrix} & 5 \\ \frac{T}{c_v}; & -\sqrt{\left(\frac{1}{c_v}-\frac{1}{c_p}\right)\frac{T}{V\varkappa_s}} \\ -\sqrt{\left(\frac{1}{c_v}-\frac{1}{c_p}\right)\frac{T}{V\varkappa_s}}; & \frac{1}{V\varkappa_s} \\ 5 & 5 \end{pmatrix}$

7. $g_{ik}(c_p, \alpha_v, \alpha_s) = \begin{pmatrix} 6 & 6 \\ \frac{T}{c_p}\left(\frac{\alpha_s+\alpha_p}{\alpha_s}\right); & -\frac{1}{V\alpha_s} \\ -\frac{1}{V\alpha_s}; & \frac{c_p}{TV^2\alpha_p\alpha_s} \\ 6 & 6 \end{pmatrix}$

8. $g_{ik}(c_p, \alpha_p, \beta_v) = \begin{pmatrix} 1 & 1 \\ \frac{T}{c_p-\alpha_p\beta_v pVT}; & -p\beta_v\frac{T}{c_p-\alpha_p\beta_v pVT} \\ -p\beta_v\cdot\frac{T}{c_p-\alpha_p\beta_v pVT}; & \frac{p\beta_v}{\alpha_p V}\cdot\frac{c_p}{c_p-\alpha_p\beta_v pVT} \\ 1 & 1 \end{pmatrix}$

Table 3 (contiued).

9. $g_{ik}(c_p, \alpha_p, \beta_s) =$ undefined $(c_p = pVT\alpha_p\beta_s)$

$$\begin{pmatrix} \frac{g_{12}^2}{g_{22}} + \frac{T}{c_p}; & -\frac{\alpha_p VT}{c_p} g_{22} \\ -\frac{\alpha_p VT}{c_p} g_{22}; & -p_s\beta g_{12} \end{pmatrix}$$

10. $g_{ik}(c_p, \alpha_p, \varkappa_T) =$

$$\begin{pmatrix} 1 & 1 \\ \frac{\varkappa_T}{\alpha_p} \quad \frac{1}{\frac{\varkappa_T c_p}{\alpha_p T} - \alpha_p V}; & \frac{1}{\alpha_p V - \frac{\varkappa_T c_p}{\alpha_p T}} \\ \frac{1}{\alpha_p V - \frac{\varkappa_T c_p}{\alpha_p T}}; & \frac{c_p}{TV\varkappa_T} \quad \frac{\varkappa_T}{\alpha_p} \quad \frac{1}{\frac{\varkappa_T c_p}{\alpha_p T} - \alpha_p V} \\ 1 & 1 \end{pmatrix}$$

11. $g_{ik}(c_p, \alpha_p, \varkappa_s) =$

$$\begin{pmatrix} 1 & 1 \\ \frac{T}{c_p}\left(1 + \frac{\alpha_p^2 TV}{c_p \varkappa_s}\right); & -\frac{\alpha_p T}{c_p \varkappa_s} \\ -\frac{\alpha_p T}{c_p \varkappa_s}; & \frac{1}{V\varkappa_s} \\ 1 & 1 \end{pmatrix}$$

12. $g_{ik}(c_p, \alpha_s, \beta_v) =$

$$\begin{pmatrix} 2 \quad 16 & 16 \\ \frac{1}{pV\alpha_s\beta_v}; & -\frac{1}{V\alpha_s} \\ -\frac{1}{V\alpha_s}; & \frac{pc_p\beta_v}{\alpha_s V} \cdot \frac{1}{c_p - pVT\alpha_s\beta_v} \\ & 2 \end{pmatrix}$$

13. $g_{ik}(c_p, \alpha_s, \beta_s) =$

$$\begin{pmatrix} 2 & 11 \\ \frac{T}{c_p} + \frac{1}{pV\alpha_s\beta_s}; & -\frac{1}{V\alpha_s} \\ -\frac{1}{V\alpha_s}; & \frac{p\beta_s}{V\alpha_s} \\ 11 & 14 \end{pmatrix}$$

Table 3 (contiued).

14. $g_{1k}(c_p, \alpha_s, \varkappa_T) = \begin{pmatrix} {\scriptstyle 12\ \ 13\ \ 15\ \ 17} & {\scriptstyle 11} \\ \dfrac{T}{2c_p}\left(1+\sqrt{1+4\dfrac{\varkappa_T c_p}{T\alpha_s^2 V}}\right); & -\dfrac{1}{V\alpha_s} \\ -\dfrac{1}{V\alpha_s}; & \dfrac{1}{2V\varkappa_T}\left(1+\sqrt{1+\dfrac{4\varkappa_T c_p}{T\alpha_s^2 V}}\right) \\ {\scriptstyle 11} & {\scriptstyle 13} \end{pmatrix}$

15. $g_{1k}(c_p, \alpha_s, \varkappa_s) = \begin{pmatrix} {\scriptstyle 14} & {\scriptstyle 11} \\ \dfrac{T}{c_p}+\dfrac{\varkappa_s}{V\alpha_s^2}; & -\dfrac{1}{V\alpha_s} \\ -\dfrac{1}{V\alpha_s}; & \dfrac{1}{V\varkappa_s} \\ {\scriptstyle 11} & {\scriptstyle 14} \end{pmatrix}$

16. $g_{1k}(c_p, \beta_v, \beta_s) = \begin{pmatrix} {\scriptstyle 4} & {\scriptstyle 4} \\ \dfrac{T\beta_s}{c_p(\beta_s-\beta_v)}; & -\dfrac{\beta_v\beta_s pT}{c_p(\beta_s-\beta_v)} \\ -\dfrac{\beta_v\beta_s pT}{c_v(\beta_s-\beta_v)}; & \dfrac{\beta_v\beta_s^2 p^2 T}{c_v(\beta_s-\beta_v)} \\ & {\scriptstyle 4} \end{pmatrix}$

17. $g_{1k}(c_p, \beta_v, \varkappa_T) = \begin{pmatrix} {\scriptstyle 19} & {\scriptstyle 19\ \ 12\ \ 18} \\ \dfrac{1}{\dfrac{c_p}{T}-V\varkappa_T(p\beta_v)^2}; & \dfrac{1}{\beta_v\varkappa_T pV-\dfrac{c_p}{pT\beta_v}} \\ {\scriptstyle 12\ \ 19} & {\scriptstyle 19} \\ \dfrac{1}{\beta_v\varkappa_T pV-\dfrac{c_p}{pT\beta_v}}; & \dfrac{1}{V\varkappa_T-\dfrac{T}{c_p}(pV\varkappa_T\beta_v)^2} \end{pmatrix}$

18. $g_{1k}(c_p, \beta_v, \varkappa_s) = \begin{pmatrix} {\scriptstyle 12\ \ 16} & \\ \dfrac{1}{2}\ \dfrac{1}{V\varkappa_s\beta_v^2 p^2}\left(1+\sqrt{1-\dfrac{4TV\varkappa_s\beta_v^2 p^2}{c_p}}\right); & g_{12}=g_{21} \\ -\dfrac{1}{2}\ \dfrac{1}{V\varkappa_s\beta_v p}\left(1+\sqrt{1-\dfrac{4TV\varkappa_s\beta_v^2 p^2}{c_p}}\right); & \dfrac{1}{V\varkappa_s} \end{pmatrix}$

Table 3 (contiued).

19. $g_{ik}(c_p, \beta_s, \varkappa_T) = \begin{pmatrix} 17 & 20 \\ \dfrac{TV\varkappa_T}{c_p\left(V\varkappa_T - \dfrac{c_p}{Pp^2\beta_s^2}\right)}; & \dfrac{-1}{p\beta_s V\varkappa_T - \dfrac{c_p}{pT\beta_s}} \\ \dfrac{-1}{p\beta_s V\varkappa_T - \dfrac{c_p}{Tp\beta_s}}; & \dfrac{1}{V\varkappa_T - \dfrac{c_p}{Tp^2\beta_s^2}} \\ 20 & 20 \end{pmatrix}$

20. $g_{ik}(c_p, \beta_s, \varkappa_s) = \begin{pmatrix} 21 & 19 \\ \dfrac{T}{c_p} + \dfrac{1}{V\varkappa_s(p\beta_s)^2}; & -\dfrac{1}{V\varkappa_s p\beta_s} \\ -\dfrac{1}{V\varkappa_s p\beta_s}; & \dfrac{1}{V\varkappa_s} \\ 21 & 19 \quad 12 \end{pmatrix}$

21. $g_{ik}(c_p, \varkappa_T, \varkappa_s) = \begin{pmatrix} 20 & 20 \\ \dfrac{\varkappa_T}{\varkappa_s}\dfrac{T}{c_p}; & -\sqrt{\dfrac{T}{c_p V\varkappa_s}\left(\dfrac{x_T - x_\varepsilon}{\varkappa_s}\right)} \\ -\sqrt{\dfrac{T}{c_p V\varkappa_s}\left(\dfrac{\varkappa_T - \varkappa_s}{\varkappa_s}\right)}; & \dfrac{1}{V\varkappa_s} \\ 20 & \end{pmatrix}$

22. $g_{ik}(v_v, \alpha_p, \alpha_s) = \begin{pmatrix} 1 & 1 \\ \dfrac{T}{c_v}; & -\dfrac{1}{V\alpha_s} \\ 1 & 1 \\ -\dfrac{1}{V\alpha_s}; & \dfrac{c_v}{TV^2\alpha_s}\left(\dfrac{1}{\alpha_s} + \dfrac{1}{\alpha_p}\right) \end{pmatrix}$

23. $g_{ik}(c_v, \alpha_p, \beta_v) = \begin{pmatrix} 1 & 1 \\ \dfrac{T}{c_v}; & -\dfrac{p\beta_v T}{c_v} \\ -\dfrac{p\beta_v T}{c_v}; & \dfrac{p\beta_v}{\alpha_p V} + \dfrac{p^2\beta_v^2 T}{c_v} \\ 1 & 1 \end{pmatrix}$

Table 3 (contiued).

24. $g_{ik}(c_v, \alpha_p, \beta_s) = \begin{pmatrix} \frac{T}{c_p}; & \frac{1}{V\alpha_p} - \frac{pT\beta_s}{c_v} \\ \frac{1}{V\alpha_p} - \frac{pT\beta_s}{c_v}; & \frac{Tp^2\beta_s^2}{c_v} - \frac{p\beta_s}{V\alpha_p} \\ & 1 \end{pmatrix}$

25. $g_{ik}(c_v, \alpha_p, \varkappa_T) = \begin{pmatrix} & 27 \\ \frac{T}{c_v}; & -\frac{\alpha pT}{\varkappa_T c_v} \\ -\frac{\alpha_p T}{\varkappa_T c_v}; & \frac{\alpha_p^2 T}{\varkappa_T^2 c_v} - \frac{1}{V\varkappa_T} \\ 27 & 24 \end{pmatrix}$

26. $g_{ik}(c_v, \alpha_p, \varkappa_s) = \begin{pmatrix} \frac{T}{c_v}; & \frac{1 - \sqrt{1 + \frac{4\alpha_p^2 VT}{c_v \varkappa_s}}}{2\alpha_p V} \\ \frac{1 - \sqrt{1 + \frac{4\alpha_p^2 VT}{c_v \varkappa_s}}}{2\alpha_p V}; & \frac{1}{V\varkappa_s} \\ 28 & 28 \end{pmatrix}$

27. $g_{ik}(c_v, \alpha_s, \beta_v) = (c_v = pVT\alpha_s\beta_v)$ undefined $\begin{pmatrix} \frac{T}{c_v}; & -\frac{1}{V\alpha_s} \\ -\frac{1}{V\alpha_s}; & g_{22} \end{pmatrix}$

28. $g_{ik}(c_v, \alpha_s, \beta_s) = \begin{pmatrix} 1 & 26 \\ \frac{T}{c_v}; & -\frac{1}{V\alpha_s} \\ -\frac{1}{V\alpha_s}; & \frac{p\beta_s}{\alpha_s V} \\ 26 & 26 \end{pmatrix}$

Table 3 (contiued).

29. $g_{ik}(c_v, \alpha_s, \varkappa_T) = \begin{pmatrix} & 28 & & 28 \\ & \frac{T}{c_v}; & & -\frac{1}{V\alpha_s} \\ & -\frac{1}{V\alpha_s}; & & \frac{1}{V\varkappa_T} + \frac{c_v}{TV^2\alpha_s^2} \\ & 28 & & 28 \end{pmatrix}$

30. $g_{ik}(c_v, \alpha_s, \varkappa_s) = \begin{pmatrix} & 29 & & 29 \\ & \frac{T}{c_v}; & & -\frac{1}{\alpha_s V} \\ & -\frac{1}{\alpha_s V}; & & \frac{1}{V\varkappa_s} \\ & 29 & & 29 \end{pmatrix}$

31. $g_{ik}(c_v, \beta_v, \beta_s) = \begin{pmatrix} & 26 & & 26 \\ & \frac{T}{c_v}; & & -\frac{p\beta_v T}{c_v} \\ & -\frac{p\beta_v T}{c_v}; & & \frac{p^2\beta_v\beta_s T}{c_v} \\ & 26 & & 26 \end{pmatrix}$

32. $g_{ik}(c_v, \beta_v, \varkappa_T) = \begin{pmatrix} & 31 & & 31 \\ & \frac{T}{c_v}; & & -\frac{p\beta_v T}{c_v} \\ & -\frac{p\beta_v T}{c_v}; & & \frac{1}{V\varkappa_T} + \frac{p^2\beta_v^2 T}{c_v} \\ & 31 & & 31 \end{pmatrix}$

33. $g_{ik}(c_v, \beta_v, \varkappa_s) - \begin{pmatrix} & 30 & & 30 \\ & \frac{T}{c_v}; & & -\frac{p\beta_v T}{c_v} \\ & -\frac{p\beta_v T}{c_v}; & & \frac{1}{V\varkappa_s} \\ & 30 & & 30 \end{pmatrix}$

Table 3 (contiued).

34. $$g_{ik}(c_v, \beta_s, \varkappa_T) = \begin{pmatrix} {}^{32} & {}^{32} \\ \frac{T}{c_v}; & -\frac{p\beta_s T}{2c_v}\left(1 \pm \sqrt{1-\frac{4c_v}{V\varkappa_T p^2\beta_s^2 T}}\right) \\ g_{21}=g_{12}; & \frac{p^2\beta_s^2 T}{2c_v}\left(1 \pm \sqrt{1-\frac{4c_v}{V\varkappa p^2\beta_s^2 T}}\right) \\ {}_{32} & {}_{32} \end{pmatrix}$$

35. $$g_{ik}(c_v, \beta_s, \varkappa_s) = \begin{pmatrix} {}^{33} & {}^{33} \\ \frac{T}{c_v}; & -\frac{1}{p\beta_s V\varkappa_s} \\ -\frac{1}{p\beta_s V\varkappa_s}; & \frac{1}{V\varkappa_s} \\ {}_{33} & {}_{33} \end{pmatrix}$$

36. $$g_{ik}(c_v, \varkappa_T, \varkappa_s) = \begin{pmatrix} {}^{35} & {}^{35} \\ \frac{T}{c_v}; & \sqrt{\frac{T}{Vc_v}\left(\frac{1}{\varkappa_s}-\frac{1}{\varkappa_T}\right)} \\ \sqrt{\frac{T}{Vc_v}\left(\frac{1}{\varkappa_s}-\frac{1}{\varkappa_T}\right)}; & \frac{1}{V\varkappa_s} \\ {}_{35} & {}_{35} \end{pmatrix}$$

37. $$g_{ik}(\alpha_p, \alpha_s, \beta_v) = \begin{pmatrix} {}^{12} & {}^{12} \\ \frac{1}{V\alpha_s p\beta_v}; & -\frac{1}{V\alpha_s} \\ -\frac{1}{V\alpha_s}; & \frac{p\beta_v}{V}\left(\frac{1}{\alpha_p}+\frac{1}{\alpha_s}\right) \\ {}_{12} & {}_{12} \end{pmatrix}$$

38. $$g_{ik}(\alpha_p, \alpha_s, \beta_s) = \begin{pmatrix} {}^{37} & {}^{37} \\ \frac{1}{pV\beta_s}\left(\frac{1}{\alpha_s}+\frac{1}{\alpha_p}\right); & -\frac{1}{V\alpha_s} \\ -\frac{1}{V\alpha_s}; & \frac{p\beta_s}{V\alpha_s} \\ {}_{37} & {}_{37} \end{pmatrix}$$

Table 3 (contiued).

39. $g_{1k}(\alpha_p, \alpha_s, \varkappa_T) = \begin{pmatrix} 38 & 38 \\ \frac{\varkappa_T}{V\alpha_s\alpha_p}; & -\frac{1}{V\alpha_s} \\ -\frac{1}{V\alpha_s}; & \frac{\alpha_p}{V\varkappa_T}\left(\frac{1}{\alpha_p}+\frac{1}{\alpha_s}\right) \\ 38 & 38 \end{pmatrix}$

40. $g_{1k}(\alpha_p, \alpha_s, \varkappa_s) = \begin{pmatrix} 39 & 39 \\ \frac{\varkappa_s}{V\alpha_s}\left(\frac{1}{\alpha_s}+\frac{1}{\alpha_p}\right); & -\frac{1}{V\alpha_s} \\ -\frac{1}{V\alpha_s}; & \frac{1}{V\varkappa_s} \\ 39 & 39 \end{pmatrix}$

41. $g_{1k}(\alpha_p, \beta_v, \beta_s) = \begin{pmatrix} 38 & 38 \\ -\frac{1}{pV\alpha_p(\beta_v-\beta_s)}; & -\frac{1}{V\alpha_p}\frac{\beta_v}{\beta_s-\beta_v} \\ -\frac{1}{V\alpha_p}\frac{\beta_v}{\beta_s-\beta_v}; & -\frac{p}{V\alpha_p}\frac{\beta_v\beta_s}{\beta_v-\beta_s} \\ 38 & 38 \end{pmatrix}$

42. $g_{1k}(\alpha_p, \beta_v, \varkappa_T)$ undefined $= (\alpha_p = p\beta_v\varkappa_T) \begin{pmatrix} -\frac{1}{\beta_v p}\, g_{12}; & -\frac{\alpha_p}{\varkappa_T}\, g_{11} \\ g_{21} = g_{12}; & \frac{1}{V\varkappa_T} - \frac{\alpha_p^2}{\varkappa_T^2}\frac{g_{12}}{\beta_v p} \end{pmatrix}$

43. $g_{1k}(\alpha_p, \beta_v, \varkappa_s) = \begin{pmatrix} 41 & 41 \\ \frac{1}{V\beta_v p}\left(\frac{1}{\varkappa_s\beta_v p}-\frac{1}{\alpha_p}\right); & \frac{1}{V}\left(\frac{1}{\alpha_p}-\frac{1}{\varkappa_s\beta_v p}\right) \\ \frac{1}{V}\left(\frac{1}{\alpha_p}-\frac{1}{\varkappa_s\beta_v p}\right); & \frac{1}{V\varkappa^s} \\ & 41 \end{pmatrix}$

Table 3 (contiued).

44. $g_{ik}(\alpha_p, \beta_s, \varkappa)_T = \begin{pmatrix} 39 & 39 \\ \frac{\varkappa_T}{V\alpha_p}\left(\frac{1}{\varkappa_T\beta_s p-\alpha_p}\right); & -\frac{1}{V}\left(\frac{1}{\varkappa_T\beta_s p-\alpha_p}\right) \\ -\frac{1}{V}\frac{1}{\varkappa_T\beta_s p-\alpha_p}; & \frac{\beta_s p}{V}\left(\frac{1}{\varkappa_T\beta_s p-\alpha_p}\right) \\ 39 & 39 \end{pmatrix}$

45. $g_{ik}(\alpha_p, \beta_s, \varkappa_s) = \begin{pmatrix} 44 & 44 \\ \frac{1}{p^2\beta_s^2 V\varkappa_s}+\frac{1}{\alpha_p p\beta_s V}; & \frac{1}{p\beta_s V\varkappa_s} \\ -\frac{1}{p\beta_s V\varkappa_s}; & \frac{1}{V\varkappa_s} \\ 44 & 44 \end{pmatrix}$

46. $g_{ik}(\alpha_p, \varkappa_T, \varkappa_s) = \begin{pmatrix} 44 & 45 \\ \frac{1}{V}\left(\frac{1}{\varkappa_s}-\frac{1}{\varkappa_T}\right)\frac{\varkappa_T^2}{\alpha_p^2}; & -\frac{1}{V}\left(\frac{1}{\varkappa_s}-\frac{1}{\varkappa_T}\right)\frac{\varkappa_T}{\alpha_p} \\ -\frac{1}{V}\left(\frac{1}{\varkappa_s}-\frac{1}{\varkappa_T}\right)\frac{\varkappa_T}{\alpha_p}; & \frac{1}{V\varkappa_s} \\ 45 & \end{pmatrix}$

47. $g_{ik}(\alpha_s, \beta_v, \beta_s) = \begin{pmatrix} 37 & \\ \frac{1}{p\beta_p\alpha_s V}; & -\frac{1}{V\alpha_s} \\ -\frac{1}{V\alpha_s}; & \frac{p\beta_s}{\alpha_s V} \\ & 37 \end{pmatrix}$

48. $g_{ik}(\alpha_s, \beta_v, \varkappa_T) = \begin{pmatrix} 14 & \\ \frac{1}{p\beta_v\alpha_s V}; & -\frac{1}{V\alpha_s} \\ -\frac{1}{V\alpha_s}; & \frac{1}{V}\left(\frac{1}{\varkappa_T}+\frac{p\beta_v}{\alpha_s}\right) \\ 46 & 47 \end{pmatrix}$

Table 3 (contiued).

49. $g_{ik}(\alpha_s, \beta_v, \varkappa_s) = \begin{pmatrix} \overset{48}{\dfrac{1}{pV\beta_v\alpha_s}}; & \overset{48}{-\dfrac{1}{V\alpha_s}} \\ -\dfrac{1}{V\alpha_s}; & \dfrac{1}{V\varkappa_s} \\ 48 & 48 \end{pmatrix}$

50. $g_{ik}(\alpha_s, \beta^s, \varkappa_T) = \begin{pmatrix} \overset{49}{\dfrac{\varkappa_T}{(p\beta_s\varkappa_T - \alpha_s)V\alpha_s}}; & \overset{49}{-\dfrac{1}{V\alpha_s}} \\ -\dfrac{1}{V\alpha_s}; & \dfrac{p\beta_s}{\alpha_s V} \\ 49 & 49 \end{pmatrix}$

51. $g_{ik}(\alpha_s, \beta_s, \varkappa_s) =$ ($\alpha_s = p\beta_s\varkappa_s$) undefined $\begin{pmatrix} & \overset{48}{} \\ g_{11}; & -\dfrac{1}{V\alpha_s} \\ -\dfrac{1}{V\alpha_s}; & \dfrac{1}{V\varkappa_s} \\ 48 & \end{pmatrix}$

52. $g_{ik}(\alpha_s, \varkappa_s, \varkappa_T) = \begin{pmatrix} \overset{48}{\dfrac{\varkappa_T\varkappa_s}{(\varkappa_T - \varkappa_s)V\alpha_s^2}}; & \overset{48}{-\dfrac{1}{V\alpha_s}} \\ -\dfrac{1}{V\alpha_s}; & \dfrac{1}{V\varkappa_s} \\ 48 & 48 \end{pmatrix}$

53. $g_{ik}(\beta_v, \beta_s, \varkappa_T) = \begin{pmatrix} \overset{50}{\dfrac{1}{p^2V\varkappa_T\beta_p(\beta_s - \beta_v)}}; & \overset{52}{-\dfrac{1}{pV\varkappa_T(\beta_s - \beta_v)}} \\ -\dfrac{1}{pV\varkappa_T(\beta_s - \beta_v)}; & \dfrac{\beta_s}{V\varkappa_T(\beta_s - \beta_v)} \\ 52 & 50 \end{pmatrix}$

Table 3 (contiued).

54. $$g_{ik}(\beta_v, \beta_s, \varkappa_s) = \begin{pmatrix} 53 & 53 \\ \dfrac{1}{p^2\beta_s\beta_v V\varkappa_s}; & -\dfrac{1}{p\beta_s V\varkappa_s} \\ -\dfrac{1}{p\beta_s V\varkappa_s}; & \dfrac{1}{V\varkappa_s} \\ 53 & 53 \end{pmatrix}$$

55. $$g_{ik}(\beta_v, \varkappa_T, \varkappa_s) = \begin{pmatrix} 54 & 54 \\ \dfrac{1}{Vp^2\beta_v^2}\left(\dfrac{1}{\varkappa_s}-\dfrac{1}{\varkappa_T}\right); & -\dfrac{1}{p\beta_v V}\left(\dfrac{1}{\varkappa_s}-\dfrac{1}{\varkappa_T}\right) \\ -\dfrac{1}{p\beta_v V}\left(\dfrac{1}{\varkappa_s}-\dfrac{1}{\varkappa_T}\right); & \dfrac{1}{V\varkappa_s} \\ 54 & 54 \end{pmatrix}$$

56. $$g_{ik}(\beta_s, \varkappa_T, \varkappa_s) = \begin{pmatrix} 55 & 55 \\ \dfrac{1}{p^2 V\beta_s^2\varkappa_s}\cdot\dfrac{\varkappa_T}{\varkappa_T-\varkappa_s}; & -\dfrac{1}{p\beta_s V\varkappa_s} \\ -\dfrac{1}{p\beta_s V\varkappa_s}; & \dfrac{1}{V\varkappa_s} \\ 55 & 53 \end{pmatrix}$$

II.
Existence of Solubility of Equations of State

The g_{ik} $i, k = 1, 2$ matrix elements are given on the presented list. Now if the occurring characteristics are also given functions of state variables, then the determination of equations of state may be obtained by:

$$T(S, V) - T(S_0, V_0) = \int_{S_0}^{S} g_{11}\,\mathrm{d}S + \int_{V_0}^{V} g_{12}\,\mathrm{d}V$$

$$-(P(S, V) - P(S_0, V_0)) = \int_{S_0}^{S} g_{21}\,\mathrm{d}S + \int_{V_0}^{V} g_{22}\,\mathrm{d}V \qquad (21)$$

These formulas need some explanation, namely:

1. The integrals are line integrals so the method of integration must be prescribed or the independence must be ensured on the path, where the integration is carried out.
2. The integrals depend on the functions $T(S, V)$, $P(S, V)$ itself, thus the integral (21)–(22) form a system of integral equations.

Note 1. may be avoided in a simple way. Recalling that denoting $x_1 = S$; $x_2 = V$ then:

$$g_{ik} = \frac{\partial^2 E}{\partial x_i \, \partial x_k} \tag{22}$$

and the mathematical conditions of the independence of the integrals on the path of integration are:

$$\frac{\partial g_{11}}{\partial x_2} = \frac{\partial g_{12}}{\partial x_1} \tag{23}$$

$$\frac{\partial g_{21}}{\partial x_2} = \frac{\partial g_{22}}{\partial x_1} \tag{24}$$

or in a shorter form:

$$g_{iik} = g_{iki} \qquad i = k \neq 1, 2 \tag{25}$$

These equations will be called *three index symmetry* conditions. These requirements are neither superfluous nor useless, namely: the characteristics are measured and theoretical or empirical approximated functions of variables, therefore g_{it} must be regarded not only as definitions given (19) resp. (22), but functions built from variables of state on the one hand and from the characteristics on the other hand. Therefore, the validity of the equations (25) are not ensured principally. The formulas (25) are not useless, because if given three characteristics (1)–(8) denoting γ_1, γ_2, γ_3 then the requirement of equality: g_{iik} g_{iki} serve two functions between the variables of state, so these are equations of state as the purpose and result of the present work. These equations (25) usually state the same, by the reason that between the independent variables declared in (1)–(8) the entropy variable usually does not occur, therefore in the sufficient conditions (23), (24) the entropy variable does not occur explicitly. The equations (23), (24) are therefore two required equations for the state variables P, V, T and must state either the same, or equation of state $\Phi(P,.V,T) = 0$ does not exist at all.

It seems to be a very advantageous circumstance that the formulas (23), (24) can be handled because, when performing the prescriptions on the base of matrices from any of 1–56, the derivatives in (23), (24) will again be simple linear functions of g_{ik} quantities and the necessary requirement can be controlled in a simple way:

Regarded the matrices 1–56 generally in all elements they must be regarded as functions of characteristics γ_1, γ_2, γ_3 and of the state variables, S, V and of state functions $P(S, V)$, $T(S, V)$, so that:

$$g_{ik} = g_{ik}(\gamma_1, \gamma_2, \gamma_3, T(S, V), P(S, V), S, V) \qquad i, k = 1, 2 \tag{26}$$

Expanding the derivatives (23) and (24):

$$\left(\frac{\partial g_{11}}{\partial x_2}\right)_{x_1} = \sum_{j=1}^{3} \left(\frac{\partial g_{11}}{\partial \gamma_j}\right)_{T,P} \left(\frac{\partial \gamma_j}{\partial x_2}\right)_{x_1} + \left(\frac{\partial g_{11}}{\partial T}\right)_{\gamma,P} \left(\frac{\partial T}{\partial x_2}\right)_{x_1} +$$

$$+ \left(\frac{\partial g_{11}}{\partial P}\right)_{\gamma,T} \left(\frac{\partial P}{\partial x_2}\right)_{x_1} + \left(\frac{\partial g_{11}}{\partial x_2}\right)_{\gamma,T,P} \tag{27}$$

$$\left(\frac{\partial g_{12}}{\partial x_1}\right)_{x_2} = \sum_{j=1}^{3} \left(\frac{\partial g_{12}}{\partial \gamma_j}\right)_{P,T} \left(\frac{\partial \gamma_j}{\partial x_1}\right)_{x_2} \left(\frac{\partial g_{12}}{\partial T}\right)_{\gamma,P} \left(\frac{\partial T}{\partial x_1}\right)_{x_2} +$$

$$+ \left(\frac{\partial g_{12}}{\partial P}\right)_{\gamma,T} \left(\frac{\partial P}{\partial x_1}\right)_{x_2} + \left(\frac{\partial g_{12}}{\partial x_1}\right)_{\varphi,T,P} \tag{28}$$

discussing the right hand sides of (27) and (28) it can be seen that all the quantities in the bracket are given if γ_i $i=1, 2, 3$ are given, while the other derivatives are equal to quantities:

$$\left(\frac{\partial T}{\partial x_1}\right)_{x_2} = g_{11} \qquad \left(\frac{\partial T}{\partial x_2}\right)_{x_1} = g_{12}$$

$$\left(\frac{\partial P}{\partial x_1}\right)_{x_2} = -g_{12} \qquad \left(\frac{\partial T}{\partial x_2}\right)_{x_1} = -g_{22} \tag{29}$$

Consider the quantities $\dfrac{\partial \gamma_j}{\partial x_i}$ in details:

$$\left(\frac{\partial \gamma_j}{\partial x_i}\right)_{x_k} = \left(\frac{\partial \gamma_j}{\partial T}\right)_{P,x_k} \left(\frac{\partial T}{\partial x_i}\right)_{x_k} + \left(\frac{\partial \gamma_j}{\partial P}\right)_{T,x_k} \left(\frac{\partial P}{\partial x_i}\right)_{x_k} + \left(\frac{\partial \gamma_j}{\partial x_i}\right)_{P,T,x_k} =$$

$$= \left(\frac{\partial \gamma_j}{\partial T}\right)_{P,x_k} g_{11} + \left(\frac{\partial \gamma_j}{\partial P}\right)_{T,x_k} g_{21} + \left(\frac{\partial \gamma_j}{\partial x_i}\right)_{P,T,x_k} \tag{30}$$

$$j=1, 2, 3; \qquad i=1, 2; \qquad k \neq i = 1, 2$$

Substituting (29) and (30) into (28) the equations (without preliminary knowledge of the dependence T and P on S and V variables) give two equations between state functions $T(S, V)$, $P(S, V)$ and the declared state variables S, V. This statement was mentioned earlier and was proved by the discussion of the equations (26)–(30).

Using this fact for further calculations [and this is the point, where the equation of state in the form of (25) cannot be used explicitly] the second equation of state can be obtained from any of (21), (22) written either in the form of integral equation:

$$T(S, V) - T(S_0, V_0) = \int_{S_0}^{S} \tilde{g}_{11}(T(S, V), P(V, T), S, V)\, \mathrm{d}S +$$

$$+ \int_{V_0}^{V} \tilde{g}_{12}(T(S, V), P(V, T), S, V)\, \mathrm{d}V \tag{31}$$

The symbol $\sim$ means that the form of function g_{ik} changed because the dependence of γ_i characteristics were taken into account written $\tilde{g}$ instead of g, moreover $P(V, T)$ is known by preparing (or numerating) of (25) i.e. (27)–(30). Taking into account the form of (31) $P(V, T)$ is again a known quantity in it and this fact can be expressed with the shorter symbol of $\bar{g}_{11}$ $\bar{g}_{12}$

$$T(S, V) - T(S_0, V_0) = \int_{S_0}^{S} \bar{g}_{11}(T(S, V), S, V)\, \mathrm{d}S + \int_{V_0}^{V} \bar{g}_{12}(T(S, V), S, V)\, \mathrm{d}V \tag{32}$$

It is not necessary to solve the second equation concerning $P(S, V)$ in equations (21), because the (27)–(28) determine the relationship. For further simplification it is necessary to determine a standard state where the entropy is regarded to be zero, and at the same time do determine V_0 as known by practical reasons, namely either the minimal volume where experiments were carried out, or the minimal estimated value, which is large related to molecular dimensions. One cannot state that $V_0 = 0$ because the thermocynamical statements very seldom consider states with volume zero.

The equation (32) may be written either in the form of integral equation and $T(S_0, V_0) = T_0$ must be given:

$$T - T_0 = \int_{S_0}^{S} \bar{g}_{11}(T, S, V)\, dS + \int_{V_0}^{V} \bar{g}_{12}(T, S, V)\, dV \tag{33}$$

or in a form of system of differential equations:

$$\begin{aligned} \left(\frac{\partial T}{\partial S}\right)_V &= \bar{g}_{11}(T(S, V), S, V) \\ \left(\frac{\partial T}{\partial V}\right)_S &= \bar{g}_{12}(T(S, V), S, V) \end{aligned} \tag{34}$$

that is the type of system of partial differential equations mentioned as "Überstimmte differentialgleichung" [14].

The detailed method of solution, including the case, where two unknown functions are [e.g. our equations (21)], may be found in [15]. With the help of our three index symmetry condition equation (25) the system of equations may be reduced to differential equations consisting of only one (namely $T(S, V)$) unknown function.

III.
Application of Solution Method on a Well-Known Example

An example is presented, where the determination of equations of state can be easily demonstrated. Let three characteristics be given:

$$c_p = \text{const}; \qquad c_v = \text{const} \qquad \varkappa_T = \frac{1}{P} \tag{35}$$

the related g_{ik} matrix can be found on Table 3.1 on the list number 5:

$$g_{11} = \frac{T}{c_v}; \qquad g_{12} = -\sqrt{\frac{c_p - c_v}{c_v} \cdot \frac{T}{c_v \varkappa_T V}}; \qquad g_{22} = \frac{c_p}{c_v \varkappa_T V} \tag{36}$$

the three index symmetry condition of existence Eq. (25) and the related formulas (26)–(31) serve:

$$g_{112} = \frac{1}{c_v}\left(\frac{\partial T}{\partial V}\right)_S = \frac{1}{c_v} g_{12} \tag{37}$$

$$g_{121}=\frac{\partial}{\partial S}\left(-\sqrt{\frac{c_p-c_v}{c_v^2}\cdot\frac{PT}{V}}\right)=-\sqrt{\frac{c_p-c_v}{c_v^2V}}\cdot\frac{\partial}{\partial S}\sqrt{PT}-\sqrt{\frac{c_p-c_v}{c_v^2V}}\left(\frac{1}{2\sqrt{PT}}\left(T(-g_{12})+Pg_{11}\right)\right)$$

$$\frac{1}{c_v}g_{12}=-\sqrt{\frac{c_p-c_v}{c_v^2}}\frac{1}{2\sqrt{PVT}}\left(T(-g_{12})+Pg_{11}\right) \tag{38}$$

Regarded (36):

$$\frac{1}{c_v}\sqrt{\frac{c_p-c_v}{c_v^2}}\sqrt{\frac{PT}{V}}=\sqrt{\frac{c_p-c_v}{c_v^2}}\frac{1}{2}\frac{1}{\sqrt{PVT}}\left[-g_{12}T+Pg_{11}\right]$$

$$\frac{1}{c_v}PT=\frac{1}{2}\left[-T\sqrt{\frac{c_p-c_v}{c_v^2}\frac{PT}{V}}+\frac{PT}{c_v}\right] \tag{39}$$

and:

$$P=-\sqrt{(c_p-c_v)\frac{PT}{V}};\quad PV=(c_p-c_v)T \tag{40}$$

this is the equation of state for perfect gases. Trying to fulfil the condition:

$$g_{212}=g_{221} \tag{41}$$

$$\frac{\partial}{\partial V}\sqrt{\frac{c_p-c_v}{c_v^2}\frac{PT}{V}}=\frac{\partial}{\partial S}\frac{c_pP}{c_vV}$$

$$-\sqrt{\frac{c_p-c_v}{c_v^2}}\frac{1}{2}\sqrt{\frac{V}{PT}}\left(VP\left(\frac{\partial T}{\partial V}\right)_S+VT\left(\frac{\partial P}{\partial V}\right)_S-PT\right)=V\frac{c_p}{c_v}\left(\frac{\partial P}{\partial S}\right)_V \tag{42}$$

Regarded (36):

$$-\sqrt{\frac{c_p-c_v}{c_v^2}}\frac{1}{2}\sqrt{\frac{V}{PT}}\left(VP\frac{T}{c_v}+VT\left(-\frac{c_pP}{c_vV}\right)-PT\right)=-V\frac{c_p}{c_v}\sqrt{\frac{c_p-c_v}{c_v^2}}\sqrt{\frac{PT}{V}} \tag{43}$$

after abbreviations we gain:

$$\sqrt{(c_p-c_v)\frac{PV}{T}}=c_v-c_p;\qquad PV=(c_p-c_v)T \tag{44}$$

the equation agrees with (40).

Equation (40) may be subsituted into (33) to gain an integral equation for $T(S, V)$ of for (34) to get a system of differential equations to the only function $T(S, V)$. Really the mentioned type of differential equations "Überbestimmt" means that instead of the usual boundary condition that makes the problem unique and correct, here a second differential equation must be fulfilled and only one initial condition must be fulfilled, namely:

$$T(0, V_0)=T_0 \tag{45}$$

Because of the simple structure of (36) the form of differential equation seems to be fruitful:

$$\left(\frac{\partial T}{\partial V}\right)_S=\bar{g}_{12}=\sqrt{\frac{c_p-c_v}{c_v^2}\frac{PT}{V}}=\sqrt{\frac{(c_v-c_p)^2}{c_v^2}\frac{T^2}{V^2}} \tag{46}$$

$$\left(\frac{\partial T}{\partial V}\right)_S = \frac{c_p - c_v}{c_v} \cdot \frac{T}{V}; \qquad T(S,V) = T_0(S)\left(\frac{V}{V_0}\right)^{\frac{c_p - c_v}{c_v}} \tag{47}$$

Where $T_0(S)$ depends only on S. As mentioned above the boundary condition is not given, but Eq. (47) has another equation, namely:

$$\left(\frac{\partial T}{\partial S}\right)_V = \bar{g}_{11} \tag{48}$$

Substituting (36) and (47) we gain:

$$\frac{dT_0}{dS}\left(\frac{V}{V_0}\right)^{\frac{c_p - c_v}{c_v}} = \frac{1}{c_v} T_0(S)\left(\frac{V}{V_0}\right)^{\frac{c_p - c_v}{c_v}} \tag{49}$$

$$\ln \frac{T_0(S)}{T_0(0)} = \frac{S}{c_v} \tag{50}$$

and using (47) again:

$$S = c_v\left[\ln\left(TV^{1-\frac{c_p}{c_v}}\right) - \ln\left(T_0(0)V_0^{1-\frac{c_p}{c_v}}\right)\right] \tag{51}$$

that is exactly the entropy function of perfect gases.

SYMBOLS

c_p — isobar specific heat, $kJkmol^{-1}K^{-1}$
c_v — isochor specific, $kJkmol^{-1}K^{-1}$
D — determinant of stability matrix, $K^2Pa \cdot J^{-1}m^{-3}$
g_{12}, g_{21} — nondiagonal elements of stability matrix, $K \cdot Pa \cdot J^{-1}$
g_{11}, g_{22} — diagonal elements of stability matrix K^2J^{-1} and $Pa \cdot m^{-3}$
l_T — latent heat, $kJ \cdot m^{-3}$
N_1 — integer number $i = 1, 2, 3, 4$ $N_i = 1, 2, \ldots, 56$.
P — pressure, Pa
R — gas constant, $Pa \cdot m^3K^{-1}kmol^{-1}$
S — entropy, $kJK^{-1}kmol^{-1}$
T — temperature, K
V — volume, m^3
x_1, x_2 — extensive variables: entropy, volume
Z — compressibility, dimensionless

Greek symbols

α — coefficient of thermal expansion, K^{-1}
α_p — isobar coefficient of thermal expansion, K^{-1}
α_s — adiabatic coefficient of thermal expansion, K^{-1}
β_v — isochor coefficient of pressure variation with temperature, K^{-1}
β_s — isobar coefficient of pressure variation with temperature, K^{-1}
γ — coefficient of pressure variation with temperature, K^{-1}
ε — compressibility factor, Pa^{-1}
γ_1 — $i = 1, 2, 3$ characteristics
μ — Joule–Thomson coefficient, $m^3 \cdot Kmol \cdot K \cdot kJ^{-1}$
μ_S — see Equ. (10), $K \cdot Pa^{-1}$
σ — coefficient of pressure variation, K^{-1}
$\varkappa_S$ — adiabatic compressibility factor, Pa^{-1}
$\varkappa_T$ — isotherm compressibility factor, Pa^{-1}

Subscripts

i, j, k — integers
p, s, v, T — refer to the declared other variable.

REFERENCES

1. FÁY, G. and TŐRÖS, R.: Hung. J. Ind. Chem. *1981*, 9, 209–220.
2. FÁY, G. and TŐRÖS, R.: Hung. J. Ind. Chem. *1981*, 9, 221–232.
3. FÁY, G., FÜLÖP, J. and TŐRÖS, R.: Hung. J. Ind. Chem. *1983*, 11, 3–12.
4. REID, R. C. and SHERWOOD, T. K.: The Properties of Gases and Liquids, McGraw Hill Book Comp. N.Y.–San Francisco–Toronto–London–Sidney, *1966*.
5. Calculation of the Thermodynamic Characteristics of Gases and Liquids (in Hungarian), Műszaki Könyvkiadó Budapest, *1972*.
6. Energy Res. Abstr. *1983* (8/10), Data Library for Equations of State 77903 SESAME '83: Report on the Los Alamos Equations of State Library, Los Alamos National Laboratory, Los Alamos NM USA.
7. Vegyészmérnöki számítások termodinamika alapjai, Szerk.: SZOLCSÁNYI PÁL, Műszaki Könyvkiadó, Bp. *1975*., pp. 31., 43.
8. SILVER, R. S.: An Introduction to Thermodynamics, Cambridge, Univ. Press, pp. 80–82, 1971.
9. JÁVORSZKY, B. M. and DETLAF, A. A.: Fizikai zsebkönyv, Műszaki Könyvkiadó, Budapest, *1974*.
10. PERRY, J. H.: Chemical Engineers Handbook, McGraw-Hill Publ. Co Ltd. 1950, New York, Toronto, London.
11. FALTIN, H.: Műszaki Hőtan, Műszaki KK., Bp. p. 30 *1970*.
12. D'ANS-LAX: Taschenbuch für Chemiker und Physiker, Springer Verlag, Berlin, Heidelberg, New York, *1967* Band I.S.1390.
13. GYARMATI, I.: Bevezetés az irreverzibilis termodinamikába. Jegyzetellátó, Budapest, *1960*.
14. BIEBERBACH, L.: Einführung in die Theorie der Differentialgleichungen in Reellen Gebiet, Springer Verlag, Berlin, Göttingen, Heidelberg, *1956* S.237–279.
15. GOURSAT: Cours d'analyse mathematique IV. Ed. II. Gauthier-Villars, Paris, *1927*.

РЕЗЮМЕ

В работе представлена методика вычисления 2-ой степени свободы однородных термодинамических уравнений состояния с помощью термодинамических характеристик. В предыдущих наших работах [1, 2] были проведены вычисления зависимостей между термодинамическими величинами. Первая часть этой статьи [3] занимается вычислением более простых случаев термодинамищеских уравнений состаяния при специальном выборе переменных. В данной работе для вычисление ураенений состаяная использована матрикса 2-ой частной производной внутренней энергии. Далее дискутируется критерии экзистенции решений.

HUNGARIAN JOURNAL
OF INDUSTRIAL CHEMISTRY
VESZPRÉM
Vol. 13. pp. 69–79 (1985)

HEURISTIC PROCEDURES FOR STRUCTURAL ANALYSIS OF CHEMICAL INDUSTRIAL SYSTEMS. I.

HEURISTIC APPROACH FOR ANALYSIS OF TOPOLOGIC MODELS

J. Lazarov

(Central Laboratory of Chemical Engineering, Bulgarian Academy of Sciences, 1040 Sofia)

Received: August 10, 1984

In this paper an heuristically adequate declarative representation of three classes of topologic models of chemical industrial systems (CIS) – parametric flow, information and signal graphs, is discussed. The structural analysis of topologic models is considered as a decomposition problem, which is solvable by a heuristic reduction system. A general algorithm of heuristic procedures in production systems is given. The reduction system is represented by a set of heuristic production systems and determinate methods for the identification of the strongly connected components of digraphs, the identification of the cycles of cyclic digraphs, optimal decomposition of cyclic digraphs and for the synthesis of the optimal sequence of the units of CIS. The formal descriptions in the graph theory terms of the sets of operators for the transformation of heuristic states, of the sets of heuristics and of the criteria for terminating the search for each of the heuristic procedures are given. The computerized procedures show a high effectiveness.

1. Representation in Heuristic Systems

The structural analysis is the first phase of the realization of the decomposition approach for solving large-scale multi-connected problems for the simulation of the steady state operations of chemical industrial systems (CIS) [3, 4, 7, 9, 14]. CIS can be represented by flow sheets (parametric flow graphs) or information-topologic models (information and signal graphs, information bigraphs and information-flow multi-graphs) [3, 9]. Possibilities exist for the general representation of the models. For example, the structural analysis of signal graphs for the simulation of linear control systems of CIS includes the identification of simple cycles and paths of digraphs. The structural analysis of information graphs for the solving of the systems of equations is identical to the one of parametric flow graphs. In addition, an approach for structural analysis generalizing these three classes topologic models is described.

For the decomposition solution of a given problem, Z can be reduced to finding a set of alternative sets of subproblems Z_i, each of which gives a solution of the problem. After this a set of alternative sets of subproblems Z_{ij} of these subproblems Z_i is found and so on, until each of the subproblems becomes obviously solvable by a determinate or intuitive method, when one reaches the hierarchic level of the identical decomposition, at which level the subproblems are invariant ones [3, 10]. The alternation of the decomposition procedures requires the approach of the theory of an optimal computing process. This formulation shows that the basic stage of the structural analysis is the optimal decomposition of the problem [15] with a priori defined criteria of suboptimality-minimum of the number of total weight p_i of the tearing arcs of the flow graph [3, 4, 9, 12, 14, 16, 17, 19, 20].

The final purpose of the structural analysis of the basic class of models — parametric flow graphs, is finding an optimal computing sequence for the units of the design system [3, 9, 14], i.e. synthesis of an optimal algorithm for the simulation of the steady state operations of the system. This is a typical humanoid problem of the heuristic trend of the artificial intelligence theory [8, 10, 11] for the solution of which it is effective to apply the adequate heuristic search.

The general idea of heuristic methods requires an heuristically adequate representation of the search space. The specificity of the space defines the possibility for the development an heuristically effective strategy. The heuristic potential of the adequate representation of the a priori known information is a function of the following basic axioms [10, 11]: the effectiveness of the heuristic search is reciprocal to the cardinality of the search space; the quantity of the initial information and the effectiveness of its use depend proportionally on the number of the representation spaces. All this requires the recurrent discovering of the general relations, reformulation of the problem by generalizing and transformation of the macroelements to new representation spaces and the decomposition of the general topology of the space to the obvious, critical and forbidden areas. These instructions or ways which are used to increase the effectiveness of the search by defining the way and search direction are the so-called heuristics. In formal terms, the heuristic is a system of operators, which transform the intuitive theory into a mathematical one and it is oriented to the development of an heuristically effective search strategy [8, 11].

The heuristic strategy is a system of two mechanism [10]: for the generation of the elements, which are potential candidates for generation in the solving sequence (a syntactic component of the strategy), and for the control of the generation (a semantic component), called the generating procedure [11]. The generating procedure (type "breadth-first process" with dominating horizontal H-moves or "depth-first process" with dominating vertical V-moves over the H-moves) carries out a traversal of the recursive tree of the logical possibilities — an implicit or an explicit one [11, 10].

Formally the problem of the heuristic search in declarative representation is represented by the four (S, S_1, S_M, Q) where S is the set of situations, S_1— the set of initial situations, S_M — the set of final situations, and Q — the set of operators for transformation of the situations in the direct T or the inverse T^{-1} traversal of the tree [10, 11, 1]. The operators $\{Q\}$ are applicable in the definite area $S_Q \subseteq S$.

The situations in the production heuristic system are represented by the system of basic signs — N-states [10]. The purpose is the optimal sequence of Q-transformations $Q: s_x \in S_1 \to s_y \in S_M$. The search space is represented algorithmically in the form of a finite digraph $G=(P, V)$ with relations $W_1: S \to P$; $W_2: S_1 \to P_1$; $W_3: S_M \to P_M$. If $s_x \to p_x \in P_1$ and $s_y \to p_y \in P_M$ then the heuristic problem is reduced to the search of solving path $h_i = (\text{beg } p_x, \text{ end } p_y)$.

The space of the reduction P-states $P=(N_x \Leftrightarrow N_y)$ is represented algorithmically by a propositional "AND/OR"-graph $G_p=(P_p, Q_p)$ [10] where $W_4: Z_{ij} \to P_p$, and P_p are conjunctive "AND" of disjunctive "OR" nodes. The arcs Q_p correspond to the operators for decomposition of the problem Z. In the set P_p one can define the subsets of directly and iteratively solved nodes as well as the boundary ones [10]. According to definition the parametric flow graph is a propositional "AND"-graph in which the solving path $g=\{\{(\text{beg } p_{px}, \text{ end } p_{py})\}/\{p_{px}, p_{py} \in P_p, x, y \in \{1, 2, \ldots, K_p\}, K_p=|P_p|\}\}$ is searched. The "AND/OR"-graph is a parametric flow multigraph in which the partial subgraph is searched, because in the set of standard programmes for simulation of CIS different solving procedures may exist for computing the subproblem Z_{ij}.

On the basis of the above mentioned, an adequate heuristic realization of the formulated decomposition problem of the structural analysis is by a reduction system in which the states in the search space are represented by the set of subproblems that are solvable by determinate methods and/or set of production systems.

The basic heuristic in the reduction system for superpositional realization of the structural analysis is the formulation of the reduction representation as a process for decomposition of the problem for the search of the path g in the "AND"-graph to subproblems for the search of the solving subpaths g_i of the path g with next composition of g_i in a solving path g.

The reduction system reduces the initial heuristic problem to the equivalent set of subproblems $(S, S_1, \{S_M^1\}, Q)$, $(S, \{S_M^1\}, \{S_M^2\}, Q)$, $\ldots$, $(S, \{S_M^{n-1}\}, \{S_M^n\}, Q)$ for which a preliminary identification of the set of states $\{S_M^i\}$ is necessary [10]. For this purpose it is most convenient to identify the key operators $Q_K \subseteq Q_p$, i.e. the operators whose application is absolutely necessary for solving the problem. The key states S_K in the decomposition of the parametric flow graphs are a consequence from the formulation of the problem for structural analysis [3, 9, 14] and from the characteristic subsets of nodes of the propositional "AND"-graph [10]: $G<\{Q_K\}>\{G_i\}<\{Q_K\}>\{P\}$. The key operators (basic stages) in most of the known methods for structural analysis are the following: 1. Identification of the strongly connected components of finite digraphs; 2. Identification of the basic system of cycles of the cyclic digraphs; 3. Optimal decomposition of the cyclic digraphs; 4. Synthesis of the solving path of the propositional "AND"-graph. They are discussed in the same sequence later.

In this paper, the general algorithmization of the heuristic search in production systems is considered, as well as the formalization of the heuristic adequate representation of the search spaces, the set of heuristics and the set of operators for the transformation of the states. They are used when designing modular heuristic procedures of a programme system for the structural analysis of CIS.

2. Algoritmization of the Heuristic Procedures in Production Systems

The basic stage [10, 8] in the design of the heuristic procedures consists of the determination of the space of the N-states — the sets S, S_1, S_M and teh set of operators for the transformation of N-states, and the set of heuristics. Let us decompose the set of heuristics E to subsets of heuristics, which are applicable in E_1-initial states, E_M-final states, E_h-mediate states, and heuristics E_C of the criterion for the terminating of the search. This decomposition has essential significance [8] for the organization of the search of the heuristics.

The formal description of the heuristics is a complicate problem [8, 10] in the heuristic search algorithmization. This involves the problem of developing a heuristic procedure, which uses a library of heuristics. An idea for solving this problem is the application of the structure of the programme systems for the simulation of CIS [4, 9, 14], i.e. the heuristic procedures have to be of a variable or fixed structure. An heuristic procedure which uses a library of heuristics must have a fixed structure and must consist of the following parts: a supervisor and a library of standard heuristics. The supervisor carries out the heuristic strategy. Each procedure from the library is a logical model of one heuristic. The basic part of the supervisor is an organizing programme, which carries out the following operations: calls by identificator the procedure from the library, which realizes the certain heuristic; renames the formal heuristic to the actual one; synthesizes the conjunctive-disjunctive function of the set of heuristics. In connection with this the heuristics must be divided into conjunctive "AND" and disjunctive "OR" heuristics. The set of "AND"-heuristics requires the application of all the heuristics from the set, while the application of only one "OR"-heuristic from the set is sufficient. Here two problems arise: the optimal sequence for the application of "AND"-heuristics (an identical problem to structural analysis), and heuristic search of fuzzy "OR"-heuristics. The formal description of heuristics, bearing in mind the above mentioned, is to be realized as a logical test. The essence of this approach leads to the procedural representation of the heuristic search, whose basis is the declarative representation. Furtheron, we shall consider the declarative representation.

The operation of the heuristic strategy by generating procedures from the type "left-depth-first process" for uni-directional search (a basic cycle of the supervisor) is in general the following iterative sequence:

1. Forming the level $D=0$ of the implicit tree.
2. Heuristic test: $E_1(s_i)/s_i \in S_1$? No-stop. Yes-go to step 5.
3. Heuristic test of the current N-state: $E_h(s_i)/s_i \in h_j$? No-test: V-move — go to step 8; H-move — go to step 10. Yes-test: H-move — go to step 9; V-move-test: $D \neq 0$? No-go to step 5.
4. Heuristic test: $E_C(h_j)/h_j \Rightarrow M$? Yes-heuristic test: $E_C(D)/D=M$? Yes-go to step 6.
5. Left direct T–V-move; $D:=D+1$; go to step 3.
6. Heuristic test: $E_M(s_i)/s_i \in S_M$? No-go to step 8. Yes-write: $h_j=(s_0, s_1, \ldots, s_i)$.
7. Heuristic test: $E_C(j)/j=1$? Yes-stop.
8. H-move; go to step 10.
9. Test: $D=0$? Yes-go to step 1. No-test: T-move — go to step 6; T^{-1}-move — go to step 8.

10. Right inverse T^{-1}–V-move: $D:=D-1$. Test–V-move — go to step 9; H-move — go to step 5.

An explanation. One example of the heuristic test from step 3 is the following heuristic: a mediate N-state s_i can be only a potential candidate for generation in the solving sequence h_j. The test from step 7 is the satisfaction of the criterion for terminating the search after one solving path h is determined.

3. Identification of strongly connected components of digraphs

Literature abounds in methods and their modifications for the identification of strongly connected components of digraphs from which the most effective is considered to be [1] the recursive TARJAN's algorithm [18]. High efficiency have the algorithms [6, 9] as well. In this paper, corresponding to the declarative representation of the reduction system in p.1, for identification of strongly connected components of digraphs, a more effective determinate method [5] is developed. It is based on the analysis of the recurrent properties of the adjacency matrix $A=\|a_{ij}\|$ of a digraph with Hamilton's path. In the remaining cases an improved [5] modification of the classic matrix method [4] is developed. Both these methods are applied, because they generate heuristics for the heuristic procedures.

4. Identification of the basic system cycles of cyclic digraphs

There are many algorithms [1–4, 9, 14] for the identification of cycles and paths in digraphs, except heuristic. In the present paper in keeping with the general treatment plan, the uni-directional and bi-directional heuristic procedures in production systems are developed as follows.

The set of N-states is $S\to P$, $P\in G$, and the initial and the final states are $S_1=S_M\to\{p_j/P_j\in G_j \vee a_{jj}^m=\text{true}\}$. The operator for the transformation of the N-states is $Q=\{\{v_j\in V\}\&\{p_iR^-v_j\}\&p_i\&\{v_jR^+p_l\}\}$. The sets of heuristics are the following: $E_1=\{\text{beg }(\text{cir}_i\ G)=\text{end }(\text{cir}_i\ G)=p_j/a_{jj}^m=\text{true}\}$, $\{\text{cir}_i\ G_l\in G_j/G_i,\ l\neq j\}$, $\{\text{rank }(\text{cir}_i\ G=m \vee 2, 3, \ldots, |G_j|\}$; $E_C=\{I_D=|P_j|/\{p_j\in P_j,\ a_{jj}^m=\text{true}\} \vee \{P_j\in G_j\}\}$, $\{h_i\neq ah_j+bh_k\}$, $\{M_l=\text{rank }(\text{cir}_i\ G)\}$, $\{D_l^{\max}=M_l\}$; $E_M=E_1\&E_C$; $E_h=\{q(q(p_i))\notin Q\}$, $\{q\in Q:p_i\to p_j/i\neq j,\ \{p_i,\ p_l\}\in h_l\}$, $\{q\in Q:p_i\to p_j/\{p_i,\ p_j\}Rv,\ v\in(V-V_0)\}$, $\{q\in Q:p_i\to\to p_j/\{p_i, p_j\{Rv, v\in V_c, V_c\in(V-V_0)\}, \{q\in Q:p_i\to p_j/\{p_i, p_j\}Rv, v\in(V_c-V_n), V_n\subset V_c\}$.

The states $S_1=S_M$ are preliminary known, thus we can develop a bi-directional procedure by applying two uni-directional searches $S_1\to S_h$ and $S_M\to S_h$ in the direction T and T^{-1} respectively where S_h is an equidistant state with respect to S_1 and S_M.

The procedure is also identical for the determination of the path or all the paths $\{p_i\to p_j\}$ where $S_1\neq S_M$; an additional heuristic can, for example, be the selective application of the operator Q in respect to the status (weight, length, cost, capacity, etc.) of the arcs.

5. Heuristic optimal decomposition of the cyclic digraphs

In the structural analysis, the optimal decomposition is considered as a process of elimination of all the cycles $\{\text{cir}_i\, G\}$ in cyclic digraphs by means of tearing a given number of arcs $V_s \subset V$. Let us introduce the relationship $S_G \subset R(V)$ in the cyclic digraph $G=(P,\ V)$ having the property: $\forall\, V_s \in S_G \Rightarrow$ $\Rightarrow \{\text{cir}_i\, G\} = \emptyset / G_s = (P,\ V - V_s)$, and the relationship of equivalence in S_G EQ: $^1_s\forall\, V,\colon\ V^2_s \in S_G \Rightarrow V^1_s EQ\, V^2_s / W_5(V^1_s) = W_5(V^2_s)$ where the bijection W_5 is $W_5 : V \to$ $\to (V - V_s)/W_5^{-1}(0) = \emptyset \,\&\, W_5(V_s) = \cup\, W_5(v)/v \in V_s\}$. The factor-set S_G/EQ has the least number of elements $V_s : \inf S_G/EQ \to V^0_s \in S_G/W_5(V^0_s) \leq W_5(V_s) \Leftrightarrow \min\, W_5(V_s)$ because the following ordering relationship in the factor-set S_G/EQ exists: $\{V^1_s\} \leq \{V^2_s\} \Leftrightarrow \{\exists\, v^1_s \in V^1_s \,\&\, \exists\, v^2_s \in V^2_s\} \to W_5(V^1_s) \leqq W_5(V^2_s)\}$.

The methods for optimal decomposition can be divided into two groups: analytic (linear and dynamic programming [19]) and algorithmic (permutation in the matrix A, techniques for the simplification of graphs [12, 14, 16], and reduction of the cyclic matrix [15, 4, 9]), topologic oriented [15, 9] and non-oriented [4, 14] respectively. The treatment of the general problem for structural analysis of the classes topologic models of CIS requires the method of optimal decomposition to satisfy the conditions: $p_i \neq \text{idem}$ and $p_i = \text{idem}$ (characteristic case for information graphs); $|\{V_s\}| = 1$ and $|\{V_s\}| > 1$, and to be topologic oriented using the cyclic matrix; and the heuristic approach requires possibilities for heuristic representation. These requirements are satisfied by the LEE and RUDD's method [15] for combinatorial reduction of the cyclic matrix by a number of principles, which are heuristically presentable by declarative representation of the search.

Let $C = \|c_{ij}\|$ is formed in p.4 cyclic matrix of the digraph G. By Col$C$ we mark the set of columns and by Row$C$ — the set of rows. There are bijections $W_6 : \text{cir}_i\, G \to \text{row}_i\, C$, $W_7 : v_j \to \text{col}_j\, C$. If $\text{Col}_i\, C$ is the set of columns of the cycle $\text{cir}_i\, G$ and $\text{Row}_j\, C$ — the set of cycles which include the arc v_j, then for each row $\text{row}_i\, C$ we form the set which includes all columns $\text{col}_j\, C$ with non-zero elements in the row $\text{row}_i\, C$, i.e. $(\text{row}_i\, C)_j = \bigcup_j \text{col}_j C / c_{ij} = 1$. For each column $\text{col}_j\, C$ we form the set $(\text{col}_j\, C)_i = \bigcup_i \text{row}_i\, C / c_{ij} = 1$ which includes each row $\text{row}_i\, C$ with non-zero elements in the column $\text{col}_j\, C$.

The general scheme of the algorithms of LEE and RUDD's method is the following:

1. Test: $p_i = \text{idem}$? No-go to step 6.
2. Operation of the 1st algorithm.
3. Test: $\text{cir}_i\, G = \emptyset$? Yes-stop. No-go to step 5.
4. Operation of the 2nd algorithm.
5. Test: $p_i = \text{idem}$? Yes-go to step 4. No-go to step 7.
6. Operation of the 3rd algorithm. Go to step 3.
7. Operation of the 4th algorithm. Stop.

5.1. Dominance Principles

The introduced [15, 9, 3] dominance principles are heuristics for reducing the extended cyclic matrix, which includes the frequency f of the arcs and the rank r of the cycles. The formal description of the principles is the following:

Principle 1 (compression of the cyclic matrix):

$$C \Rightarrow \{C^*/V_s \not\subset (V - V_0)V_s \not\subset V_i, f_i = 0\}.$$

Principle 2 (dominance of a column over a row):

$$\mathrm{col}_j\, C < \mathrm{dom} > \mathrm{row}_i\, C \Rightarrow \{\{v_j \in V_s / v_j \in (\mathrm{row}_i\, C)_j\} < \mathrm{tear} > \mathrm{cir}_i\, G\}.$$

Principle 3 (dominance of a column over a set of rows):

$$\mathrm{col}_j\, C < \mathrm{dom} > \{\mathrm{row}_i\, C\} \Rightarrow \{\{v_j \in V_s / v_j \in \}(\mathrm{row}_i\, C)_j\}\} < \mathrm{tear} > \{\mathrm{cir}_i\, G\}.$$

Principle 4 (dominance of a column over a column):

$$\mathrm{col}_j\, C < \mathrm{dom} > \mathrm{col}_i\, C \Rightarrow \{\mathrm{col}_i\, C \overrightarrow{\subset\subset} \mathrm{col}_j\, C / f_j \geq f_i,\ (\mathrm{col}_j\, C)_m = (\mathrm{col}_i\, C)_n\}.$$

Principle 5 (strong dominance of a column over a column):

$$\mathrm{col}_j\, C < \mathrm{dom} > \mathrm{col}_i\, C \Rightarrow \{\mathrm{col}_i\, C \overrightarrow{\subset\subset} \mathrm{col}_j\, C / p_i \geq p_j,\ (\mathrm{col}_j\, C)_m = (\mathrm{col}_i\, C)_n\}.$$

Principle 6 (strong dominance of a set of columns over a column):

$$\{\mathrm{col}_j\, C\} < \mathrm{dom} > \mathrm{col}_i\, C \Rightarrow \mathrm{col}_i\, C \overrightarrow{\subset\subset} \{\mathrm{col}_j\, C / p_i \geq \sum_j p_j,\ f_i \cong f_j,\ \bigcup_m (\mathrm{col}_j\, C)_m = (\mathrm{col}_i\, C)_n\}.$$

Principle 7 (strong dominance of a set of columns over a set of columns):

$$\{\mathrm{col}_j\, C\} < \mathrm{dom} > \{\mathrm{col}_i\, C\} \Rightarrow \{\{\mathrm{col}_i\, C\} \overrightarrow{\subset\subset} \{\mathrm{col}_j\, C\} / \sum_i p_i =$$

$$= \sum_j p_j,\ \bigcup_m (\mathrm{col}_j\, C)_m = \bigcup_n (\mathrm{col}_i\, C)_n\}.$$

Principle 8 (dominance of a row over a row):

$$\mathrm{row}_j\, C < \mathrm{dom} > \mathrm{row}_i\, C \Rightarrow \{\mathrm{cir}_i\, G \overrightarrow{\subset\subset} \mathrm{cir}_j\, G / (\mathrm{row}_j\, C)_m \geq (\mathrm{row}_i\, C)_n\}.$$

Principle 9 (dominance of a set of rows over a row):

$$\{\mathrm{row}_i\, C\} < \mathrm{dom} > \mathrm{row}_j\, C \Rightarrow \{\mathrm{cir}_j\, G \overrightarrow{\subset\subset} \{\mathrm{cir}_i G\} / (\mathrm{row}_j C)_n \subset (\mathrm{row}_i\, C)_n\}.$$

Principle 10 (dominance of an essential column in tearing):

$$\mathrm{col}_j\, C < \mathrm{dom} > \mathrm{col}_i\, C \Rightarrow \{v_j \overrightarrow{\subset\subset} S_G / EQ / (\mathrm{row}_n\, C)_j = \mathrm{col}_j\, C,\ r_n = 1\} < \mathrm{tear} > \mathrm{cir}_n\, G.$$

Principle 11 (dominance of an essential set of columns in tearing):

$$\{\mathrm{col}_j\, C\} < \mathrm{dom} > \{\mathrm{col}_i\, C\} \Rightarrow \{\{\mathrm{col}_j\, C\} \overrightarrow{\subset\subset} \{v_j\} \in$$

$$\in S_G / EQ / \{\mathrm{cir}_n\, G\} \subseteq (\mathrm{row}_n\, C)_j\} < \mathrm{tear} > \{\mathrm{cir}_n\, G\}\}.$$

Principle 12 (dominance of a column in partitioning):

$$\mathrm{col}_j\, C < \mathrm{dom} > \mathrm{col}_i\, C \Rightarrow \{\mathrm{col}_k\, C,\ \mathrm{col}_1\, C\} / \cup \{\mathrm{col}_k\, C,\ \mathrm{col}_1\, C\} = \mathrm{col}_j\, C,\ \{\text{Principle 5}\},$$

$$\{\text{Principle 6}\},\ f_i \leq f_j,\ p_j \geq p_i\}.$$

The application of the following principles 1, 8, 9 and 4 or 5 does not influence the optimality of the solution and is carried out in the initial phase of the optimal decomposition. As a result of this application, an independent system of columns is determined.

5.2. 1st Algorithm

The 1st algorithm is a realization of the 10th principle, when the system of columns in the matrix C is an independent one. The arcs $v_j \in (\mathrm{row}_i\, C)_j$ with rank $r_i = 1$ are torn, after which the 2nd principle is applied.

5.3.2nd Algorithm

The 2nd algorithm is a realization of the 11th principle, if in the case of an independent system of the column, the requirements of the 10th principle are not satisfied. The combinatorial essence of the 11th principle is presented by heuristic production system.

The set of N-states is $S \to \{\mathrm{col}_j\, C^*\}$, the initial states are $S_1 \to \{\mathrm{col}_i\, C^*/n \leq \leq |\{\mathrm{col}_j\, C^*\}| - |\{\mathrm{col}_i\, C^*\}| + 1,\ v_n \in \{\mathrm{col}_i\, C^*\}$, the final states are generated by the mechanism for generation in the process of heuristic search. The recurrently applied operator for the transformation of the N-states over the set $\{\mathrm{col}_j C^*\}$ is in itself a generation of combinations without repeating C_N^K of the class $K = 2, N$ with elements $N = 1, |\{\mathrm{col}_j C^*\}|$. The set of heuristics is the following: $E_1 = \{\mathrm{col}_m C \in S_1/m \leq N - K + 1\}$; $E_M = \{\mathrm{col}_m C \in S_M/m \leq N\}$; $E_h = \{\mathrm{col}_m C \in S_i/m \leq \leq N - K + 1 + i\}$, $\{q \in Q : \{\mathrm{col}_i C, \mathrm{col}_j C\} \in h_l/i \neq j\}$, $\{q(q(\mathrm{col}_i C)) \in Q\}$; $E_C = \{I_D = N - - K + 1\}$, $\{D_I^{\max} = K - 1\}$, {Principle 11} $\to h_j\}$. The path h_j determines only one element of the set S_G/EQ. For the determination of all the elements the search continues to class N, separating the linear-inpedendent paths $\{h_1, h_2, \ldots, \in S_G/EQ/h_j \neq ah_i + bh_m\}$ which are the solutions.

5.4.3rd Algorithm

The tearing is more complicated when $p_i \neq$ idem and a set of independent non-essential columns exists. The 3rd algorithm combines the 1st and the 2nd ones in heuristic realization of the 6th principle in a production system. The heuristic representation of the 6th principle is identical to the description in p.5.3: the difference is only in the heuristic {Principle $6 \to h_j$}.

5.5.4th Algorithm

The 4th algorithm generalizes the 3rd algorithm by recursive realization of the 12th principle, that is why necessarity the heuristic representation falls away.

6. Synthesis of the solving path of the propositional "AND"-graph

There is no description of the heuristic algorithms for synthesis of the computing sequence of the units of CIS, when a tearing set of arcs exists. Further on an heuristic algorithm in declarative representation is considered.

The set of N-states is $S \to V$, $V \in G$, and the initial states are $S_1 \to \{V_0^+ \cup V_s, V_0^+ \subset V,\ V_s \subset V\}$, the final states are generated by the mechanism for generation of the elements in the process of the heuristic search. The superpositionally applied operator for the transformation of the N-states over the set $\{G_i\}$, which carries out the tests for triviality of G_j and for the solution of

the $p_i \in G_j$ is: $Q=\{p_i \Rightarrow p_{pi}/p_i \in G_j,\ |G_j|=1,\ \{p_i \Rightarrow p_{pi}/p_i R^+ v_j,\ (v_j \in V_0^+) \vee (v_j \in V_s) \vee \vee (v_j R^- p_m),\ p_m \in P_{pj}\},\ \{v_j \in V_s\}/\{v_j R^+ p_i,\ p_i \in G_j \Rightarrow g_j\}$. The sets of heuristics are the following: $E_1=E_M=\{v_i \in V_s\}, \{v_i \notin \bar{V_0}\}$; $E_C=\{I_D=|\{G_j\}|, \{M_I=|\{G_j\}|\}, \{D_I^{max}=M_I\}$, $\{g_i=|G_j|\},\ \{g=\sum_j g_j\},\ \{|g_j|=I_D\};\ E_h=\{q \in Q: v_i \to v_j/v_i,\ v_j \in V_j,\ P_j \cap (V_j - \bar{V_{0j}}) \neq \emptyset,$ $P_j,\ V_j \in G_j\},\ \{q(q(v_i)) \notin Q\},\ \{q \in Q: v_i \to v_l/\{v_i \& v_j R p_l \& v_i,\ v_j R p_m,\ p_l \in G_i, p_m \in G_{i+1}\}$, $\{q \in Q: v_i \to v_j/i \neq j,\ v_i,\ v_j \in g_l\},\ \{q \in Q: v_i \to v_j/v_i \notin (V_s \cup V_0^+ \cup (VR^+P_p),\ P_p \in g_j\}$.

7. Implementation of the Methods

On the basis of the suggested algorithms, the heuristic programme system for structural analysis of CIS, using the modular principles, is developed. The programme system is applied for proving the correctness and comparative analysis of the effectiveness of the algorithms over the set of examples from [3, 9, 12, 14, 15, 18, 19] and other examples with $|P|=23$–50, $|V|=33$–80 on a IBM 370/145 computer. The results obtained do not differ from the cited ones, excluding one equivalent solution; in several examples a number of equivalent solutions are obtained. The effectiveness of the separate algorithms is comparable to that of the best algorithms in literature [1, 4, 6, 7, 9, 12, 14, 15, 18].

The distribution of the execution time is: $t=60$–255 s, to the four stages correspondingly: $t_3=1$–5%, $t_4=60$–90% (mean 80%), $t_5=1$–13% (mean 10%) and $t_6=3$–8%; in the case of $p_i \neq$ idem an increase from $t_5=40$–65% and $t_6=1$–10% is established.

8. Conclusions

The theoretical investigations carried out and the implementation of the algorithms allow the formulation of the following significant conclusions.

1. An heuristic approach by declarative representation for structural analysis of CIS is proposed, which is a general and effective method especially for the most complicated problem [7] — the optimal decomposition.

2. The development of the hueristic procedure in procedural representation, which consists of a supervisor and a library of standard heuristics allows an improvement of the heuristic programme system for the structural analysis of the classes of models of CIS by application of the fuzzy set theory.

3. A general approach and scheme of the heuristic structural analysis of CIS, which are represented by the classes parametric flow, information and signal graphs are proposed.

4. A general scheme of the algorithm for heuristic search in declarative representation with generating procedure from the type "left-depth-first process" is proposed, which is applied to the algorithmization of all the heuristic procedures in this paper.

5. An heuristic procedure for identification of cycles and paths in digraphs is proposed.

6. An effective heuristic modification of Lee and Rudd's method for optimal decomposition of the cyclic digraphs is developed, having an advantage over all the known methods for the determination of only one or all the optimal tearing sets of arcs.

7. The heuristic procedure for optimal decomposition of the cyclic digraphs allowed the establishment of the fact that the same problem has a multimodal object function, which has a set of equivalent and probably non-equivalent extrema. This rises the problem for vector optimal decomposition.

8. An heuristic procedure for synthesis of the computing sequence of units of CIS when a tearing set of arcs is given.

9. A programme system for heuristic structural analysis of CIS on the basis of the modular principles is developed. It showed high efficiency in solving a set of examples.

9. Notation

$R(R^+, R^-)$-incidence relationship (positive, negative) between the elements of the sets P and V of the digraph $G=(P, V)$;

$\text{beg}(\text{cir}_i\, G)$-beginning of the cycle $\text{cir}_i\, G$;

r_i, $\text{rank}(\text{cir}_i\, G)$-rank of the cycle $\text{cir}_i\, G$;

V, V_0, V_0^-, V_0^+, V_c, V_s, V_n-set of arcs, external-incidence arcs for the graph, negative or positive-incidence to the node p, cyclic arcs, tearing arcs, unnecessary for tearing arcs of the graph $G=(P, V)$;

M_I-maximal depth's searching level of the implicit tree I;

I_D-cardinality of the set of the implicit trees at level D;

$\text{Col}_i C$-set of columns of the cycle $\text{cir}_i\, G$;

$\text{Row}_j\, C$-set of cycles, which include the arc v_j from the column $\text{col}_j\, C$;

$(\text{row}_i\, C)_j$-set of columns, which includes all the columns $\text{col}_j\, C$ with $c_{ij} \neq 0$ in the row $\text{row}_i\, C$;

$(\text{col}_j\, C)_i$-set of rows, which includes all the rows $\text{row}_i\, C$ with $c_{ij} \neq 0$ in the column $\text{col}_j\, C$;

p_i-node of the graph G; weight of the arc v_i;

C^*-compressed cyclic matrix C;

$N=|\{\text{col}_j\, C^*\}|$-cardinality of the set $\{\text{col}_j\, C^*\}$;

$\{G_i\}$-set of the strongly connected components of the digraph G;

$P \Rightarrow B$ — equivalence relation; B is a consequence from P;

$\{x/P(y)\}$-set of the elements x which satisfy the condition $P(y)$;

$\overrightarrow{\subset\subset}$-inclusion map operation.

10. REFERENCES

1. AHO, A., HOPCROFT, J. and ULLMAN J.: The design and analysis of computer algorithms. Addison-Wesley Publ. Co., London, 1976, pp. 214, 216.
2. BERGE, C.: Theorie des grafes et ses applications. Dunod, Paris, 1958, p. 75.
3. KHAFAROV, V., PEROV, V. and MESHALKIN, V.: Principles of simulation of chemical industrial systems. Khimija, Moscow, 1974, pp. 128–154 (in Russian).
4. CROW, C., HAMIELEC, A., HOFFMAN, T. et al.: Chemical plants simulation. Prentice-Hall Inc., N. Y., 1969, pp. 33–47.
5. LAZAROV, J.: Hung. J. Ind. Chem., *1985*, 13, 00.
6. LEIFMAN, L.: Cybernetic, *1966*, 5, 18 (in Russian).
7. MOTIL, D., VOLIN, JU. and OSTROVSKIJ, G.: Theoret. Found. Chem. Engng., *1981*, 15, 232 (in Russian).
8. NILSON, N.: Problem-solving methods in artificial intelligence. McGraw-Hill Book Co., N. Y., 1971, pp. 91, 129.
9. OSTROVSKIJ, G. and VOLIN, JU.: Simulation of chemical industrial systems. Khimija, Moscow, 1975, p. 52 (in Russian).

10. Popov, E. and Firdman, G.: Algorithmic foundations of intelligent robots and artificial intelligence. Nauka, Moscow, 1976, p. 38 (in Russian).
11. Slagle, J.: Artificial intelligence. McGraw-Hill Book Co., N. Y., 1971, pp. 137, 163.
12. Christensen, J. and Rudd, D.: AIChEJ, *1969*, 15, 94.
13. Earnest, C., Balke, K. and Anderson, J.: of ACM., *1972*, 19, 23.
14. Kehat, E. and Schacham, M.: Proc. Techn. Int., *1973*, 18, 35, 115.
15. Lee, W. and Rudd, D.: AIChEJ. *1966*, 12, 1184.
16. Motard, R. and Westerberg, A.: AIChEJ, *1981*, 27, 725.
17. Pho, T. and Lapidus, L.: AIChEJ, *1973*, 19, 1182.
18. Tarjan, R.: SIAM J. Comput., *1972*, 1, 146.
19. Upadhye, R. and Grens, E.: II. AIChEJ, *1975*, 21, 136.
20. Westerberg, A. and Edie, F.: The Chem. Engrs., *1971*, 2, 9.

РЕЗЮМЕ

В этом статье рассматривается эвристически адекватное представление трех классов топологических моделей ХТС-параметрических потоковых, информационных и сигнальных графов, в декларативной системе. Структурный анализ топологических моделей рассматривается как декомпозиционная задача, решимая в виде эвристической редукционной системы. Дан обобщенный алгоритм эвристических продукционных процедур. Редукционная система представлена множеством эвристических продукционных систем и детерминированными методами для идентификации сильно связных компонентов орграфов, идентификации циклов циклических орграфов, оптимальной декомпозиции циклических орграфов и для синтеза оптимальной вычислительной последовательности аппаратов ХТС. Даны формальные теоретико-графовые описания множеств операторов трансформации эвристических состояний, множеств эвристик и критерии окончания поиска для каждой эвристической процедуры. Программно реализованные процедуры показывают высокую эффективность.

HUNGARIAN JOURNAL
OF INDUSTRIAL CHEMISTRY
VESZPRÉM
Vol. 13. pp. 81–92 (1985)

HEURISTIC PROCEDURES FOR STRUCTURAL ANALYSIS OF CHEMICAL INDUSTRIAL SYSTEMS. II.

A NEW APPROACH FOR PARTITIONING OF FLOWSHEETS

J. LAZAROV

(Central Laboratory of Chemical Engineering, Bulgarian Academy of Sciences, 1040 Sofia)

Received: August 10, 1984

A new approach for the identification of the components of digraphs, which are topologic models of chemical process flowsheets, is developed. It is based on the analysis of three classes recurrentness of the adjacency matrix of the digraphs with HAMILTON's path. Four fundamental types of recurrent structures of strongly and one-side connected digraphs are identified and described.

A method for improving the matrix method for the identification of the strongly connected components of the digraphs is proposed.

A new, simple and efficient method for identification of the strongly connected components of digraphs with HAMILTON's path is developed. The convergency and the asymptotic complexity of the method are proved.

An algorithm and an example are given.

In the first part [20] of this paper the problem of heuristic representation of the structural analysis of chemical industrial systems is discussed. A general heuristic description is presented for the development of the system of heuristic procedures for a priori precedence-ordering, which determines the optimal sequence in which each element of the chemical industrial system is to be computed. One of the essential parts of the same procedure, is the process method of determining the closed technological subsystems in which the problems of the structural analysis are solved one after the other, but they already have smaller dimensions.

The problem of the identification of the closed subsystems of chemical process flowsheets, which are presented by topologic models, is reduced in the graph theory terms to the identification of the components of digraphs. Henceforth, the problem is considered in this way.

In this paper, determinate methods for the identification of the components of digraphs are developed. The methods are used as generators of heuristics for the heuristic procedures, when we solve the problem of the structural analysis. This corresponds to the representation of the structural analysis of

chemical industrial systems as a reduction heuristic system in declarative representation, which is considered in part I [20].

Let us take a chemical industrial system C with topologic model T. Let us mark by $A_T=\{A_1, A_2, \ldots, A_K\}$ the set of the subsystems of the system, by $F_T=\{f_{ab}^{pq}: x_a^{(p)}=y_b^{(q)} / a \leqq m_p \& b \leqq m_q,\ p, q \leqq K\}$ the set of the topologic connection between the subsystems in T, and by $X_i=\{X_i^{(1)}, X_i^{(2)}, \ldots. X_i^{(m_i)}\}$ and $Y_i=\{Y_i^{(1)}, Y_i^{(2)}, \ldots, Y_i^{(n_i)}\}$ the set of the input-output variables of the technological flows. Let us represent the model T by finite digraph $G=<P, V, \alpha, \beta>$ by means of bijections $\varphi_1: A_T \to P$ and $\varphi_2: F_T \to V$. The functions α, β are defined by φ_1, φ_2 so that they fulfil the conditions $\alpha, \beta: P \to V$, $v=\varphi_2(f_{ab}^{pq}) \Leftrightarrow \alpha(v)=\varphi_1(A_p) \& \beta(v)=\varphi_1(A_q)$. The method to analyze system C depends on the type of model T. It is obvious that essential difficulties exist in the analysis of the closed models T. This requires a turn into equivalent open model T^0 which is gained after the elimination of several equations of the connections in every complex in the model T — the set $\varphi_1^{-1}(P_i)$. The interpretation of the problem of determining the set $\varphi_1^{-1}(P_i)$ in the terms of graph theory is reduced to an identification of the strongly connected components of the digraphs.

1. Current State of the Problem for the Identification of the Strongly Connected Components of the Digraphs

The problem of the identification of strongly connected components of finite digraphs is discussed in a number of works: [1–19] and others. The matrix method is the first well known one. Its theoretical basis is given in [3, 8, 11, 14, 15] using the adjacency matrix, its powers, the matrix of reachability and the matrix of the complexes. The adjacency matrix is defined as a square matrix $a_{ij}=T$ (true) if $\{p_i < \mathrm{adj} > p_j / \exists (p_i, p_j, 1)\}$, otherwise the logical value of the element is $a_{ij}=F$(false). Different modifications and improvements of the method are known [14, 13, 7]. The correctness of the matrix method is mathematically proved, but it requires m powers of the matrix A. The sufficient exponent m theoretically is not clarified [3, 8] and $m=|P|$ is accepted [14, 11] and seldom $m=|P|-1$ [13].

Among the other methods, the method of the sequential lumping of the cycles in a digraph has an important place, where the components are represented as pseudo-nodes [10, 16, 17]. The first to apply the method were SARGENT and WESTERBERG [16] who traced the information flows of the digraph backwards until they identified a cycle in which the nodes are lumped into a pseudo-node. CHRISTENSEN and RUDD [9] carried out the initial deleting of the nodes that have no input and output edges, which cannot be included in a cyclic net. They also added forward tracing. The algorithm operation [2] consists of tracing the path until the determination of a cycle and then integrating with the crossing cycles in a complex.

LEIFMAN's iterative algorithm [4] for determining the bicomponents of graphs is based on the transitivity of the reachability relations R of the nodes. After deleting the ended and the initial acyclic subgraphs, a node p_0 is chosen, after this all the reachable nodes $p_0 R^{+1} p_i$ are set, which are labelled by $\mu=1$. By backward reachability relation $p_j R^{-1} p_0$ the nodes $p_j \to p_0$ are set, which are labelled by $\nu=1$. According to the labelling carried out the set P is decomposed into four non-crossing subsets P_{ij}, $i, j \in \{0, 1\}$. If $P_{11} \neq \emptyset$ then G_{11} is

a biconnected component. The procedure is repeated after deleting subset G_{11}, regarding the subsets G_{00}, G_{01} and G_{10}.

Another effective method having some common features with the algorithms [2, 6, 9, 10, 16, 17] in the strategy of the path-searching is TARJAN's algorithm [18, 12]. The algorithm is based on applying the depth-first search with the reordering of the nodes. When searching forwards, regarding the edges a node x is chosen to which an ordered number in the string num (x) is given, containing the order of the search. By depth-first traversal through the edge (v, w) if the node w is in the string preceding the node v, then num $(w) <$ num (v) and the edge (v, w) is a back-edge. If node w is not an ancestor of the node v and num $(w) >$ num (v), then node w is a descendant of node v and the edge (v, w) is a forward-edge. If num $(w) <$ num (v) and node w is not an ancestor or a descendant of node v, then the edge (v, w) is a cross-edge. The negative-incident back-edges and cross-edges of node v can be positive-incident only to this node x fulfilling the condition num $(v) >$ num (x). A path μ from node v to node w exists in the component G_i by definition [3, 8]. It is proved [18] that a spanning tree of the graph exists, which together with the back-edges and the cross-edges also includes the path μ. Node v is defined as a root of the minimal spanning tree, i.e. nodes $P_i \in G_i$ define a rooted tree, which is a subgraph of the spanning forest. The determining of the roots of the spanning trees corresponding to the components permits the strongly connected components themselves to be found.

There are other methods and modifications known, which have both advantages and disadvantages regarding their effectiveness, the storage requirements, simplicity of the method and computer programme.

In this paper the theoretical and algorithmic aspects of a new approach are discussed for the identification of the strongly connected components based on recurrent properties of the adjacency matrix. The novel aspect involves the development of simple procedures, both for improving the matrix and some other known methods and their modifications, and for the development of new methods and algorithms for the identification of strongly or one-side connected components, transitive closures, paths, cycles and classes of connectedness of the finite digraphs.

2. Recurrent Properties of the Adjacency Matrix

When presenting the method axiomatically we should establish a set of formulations, axioms and theorems as in [4, 6, 18, 15]. The adjacency matrix $\|a_{ij}\|$ with the number of the vertices has a strong relationship over the natural semiring $i_s: P \to \{1, 2, \ldots, K\}$ (in the general case the unspecified relationship i_s is presented by the vector IS) over the number of the rows of the matrix A relation i_a: $\mathrm{Row}_i A \to \{1, 2, \ldots, K\}$ has the following areas: *I–a* triangular upper submatrix containing the forward directed arcs V_c for which $i=1, (K-2), j=(i+2), K$; II-an area of the principal arcs V_m — the diagonal $i, i+1$ (a principal HAMILTON's path); III-an area of the loops-the diagonal i, i; IV-a triangular lower submatrix containing backward directed arcs V_r for which $i=2, K, j=1, (i-1)$.

In this paper the concept of recurrentness in introduced, which is a convenient mean both for the development of the theoretical approach for analy-

sis and synthesis of the graph structures, and also offers different methods of finding the sets of vertices forming strongly or one-side connected components, bicomponents, paths and cycles. The main concept for the formal description of the studies consists of the recurrent structure. By "recurrent structure of the finite digraph" let us consider graph G whose set of binary relations $R \subset P^2$ contains some explicit, recurrent interrelations in the terms of the problem for the identification of the components.

Theorem 1: There are four fundamental recurrent structures of the strongly connected digraphs.

Proof: The recurrent interrelations in set $R \subset P^2$ of digraph G without external input/output arcs in the area IV of the matrix A, which allow a recurrent analysis or synthesis of graph G, can be realized by means of the following ways: 1. $j = \text{const}$, $i = (j+1), K$; 2. $i = \text{const}$, $j = 1, (i-1)$; 3. $j = K/2, 1, -1$, $i = (K-j+1), K$; 4. $j = 1, (K-l-1)$, $i = (K-l+1), K$ for $i, j = 1, 2, \ldots, K$, $l = 0, 1, \ldots, (K-1)$.

Corollary 1: The allocation of the $a_{ij} = T$ elements of the recurrent structures of the strongly connected finite digraphs in the area IV of the matrix A is according to one of the following ways: 1. Vertically; 2. Horizontally; 3. Along the second principal diagonal; 4. Along the diagonal which is parallel to the first principal diagonal.

The respective recurrent structures of the strongly connected finite digraphs with HAMILTON's path are shown in *Fig. 1* (for $q = 1$ and $i_{1,2,3,4} = 2, 2, 1, 2$). *Fig. 2* gives the allocation of the three classes recurrentness in the adjacency matrix.

The identified fundamental recurrent structures of the strongly connected digraphs with HAMILTON's path are described mathematically by the following

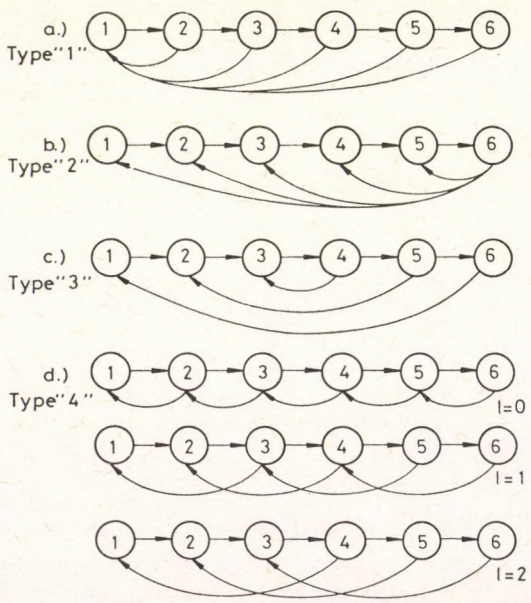

Fig. 1
Fundamental recurrent structures of strongly connected finite digraphs with HAMILTON's path p_i, p_{i+1}.

Table 1.

No. of RS	q	r	K	m_1	L	a	b b_{min}, b_{max}, Δb $j=1, 2, \ldots$ i	d	m	$A^{m+const}=idem$, $i, j=1, 2, \ldots$
1	0	$2i$	$2i+1$	$2i$	$4i$	$2i$	$0, (2j-1), 1$	1	$2i+1$	$A^{2i+3}=A^{2i+3+j}$
	1	$2i+1$	$2(i+1)$	$2i+1$	$2(2i+1)$	$2i+1$	$0, 2j, 1$		$2(i+1)$	$A^{2(i+2)}=A^{2(i+2)+j}$
2	0	$2i$	$2i+1$	$2i$	$4i$	1	$0, (2j-1), 1$	$2i$	$2i+1$	$A^{2i+3}=A^{2i+3+j}$
	1	$2i+1$	$2(i+1)$	$2i+1$	$2(2i+1)$		$0, 2j, 1$	$2i+1$	$2(i+1)$	$A^{2(i+2)}=A^{2(i+2)+j}$
3	0	$2i$	$4i$	$4i-1$	$6i-1$		$0, 2(j-1), 2$	$2i$	$4i$	$A^{4i}=A^{4i+2j}$ $A^{4i+1}=A^{4i+1+2j}$
	1	$2i+1$	$2(2i+1)$	$4i+1$	$6i+2$		$0, 4(j-1), 2$	$2i+1$	$2(2i+1)$	$A^{2(2i+1)}=A^{2(2i+1)+2j}$ $A^{4i+3}=A^{4i+3+2j}$
4	0	$2i-1$	$2i+1$	$2i$	$4i-1$	l	$l=0, 1, 2, \ldots, (i-1)$ $l_{max}=2i-1$	$2i-l$	$2i$	$A^{2i}=A^{2i+2j}$ $A^{2i-1}=A^{2i+2j-1}$
	1	$2i-1$ $+1$	$2(i+1)$	$2i+1$	$2(2i+1)-1$		$l=0, 1, \ldots, i$ $l_{max}=2i$	$2i-l$ $+1$	$2i+1$	$A^{2i}=A^{2i+2j}$ $A^{2i+1}=A^{2i+2j+1}$

parameters: $K=|P|$; $L=|V|$; $r=|V_r|$; $a=|V_a|$ where $V_a \subset V$ and $P_i \cap V_a = \max\deg^+(p_i)$; $b=|P_b|$, $P_b \pitchfork V_j$, $V_j=(p_i, p_j, 1)$ and $i<b<j$; $d=|P_d|$, $P_d \cap V_r$ for which $p_i \in P_d$, $\deg^+(p_i)_i=(V_r \cup V_m) \cap p$; $m_1=|V_m|$. The mathematical expressions are represented in *Table 1.* They are deduced regarding the independent parameter i which is the number of the recurrent structures in the respective homological order. The parameter $q=\frac{1}{2}[1+(1-)^{i \vee (i+1)}]$ is an index of the parity of the recurrent structures (when $l=0$).

Theorem 2: There are four fundamental recurrent structures of the one-side connected finite digraphs.

Corollary 2: The allocation of the $a_{ij}=T$ elements of the recurrent structures of the one-side connected digraphs in the area I of matrix A is analogous to the allocation in area IV according to *corollary 1.*

3. Improvement of the Classical Matrix Method

The fundamental result from studying the recurrent structures consists in the identification of the sufficient exponent m of the reachability power of the adjacency matrix (the sufficient exponent for identification of the cycles is $m_c \leq m$): for the first, second and third structures the sufficient exponent is $m=K$ and for the fourth structure $m=K-1$. Further investigations showed that for random strongly connected digraphs, the sufficient exponent is $m \leq K$. For the multi-connected graph, the next statement is valid: the sufficient exponent m is determined from the cardinality of set $|P_i|$ of the prioritive strongly connected component G_i therefore $m \leq |P_i^{max}|$. This essentially decreases the number of the powers of the adjacency matrix in the matrix method, because $|P|>|P_i|$. The previous determination of the sufficient exponent m, which is essentially smaller than the so far applied exponents

[3, 7, 8, 11, 13, 14] leads to an increase of the effectiveness of the matrix method and its modifications.

Further investigations of the recurrentness of a multi-connected digraph lead to the identification of six recurrent fields in the area IV of the adjacency matrix which are shown in *Fig. 2*. The existing element $a_{ij}=T$ in the fields shows the presence of the type connections of the recurrent structure. This structure is a partial subgraph, which is connected with other strongly connected partial subgraphs as follows: in the field A — additional recycle edges in the recurrent structure itself; B/D — a connection of the recurrent structure with preceding/following component (a multiplicative recurrent structure); C — a recycle edge which envelopes the recurrent structure; E/H — a separable connection (an articulation point) with preceding/following component (an additive recurrent structure). For the purpose of computing, the recurrent fields are described by recurrent expressions regarding the auxiliary parameters as well: $K_1=|P_i|$, $p=|V_r^{rs}|$, $n=\min j$ for the elements $a_{ij}=T$. The mathematical expressions from Table 2 are applied to determine the sufficient exponent m.

Table 2.

RS \ Field	Limit	A		B	C	D	E	H
		A'	A''					
1	F_T	$(n+2)$, $(n+p)$, 1		$n+1$	$n+p-1$	$n+p+1$	n	$n+p+1$
	F_U	$n+p$			K_1		1	K_1
	F_L	$n+1$		1		n		$n+p$
	F_R	$(n+1)$, $(n+p-1)$, 1		$n-1$		$n+p-1$		
2	F_T			$n+1$	$n+p+1$		$n-1$	$n+p+1$
	F_U	$n+p-1$		$n+p$	K_1			K_1
	F_L	n		1		n	1	$n+p$
	F_R	n, $(n+p-2)$, 1		$n-1$		$n+p-1$	$n-1$	
3	F_T	$(n+1)$, $(n+p-1)$, 1	$(n+2p-1)$, $(n+p-1)$, -1 / $(n+p-1)$, $(n+2p-1)$, 1	$n+1$	$n+2p$		n	$n+2p$
	F_U	$(n+2p-2)$, $(n+p)$, -1	$n+2p-1$		K_1			K_1
	F_L	n	$(n+1)$, $(n+p-1)$, 1	1		n	1	$n+2p-1$
	F_R	n, $(n+p-2)$, 1 / $(n+p-2)$, n, -1	$(n+p)$, $(n+2p-2)$, 1	$n-1$		$n+2p-2$	$n-1$	
4	F_T	$(n+1)$, $(n+p+b)$, 1	$(n+b+2)$, $(n+b+p)$, 1	$n+1$	$n+p+b+1$		n	$n+p+b+1$
	F_U	$(n+b)$, $(n+p+b)$, 1	$n+p+b$		K_1			K_1
	F_L	n, $(n+l)$, 1	n	1		n	1	$n+p+b$
	F_R	n, $(n+p+b-1)$, 1	n, $(n+p-2)$, 1	$n-1$		$n+p+b-1$	$n-1$	

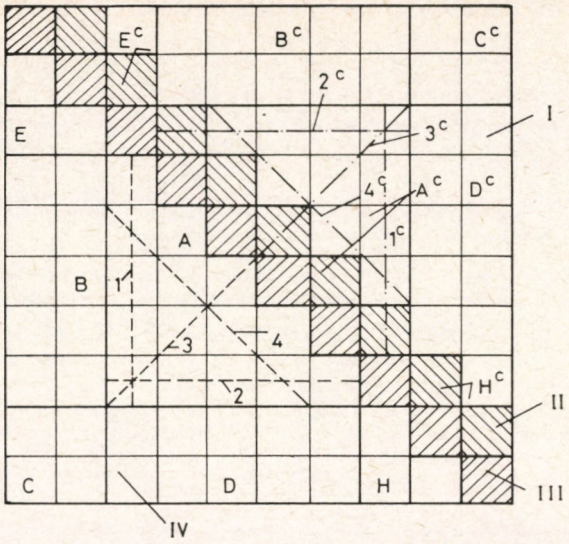

Fig. 2
A general view of the recurrentness of the adjacency matrix of a multi-connected digraph with HAMILTON's path: recurrent areas — I, II, III and IV; recurrent fields — *A*, *B*, *C*, *D*, *E* and *H*; allocation of the fundamental recurrent structures — *1*, *2*, *3* and *4*. The index "*c*" in area I is for recurrentnesses of one-side connected subgraphs (in the case of strongly parallel arcs, area II is considered as well)

The up-to-now received results are important for the improvement of the developed computer programmes for the automatic design of process systems based on the matrix method.

The upper concepts are valid for one-side connected components as well.

4. A New Method for the Identification of Strongly Connected Components of Finite Digraphs with HAMILTON's Path

The matrix method, independently from the developed improvements, uses a large number of matrixes, which is its second disadvantage. This disadvantage is intrinsic of other methods [4, 6, 9, 16]. In this connection combinatorial studies of the recurrent properties of the matrix A are carried out, particularly for the recurrent fields. On this basis, in the further analysis of the recurrentness, a new method for the identification of strongly connected components of digraphs with HAMILTON's path and forming the matrix of complexes W is developed. The main feature is that the method uses only the adjacency matrix A. It is clear that for the identification of strongly connected components of digraphs with HAMILTON's path, it is necessary to consider only the lower triangular submatrix, which is area IV of the adjacency matrix. The essence of the method consists of the analysis of the recurrent fields in area IV precisely the fields B and E.

Let us consider the mathematical formalization of the method in the terms

of the graph theory. If $(\mathrm{row}_i A)_j$ is the set of columns of the row $\mathrm{row}_i A$ with elements $a_{ij}=T$ in the adjacency matrix and $(\mathrm{col}_j A)_i$ is the set of rows with $a_{ij}=T$ to which a column $\mathrm{col}_j A$ corresponds, then for each row $i \leq K$ of the matrix A the set $\mathrm{Col}_i A = \bigcup_i \mathrm{col}_j A\{(p_i, p_j, 1) \backslash a_{ij}=T, j=1, 2, \ldots, (i-1)\}$ can be formed, and for each column $j<i$ — the set $\mathrm{Row}_j A \bigcup_j \mathrm{row}_i A\{(p_i, p_j, 1) \backslash a_{ij}=T\}$, which includes each row with elements $a_{ij}=T$ in column j of matrix A. The dominant relation is defined regarding the strong ordering relationship of the morphisms $M: G_k \to G\{G_k = <P_1, V_1, \alpha_1, \beta_1>, V_1=\{v_1 \backslash v=[i, i+1], 0 \leq i \leq n-1\}, \alpha_1(v)=\alpha_1[i, i+1]()=i \& \beta_1(v)=\beta_1([i, i+1])=i+1, G_k \in G\}$ over the semiring of the natural numbers with respect to the reachability relationship R^{+1}. If $M_1\{\mathrm{beg}\,(p_1), \mathrm{end}\,(p_{i+2})\} > M_2\{\mathrm{beg}\,(p_2), \mathrm{end}\,(p_{i+1})\} > M_3\{\mathrm{beg}\,(p_3), \mathrm{end}\,(p_i)\}$, then $(p_{i+2} R^{-1} p_1) < \mathrm{dom} > (p_{i+1} R^{-1} p_2) < \mathrm{dom} > (p_i R^{-1} p_3)$, and if the mutual reachability relationship $R=R^{-1} \circ R^{+1}$ is valid, then the strongly connected components $\bigcup_i G_1, G_2, \ldots, G_j, \ldots, = G$ exist. All this allows the following principles to be formulated:

Principle 1 (a row dominance over another row): If for a pair of rows $\mathrm{row}_i A$ and $\mathrm{row}_x A$ the expression $\min(\mathrm{row}_i A)/j \leqq \min\,(\mathrm{row}_x A)_y \backslash y\{j<i,\ x>y,\ x=j-1, \ldots, i-1\}$ is valid, then the row $\mathrm{row}_i A$ dominates over the row $\mathrm{row}_x A$: $\mathrm{row}_i A < \mathrm{dom} > \mathrm{row}_x A$. The last relationship is valid because the next interrelationship between the ranks of the cycles, including the edges $(p_i, p_j, 1)$ and $(p_x, p_y, 1)$ of a given strongly connected component of graph exists: $\mathrm{rank}\,\{\mathrm{cir}_i C \backslash (p_i, p_j, 1)\} > \mathrm{rank}\,\{\mathrm{cir}_j G \backslash (p_x, p_y, 1)\}$, and each cycle $\mathrm{cir}_i G$ belongs only to one strongly connected component [3, 8].

Principle 2 (a column dominance over a set of rows): The column $\mathrm{col}_j A$ dominates over the set of rows $\mathrm{Row}_x A$ if the row $\max\,(\mathrm{col}_j A)_i \backslash i$ dominates over each of the rows $\bigcup_{j-1}^{i-1} \mathrm{row}_x A \backslash \{(j-1) \leq x \leq (i-1)\}$ in accordance with principle 1. If the expressions $\max(\mathrm{col}_j A)_i \backslash i = k$ and $\min\,(\mathrm{row}_i A)_j \backslash j = 1$ are valid, then the row $\mathrm{row}_i A$ dominates over all the rows $1, 2, \ldots, (k-1)$, and if $k=K$ then the row $\mathrm{row}_k A$ is an absolute dominating row, and graph G is a strongly connected one.

5. Convergency and asymptotic complexity of the method

For an evaluation of the method it is necessary to find the order of the increase of the asymptotic time complexity by increasing the size of the problem.

Theorem 3: The method finds the strongly connected components of digraph G with asymptotic time complexity $0\left(\sup\left(((|G_i|-1)/(2.|G_i|)).|P|\right)\right)$.

Proof: $(|P|-1).\,|P|/2$ logical operations for a trivial finite digraph are carried out, then the complexity is $0((|P|-1)\cdot|P|/2)$. For the strongly connected digraph, the method finishes after the first logical operation, therefore $0(0)$. For proving the complexity searched, let us consider inductively graph G_i with $|G_1|=2$, $|G_2|=3$ and so on strongly connected components respectively, for each of which $|P_i|=2$. For the asymptotic time complexity, we obtain $0_2(|P|/|G_i|-|P|^2/|G_i|^2)$, $0_3(2\cdot|P|/|G_i|-3\cdot|P|^2/|G_i|^2)$, $0_4(3\cdot|P|/|G_i|-6\cdot\cdot|P|^2/|G_i|^2)$ and so on respectively. Therefore, the general expression is

$0\left(\left(\left(|G_i|-1\right)/\left(2\cdot|G_i|\right)\right)\cdot|P|\right)$. Bearing in mind that $|P|=|G_i|\cdot|P_j|$ then obviously by increasing $|P_j|$ $|G_i|$ will decrease, therefore, the gained expression of the complexity is a supremum.

The convergency of the method follows from the essence of principle 1, beginning from the last row of the adjacency matrix. For a trivial graph, $|P|$ cycles are carried out, for a strongly connected graph — one cycle, and in the generals case — $|G_i|$ cycles.

6. Algorithm

The process of identification of the set of strongly connected components G_i of a digraph with HAMILTON's path can be described by the following recurrent expression:

$$G_i \Leftrightarrow \{\text{row}_k A \backslash \min(\text{row}_k A)_j \backslash j = k+1\} \vee \{\text{Row}_n A / \max(\text{col}_j A)_i \backslash i < \text{dom} > \text{row}_n A \backslash \backslash j-1 \leq n \leq i-1,\ k_0 = K,\ k := k-1,\ \ldots,\ 1 \vee k := n-1,\ \ldots,\ 1\}. \quad (1)$$

The algorithm in accordance with expression (1) starting from $k_0 = K$ represents the following cyclic sequence which can be written in a recursive form as well.

1. Test: $k \leq 1$? Yes-stop. No-test: $a_{kn} = T(n=1,\ k-1)$? Yes-(test: $n=1$? Yes-go to step 4) go to step 3.

2. The vertex k (in the general case $IS(k)$) is a trivial strongly connected component; $k := k-1$; go to step 1.

3. Forming an analysis of the generalized field: $i = n,\ k-1,\ +1$ (or $i = k-1,\ n,\ -1$), $j = 1,\ n-1$. Test: $a_{ij} = T$? Yes-n: $= j$; test: $n = 1$? No-repeat step 3.

4. The vertices $(n,\ k)$ $\left(\text{in the general case } (IS(n),\ IS(k))\right)$ form a strongly connected component; $k := n-1$; go to step 1.

The algorithm for the identification of the one-side connected components of the finite digraphs with HAMILTON's path is an analogous one.

An example: Let us consider the operation of the algorithm over the graph shown in Figure 3, whose adjacency matrix is shown in Figure 4. The algorithm begins with the analysis of the adjacency matrix from the last row $k_0 = 6$ for $n = 1$, 8 the $a_{kn} = \text{T}$ element is searched for until $a_{97} = T$. The field of adjacency matrix A is formed with limits of rows $i = 7$, 8 and columns $j = 1$, 6. By analysis the field is established that all the elements are $a_{ij} = F$. Then in accordance with principle 2 the vertices $(n,\ k)$ are written in the matrix of complexes as $W(1, |G_i^{\max}|) = \{7,\ 8,\ 9\}$. The next row $k = n-1 = 6$ for $n = 1$, 5 is analyzed. All the elements are $a_{6n} = F$, that is why the vertex 6 is written as a trivial strongly connected component: $W(2,\ |G_i^{\max}|) = \{6\}$. For the row $k := k-1 = 5$ for $n = 4$ it is established that $a_{54} = T$. The field $i = 4,\ 4$ and $j = 1,\ 3$ is formed and analyzed in which $a_{42} = \text{T}$. According to the principle 1 for $n = 2$ the new field is formed for $i = 2,\ 4$ and $j = 1,\ 1$ for which in the row $i = 3$ for $j = 1$ it is established that $a_{31} = T$. Because $n = j = 1$ the direct writing in

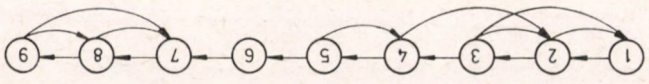

Fig. 3
An example digraph with HAMILTON's path

	1	2	3	4	5	6	7	8	9
1	F	T	F	F	F	F	F	F	F
2	F	F	T	F	F	F	F	F	F
3	T	T	F	T	F	F	F	F	F
4	F	T	F	F	T	F	F	F	F
5	F	F	F	T	F	T	F	F	F
6	F	F	F	F	F	F	T	F	F
7	F	F	F	F	F	F	F	T	F
8	F	F	F	F	F	F	T	F	T
9	F	F	F	F	F	F	T	T	F

Fig. 4
The adjacency matrix of the example digraph with generalized fields, which are formed from the algorithm.

the matrix of complexes is carried out: $W(3, |G_i^{max}|)=\{1, 2, 3, 4, 5\}$. After computing $k:=n-1=0$ and test the algorithm finishes. The rows of the matrix W are inverted symetrically: $W(1, |G_i^{max}|) \rightarrow W(3, |G_i^{max}|)$, and $W(3, |G_i^{max}|) \rightarrow \rightarrow W(1, |G_i^{max}|)$.

7. Computational Experience

For the comparative evaluation of the effectiveness of the proposed improvements and new formulations, the classic matrix method, the matrix method with appliance of the proposed principles for determining the sufficient exponent m, and the new developed method are algorithmized and programmed. Computing the large number of examples from [6, 9–11, 13, 14, 16, 17] and others by a IBM 370/145 computer, the following execution times were attained: I — from 300 until 1200 s; II — from 30 until 50 s; III — from 1 until 5 s.

8. Conclusions

On the basis of the considered formulations, principles, theorems, graph theory descriptions and examples, the following significant conclusions can be formulated:

1. A theoretical approach for the analysis and synthesis of the graph structures is proposed, which is oriented for the identification of the strongly and one-side connected components, paths, cycles and classes of the connectedness of the finite digraphs by an analysis recurrent properties of the adjacency matrix.

2. The three classes of recurrentness of the adjacency matrix of finite digraphs are identified, mathematically described and used.

3. The four fundamental types of recurrent structures of strongly connected finite digraphs with HAMILTON's path are identified and mathematically described, the four fundamental types of one-side connected recurrent structures respectivelly.

4. A method for improving the efectiveness of the classic matrix methods for identification of strongly connected components is proposed.

5. A new simple and efficient method for identification of strongly connected components of finite digraphs with HAMILTON's path is developed.

6. The efficiency and effectiveness of the proposed methods were established through the computing of a large number of examples.

9. Notation

G_i-set of strongly connected components of the digraph G;
P_i, V_i-sets of vertices and arcs of the subgraph G_i;
R-set of the binary relations in the set P;
$m_1 = |V_m|$-cardinality of the set of arcs V_m of the HAMILTON's path (p_i, p_{i+1}) in the graph G;
$r = |V_r^{rs}|$-cardinality of the set of recycle arcs V_r of given recurrent structure;
$\{(p_i, p_j, 1)/a_{ij} = T\}$-set of arcs between the vertices p_i, p_j of the graph G for which the condition $a_{ij} = T$ is satisfied;
beg(p)-initial vertex of path in the graph G;
end(p)-final vertex of path in the graph G;
deg$^+(p)$-indegree of the vertex p;
$\langle$dom$\rangle$-dominance relation;
$\langle$adj$\rangle$-adjacency relation;
row$_i$ A-row i of the adjacency matrix A with element $a_{ij} = T$(true);
$(\text{row}_i A)_j$-set of columns of the row row$_i A$ with $a_{ij} = T$;
col$_j$ A-column j of the matrix A with element $a_{ij} = T$;
$(\text{col}_j A)_i$-set of rows of the column col$_j A$ with $a_{ij} = T$;
Col$_i$ A-unification of the set of columns col$_j A$;
Row$_j$ A-unification of the set of rows row$_i A$;
$\leftrightarrow$-equivalence relation;
i_s-relationship of the labels of the vertices of the diagraph G over the semiring of the natural numbers;
min $(\text{row}_i A)_j/j$-infinitum of the set of columns $(\text{row}_i A)_j$;
max $(\text{col}_j A)_i/i$-supremum of the set of rows $(\text{col}_j A)_i$;
$=$, $\leqq$-strong ordering and ordering relationships;
rank $\{\text{cir}_i G_j\}$-rank of the cycle cir$_i G_j$ of the subgraph G_j.

REFERENCES

1. AHO, A., HOPCROFT, J. and ULLMAN, J.: The design and analysis of computer algorithms. Addison-Wesley Publ. Co., London, 1976, p. 197.
2. VOLIN, JU., OSTROVSKIJ, G. and HANSEL, K.: Theoret. Found. Chem. Engng., *1975*, 9, 254 (in Russian).
3. CHRISTOFIDES, N.: Graph theory. Academic press, N. Y., 1975, p. 29.
4. LEIFMAN, L.: Cybernetic, *1966*, 5, 18 (in Russian).
5. MOTIL, D., VOLIN, JU. and OSTROVSKIJ, G.: Theoret. Found. Chem. Engng., *1981*, 15, 232 (in Russian).
6. OSTROVSKIJ, G. and VOLIN, JU.: Simulation of chemical industrial systems. Khimija, Moscow, 1975, p. 44 (in Russian).
7. REINGOLD, E., NIEVERGELT, J. and DEO, N.: Combinatorial algorithms. Prentice-Hall Inc., New Yersey, 1977, p. 356.

8. HARARY, F.: Graph theory. Addison-Wesley Publ. Co., London, 1969, p. 232.
9. CHRISTENSEN, J. and RUDD, D.: AIChEJ., *1969*, 15, 94.
10. FORDER, G. and HUTCHISON, H.: Chem. Engng. Sci., *1969*, 24, 771.
11. HIMMELBLAU, D.: Decomposition of large-scale problems. North-Holland Publ. Co., Amsterdam. 1973, p. 34.
12. HOPCROFT, J. and TARJAN, R.: Comm. ACM., *1973*, 16, 372.
13. KEHAT, E. and SHACHAM, M.: Proc. Techn. Int., *1973*, 18, 35, 115.
14. LEDET, W. and HIMMELBLAU, D.: Adv. Chem. Engng., *1970*, 8, 185.
15. NORMAN, J.: AIChEJ., *1965*, 11, 450.
16. SARGENT, R. and WESTERBERG, A.: Trans. Inst. Chem. Engrs., *1964*, 42, T140.
17. STEWART, J.: SIAM. Numer. Anal., *1965*, 2, 345.
18. TARJAN, R.: SIAM. J. Comput., *1972*, 1, 146.
19. TARJAN, K. and GYENIS, J.: A graph-theory-based decomposition method for complex chemical systems. Paper presented at CHISA '81, Meeting, Prague.
20. LAZAROV, J.: Hung. J. Ind. Chem., *1985*, 13, 00.

РЕЗЮМЕ

В статье рассматривается новый подход идентификации компонентов орграфов, которые являются топологическими моделями химико-технологических схем. Подход основан на анализе трех классов рекуррентностей в матрице смежности орграфов с Гамильтоновым путем. Идентифицированны и описаны четыре основные типа рекуррентных структур сильно и односторонно связных орграфов.

Предложен метод совершенствования матричного метода идентификации сильно связных компонентов орграфов.

Разработан новый, элементарный и эффективный метод идентификации сильно связных компонентов орграфов, обладающих Гамильтоновый путь. Доказаны сходимость и асимптотическая сходимость метода.

Приведены алгоритм и пример.

HUNGARIAN JOURNAL
OF INDUSTRIAL CHEMISTRY
VESZPRÉM
Vol. 13. pp. 93–105 (1985)

STUDIES ON VIBRATIONAL TRANSPORT. I.

DYNAMIC STUDIES ON A PNEUMATIC BALL VIBRATOR

A. Szalay and K. Erdész

(Research Institute for Technical Chemistry of the Hungarian Academy of Sciences, Veszprém)

Received: August 17, 1984

The relationships of the hydrodynamic and kinetic characteristics of a pneumatic ball vibrator are studied. Vibrational measurements were carried out using a pendulum-type suspension mode and the results were compared to the theoretical model proposed in literature. It was concluded that the pendulum-type suspension mode offers definite advantages when the pneumatic ball vibrator is used in transport machinery, that operation below the resonance point is more advantageous and that transportation elements of low mass and high rigidity are preferred.

Introduction

Literature dealing with pneumatic ball vibrators is rather sparse [1, 2] and apart from brief schematics it does not discuss either the operations principles or the design equations of vibrators. According to manufacturers [3, 4], the advantages of ball vibrators include the lack of bearing systems, the possibility of continuous adjustment, low mass and small footprint. The main field of application is the vibration of silo walls wherein solid supporting modes and fairly high frequencies (100–500 Hz) are employed.

Directed vibration, indispensible for the vibrational transportation of particulate material cannot be produced in the above frequency range and with a solid-type suspension mode. This work was aimed at finding suspension modes, which allow the generation of directed vibration over a wide range of amplitude and frequency. The relationship of frequency and amplitude is of prime importance, because these parameters are used in various systems (vibrational transportation machines, feeders, sieves, driers, coolers, and granulators, etc.) to control the residence time and mass flow rate of the particles, which, in turn, influence the efficiency of the particular operation.

1. Operation Principle of the Vibrator

The operation principle of the vibrator is as follows: the component along a given set axis of the centrifugal force acting upon a ball or roller of mass m_g subjected to circular motion by compressed air (or other gas) varies harmonically (follows a sine or cosine function) and so, an excitation force is generated described by Eq. (1):

$$F_g = m_g R\omega^2 \sin \omega t \tag{1}$$

For the design (or selection) of a vibrator and for the determination of the excitation force, one has to know the relationships between the angular velocity, ω and flow rate, V, and pressure, p, of the compressed gas. The role of the geometric characteristics (nozzle diameter, d_f, ball rotation radius, R, rolling friction coefficient, f_g, mass of ball, and m_g, etc.) in the hydrodynamic and kinetic behaviour of the vibrator also has to be known. Furthermore, it is expedient to carry out vibration experiments in order to determine the operational stability and optimum operation mode of the vibrator.

Thus, the dynamic studies of the vibrator were aimed at the theoretical description of the above relationships, at their experimental verification and at deducing conclusions as they apply to the design and selection of vibrators and vibrational transportation machines.

2. Relationships Between the Hydrodynamic and Kinetic Characteristics of the Ball Vibrator

Ball vibrators are designed on the basis of the knowledge pertaining to the relationships among gas flow-rate, gas pressure, circumferential velocity of the ball (rotation speed), its mass and the main size parameters of the vibrator. The hydrodynamic-kinetic preconditions of ball rotation are shown in *Fig. 1.*

Forces acting upon the ball are as follows:

F_t — propulsive force of air jet flowing in:

$$F_t = \xi \times \varrho'' \frac{(u'')^2}{2} \times S_g \tag{2}$$

where ξ is the resistance coefficient and, according to [5], it is:

$$\xi = \frac{24}{Re} + \frac{3.73}{\sqrt{Re}} - \frac{4.83 \times 10^{-3}\sqrt{Re}}{1 + 3 \times 10^{-6}\sqrt{Re^3}} + 0.49 \tag{3}$$

where Re is the REYNOLDS number:

$$Re = \frac{d_1 u'' \times \varrho''}{\eta''} \tag{4}$$

S_g is the cross section area of the ball perpendicular to the direction of action of the air jet

$$S_g = \frac{d_1^2 \times \pi''}{4} \tag{5}$$

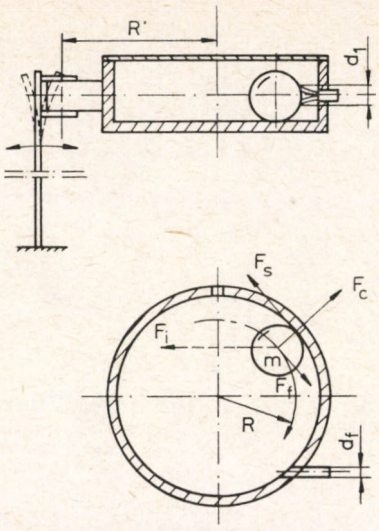

Fig. 1
Schematics of the ball vibrator and its amplification. The hydrodynamic and kinetic conditions of ball rotation

From here on, let $d_1 = d_f$.

F_c is the centrifugal force

$$F_c = m_g R(\bar{\omega})^2 \tag{6}$$

F_s is the friction force

$$F_s = f_g \times F_c \tag{7}$$

f_g is the coefficient of rolling resistance which, according to [6], is:

$$f_g = 0.00065$$

When the ball passes the nozzle, it receives a pulse, which accelerates it from velocity v_2 to v_1.
The momentum of the ball is:

$$m_g(v_1 - v_2) = F_t \times t_1 \tag{8}$$

where t_i is the duration of the pulse:

$$t_1 = \frac{d_f}{\bar{v}_g} \quad \text{and} \tag{9}$$

where $\bar{v}_g$ is the average velocity of the ball:

$$\bar{v}_g = \frac{v_1 + v_2}{2} \tag{10}$$

that is:

$$m_g(v_1 - v_2) = \xi \times \varrho'' \times \frac{(u'')^2}{2} \frac{d_f}{\bar{v}_g} \times S_g \tag{11}$$

The decrease in the kinetic energy of the ball is due to work spent on friction, i.e.:

$$F_c \times f_g 2R\pi = m_g \frac{v_1^2 - v_2^2}{2} \tag{12}$$

$$m_g R \frac{\bar{v}_g^2}{R^2} \times f_g \times 2R\pi = m_g \frac{v_1 + v_2}{2} (v_1 - v_2), \tag{13}$$

from where:

$$\bar{v}_g \times f_g 2\pi = v_1 - v_2 \tag{14}$$

Substitution into Eq. (11) results in:

$$\bar{v}_g^2 = \xi \times \varrho'' \times \frac{(u'')^2}{2} \times \frac{d_t S_g}{m_g \times f_g \times 2\pi}, \tag{15}$$

and

$$\bar{v}_g = \frac{u''}{4} \sqrt{\xi \varrho'' \times \frac{d_t^3}{m_g \times f_g}} \tag{16}$$

The rotation speed of the ball and the frequency of the excitation vibration is:

$$n = \frac{\bar{v}_g}{2R\pi} \tag{17}$$

$$f_{sz} = \frac{u''}{8R\pi} \cdot \sqrt{\xi \varrho'' \frac{d_t^3}{m_g \times f_g}} \tag{18}$$

In Eq. (16) ϱ'' is dependent on the pressure and, assuming an adiabatic change of state, it reads as:

$$\varrho'' = \varrho_n'' \left(\frac{p}{p_n}\right)^{1/\varkappa} \tag{19}$$

where: p_n, ϱ_n'' — the pressure and density of compressed air under normal conditions ($p_n = 10^5$ Pa, $T = 293$ K, $\varrho_n'' = 1.2$ kg/m^3).

Flow rate and pressure of compressed air, while passing the tubing and the nozzle, are related as:

$$p = C_1 \times \varrho'' \times \frac{(u'')^2}{2} \tag{20}$$

where: C_1 — is the coefficient of all resistances combined.
Since:

$$u'' = \frac{V''}{S_t} \tag{21}$$

where: S_t — is the cross section of the nozzle, flow rate and pressure are related as follows:

$$V'' = S_t \times \sqrt{p \left[\frac{p_n}{p_n + p}\right]^{1/\varkappa} \times \frac{2}{\varrho_n'' \times C_1}} \tag{22}$$

3. Theoretical Considerations on the Dynamic Experiments

The previous assumptions are based on the equilibrium of momentum and friction forces at rest on the penumatic ball vibrator. However, under normal conditions the vibrator is not at rest, rather it operates in a vibrating system under dynamic conditions in such a way that the vibrator excites the vibrations on the one hand, and the inertia force borne from the excited vibrations proper effect the rotating ball itself, on the other. That is why equations described in literature [1] do not directly apply. However, the deducing of new relationships is beyond the scope of this paper.

Thus, dynamic studies were conducted as follows:

— verification of Eq. (22) via measurements,
— vibrational study of a ball vibrator, i.e. determination, by measurements, of the amplitude-frequence relationship (amplification function), its comparison with the theoretical amplification function [7],
— comparison of measured data with those calculated by Eq. (18).

4. Experimental System and Measurement Method

For vibration measurement, the rotation speed of the ball in the ball vibrator has to be known. From this, the frequency of vibration can be calculated. This measurement was accomplished directly by a stroboscope of Type ORIS-TROB. Frequency was measured indirectly via a piezoelectric probe attached to the vibrating bridge, and its signal was fed to a measuring bridge, transduced, amplified and displayed both on a scope and a panel instrument. Comparison of the three measurements showed that for all practical purposes it was sufficient to use a panel instrument, because it proved difficult to synchronize the signal on the scope. One has to revert to a stroboscope only when the suspension of the vibrator is of the solid-type and no piezoelectric signal can be transmitted. The frequency values obtained by direct and indirect measurements agreed well, consequently the measurement system was set up as follows. The amplitude of vibrations was measured by a bridge, while the hydrodynamic parameters of the pneumatic vibrator (pressure, air flow rate) were measured by a Bourdon-type manometer and a rotameter (MOM, Hungary and PG, GDR, respectively).

The Measurement System

Dynamic measurements on the ball vibrator were carried out in the experimental set-up shown in *Fig. 2*. The system corresponds to a dampened vibrating system excited by a rotating mass. The experimental system consists of ball vibrator *1*, connected through ball-bearings *2* to bridge *3*, bolted onto leaf-springs *4*. Suspension of the ball vibrator ensures that the excitation force acts only in the direction $x—x$, while in the perpendicular direction, $z—z$, the vibrator rotates freely. Consequently, there is no momentum originating from the side-forces, which act upon the leaf-springs.

Compressed air driving the pneumatic ball vibrator is delivered through a flexible plastic tube connected to a central source. Thus, it contributes only a small excess mass to the vibrating mass. Rotation speed is regulated via ball-valve *5*. The flow rate and pressure of compressed air is measured by rotameter *6* and manometer *7*, respectively.

Pulses, generated by the vibrations are transmitted by piezoelectric transducer *8* to universal vibrometer *9* (Type SM 211), which transforms the values to potentials allowing for the display of path, velocity and acceleration maxima. Appropriate ranges can be selected by push-buttons. Vibration frequency was measured by frequuency meter *10* (Type VEB RFT 4311) connected to the output of vibrometer *9*. The vibrating elements of the measuring system were installed on a welded steel support-frame of high mass, *11*.

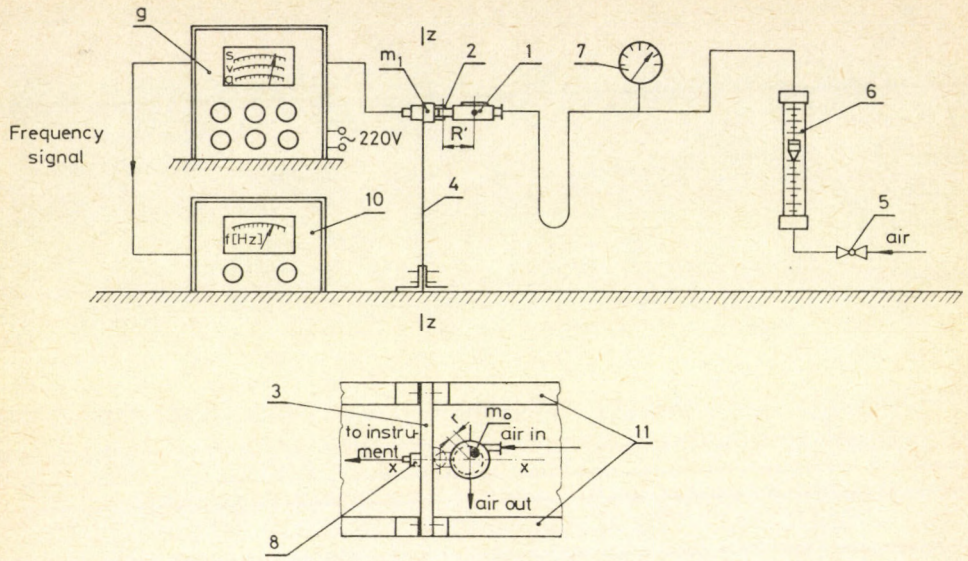

Fig. 2
Schematics of the experimental apparatus and measuring system: *1*-ball vibrator, *2*-bearing, *3*-bridge, *4*-flat springs, *5*-ball valve, *6*-rotameter, *7*-pressure gauge, *8*-piezoelectric transducer, *9*-SM 211 universal frequency meter, *10*-VEB RFT 4311 frequency meter, *11*-steel structure

In order to isolate the effects of vibration, the system was mounted on a rubber mat, with the instruments located on a special stand.

Triplicate measurements were carried out in the x—x direction at every pressure (i.e. ball rotation speed) setting. The mass and spring coefficient of the system were also varied by attaching extra mass to the bridge and replacing the leaf springs, respectively. The spring coefficient and mass of the vibrating system had to be known for the calculation of its dynamic characteristics (eigen-frequency, and static amplitude).

The spring coefficient of the leaf-springs was determined experimentally and verified by calculation. An approximately linear correlation was found between load and bending. Measured and calculated values also agreed well. This means that the method of suspension—which often leads to the correction of the constant in the formula of the spring coefficient—could be considered ideally rigid in this case.

The mass of the vibrating system was determined by direct weighing:

— mass of the vibrating ball, $m_g = 0.067$ kg
— overall mass of the house of the vibrator, bolts and ball, $M = 1.5$ kg
— attached masses were as follows:

$$m_1 = 0.179 \text{ kg}$$
$$m_2 = 0.182 \text{ kg}$$
$$m_3 = 0.177 \text{ kg}$$
$$m_{cs} = 0.065 \text{ kg}.$$

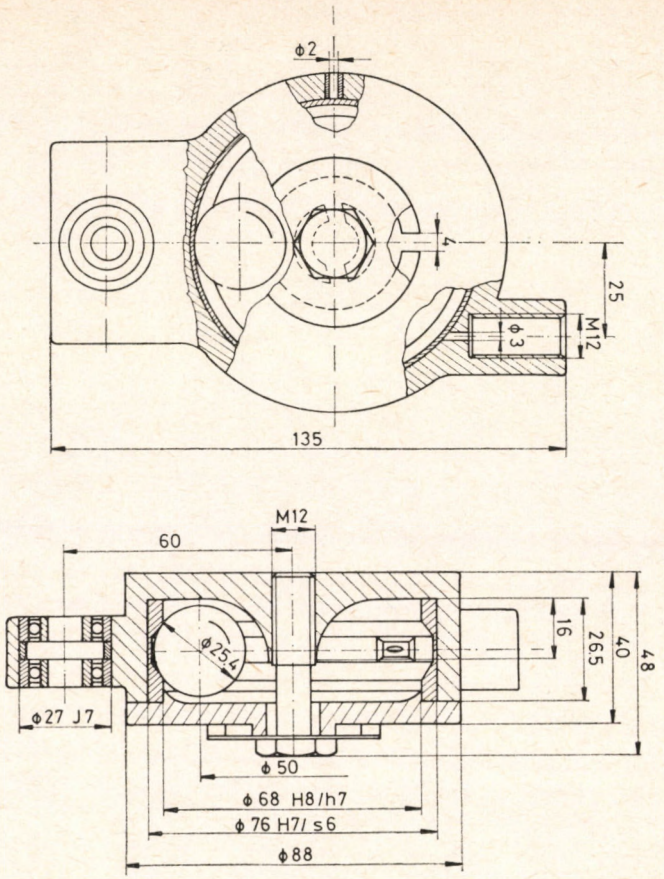

Fig. 3
Schematics of the ball vibrator

Table 1

Setpoints used in the experiments

No.	Spring coefficient	Overall vibrating mass	Eigen frequency	Static amplitude
	c, m/N	M_0, kg	$\omega_0 = \sqrt{\frac{1}{M_0 c}}$, s^{-1}	$A_{st} = \frac{m_g}{M_0} \times R$, m
I 1	2.787×10^{-4}	$M = 1.5$	48.51	1.11×10^{-3}
I 2		$M + m_1 + m_2 = 1.93$	43.17	0.87×10^{-3}
I 3		$M + m_1 + m_{cs} = 2.10$	41.34	0.79×10^{-3}
II 1	4.340×10^{-5}	$M = 1.5$	123.95	1.11×10^{-3}
II 2		$M + m_1 + m_2 = 1.93$	109.40	0.87×10^{-3}

A custom-modified ball vibrator of NETTER, Type K 05 B, shown in *Fig. 3*, was used for the experiments. The values of the major characteristics used for the calculations were as follows:

— rotaion ratdius of the vibrator ball, $R = 2.5 \cdot 10^{-3}$ m
— diameter of the nozzle, $d_f = 3 \cdot 10^{-3}$ m
— expansion section at the entry point of compressed air: $h_b = 6 \cdot .10^{-3}$ m, $l_b = 12 \cdot 10^{-3}$ m, $v_b = 1 \cdot 10^{-3}$ m.

The characteristic values set for the respective experiments are listed in *Table 1.*

5. Results

Measured values are plotted in *Fig. 4–7* as follows:

a) Coefficient C_1 was calculated by Eq. (22) from measured gas flow rates and pressures. The $p - V''$ relationship is shown at the left-hand side of the diagrams. It can be seen that measured and calculated values agree well *(Fig. 4* and *6)*. This means that Eq. (22) applies up to $p = 2 \times 10^5$. Above this limit it becomes, occasionally, linear *(Fig. 6)*.

b) Eq. (18) and the measured $p - V''$ curve were used to calculate the $V'' - f$ curve, shown at the right-hand-side of the diagrams (f_{sz} curve, *Fig. 4* and *6)*.

c) Measured $V'' - f$ data are also shown at the right-hand side of the diagrams *(Fig. 4* and *6*, curve f_m*)* and are compared with data calculated by Eq. (18). It can be seen that in real systems there is a jump in frequency (rotation speed of the ball) once a certain pressure/flow rate is reached *(Fig. 4* and *6)*.

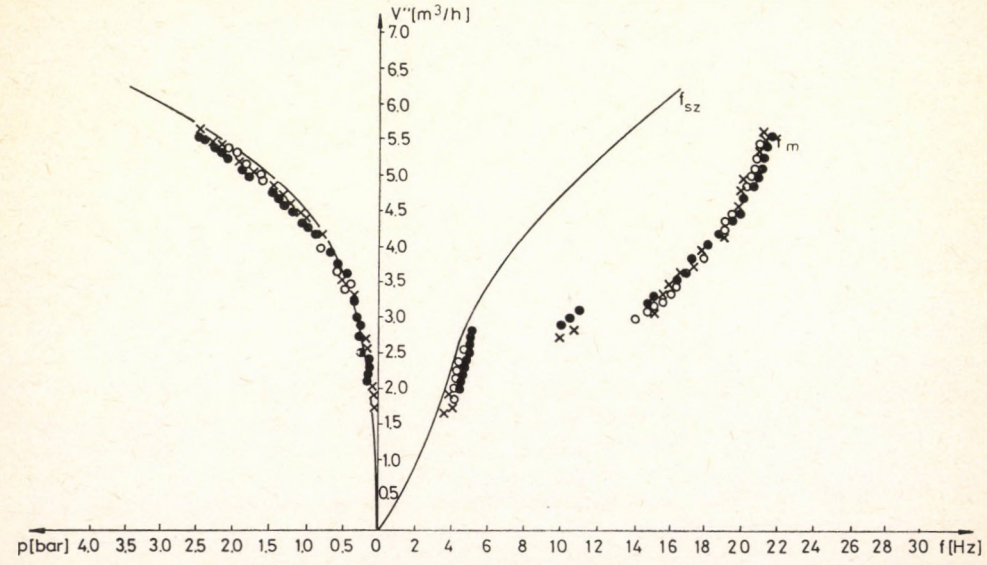

Fig. 4
Relationships between air pressure, flow rate and the frequency of the vibrating system ($c = 2.787 \times 10^{-4}$ m/N)

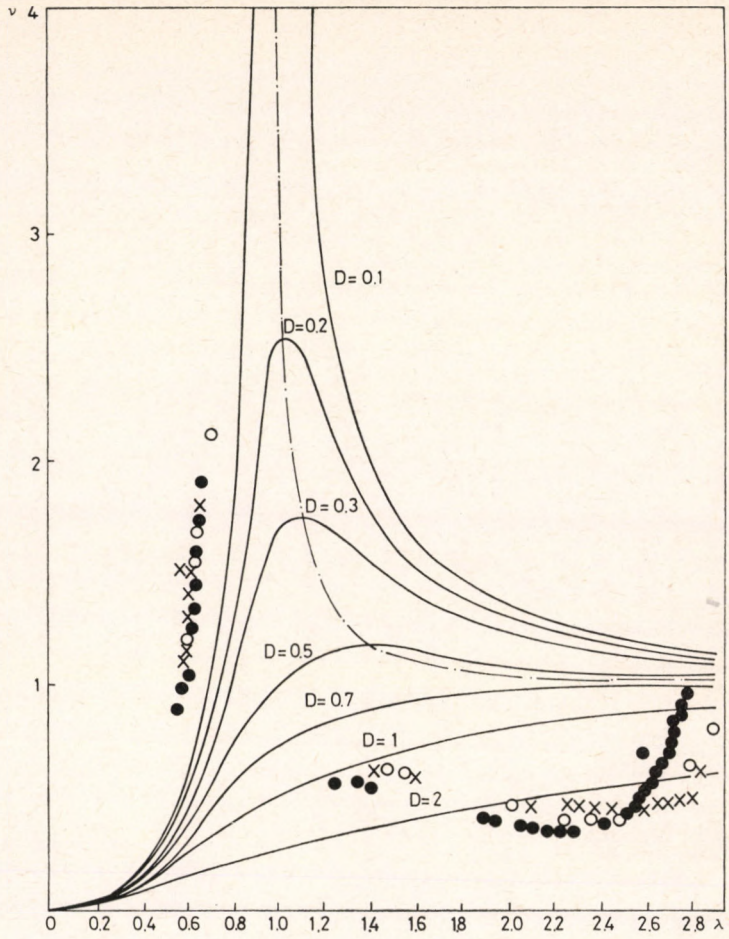

Fig. 5
Comparison of the theoretical and measured resonance curves ($c = 2.787 \times 10^{-4}$ m/N)

d) Theoretical and measured amplification functions are shown in *Fig. 5* and *7*. It can be seen that below the resonance point, actual amplification values shift towards the left, but the shape of the curve is correct. In the vicinity of the resonance point (though slightly below) there is a sudden increase in frequency. Above the resonance point, measured and calculated amplification curves fall to agree. In this range, the amplification of applitude for system B should approach the $\nu = 1$ value from above ($\nu > 1$). Actually, measured data first decrease from a $\nu < 1$ value, then increase comparatively rapidly, though never reach (in the range tested) the theoretical value, $\nu = 1$.

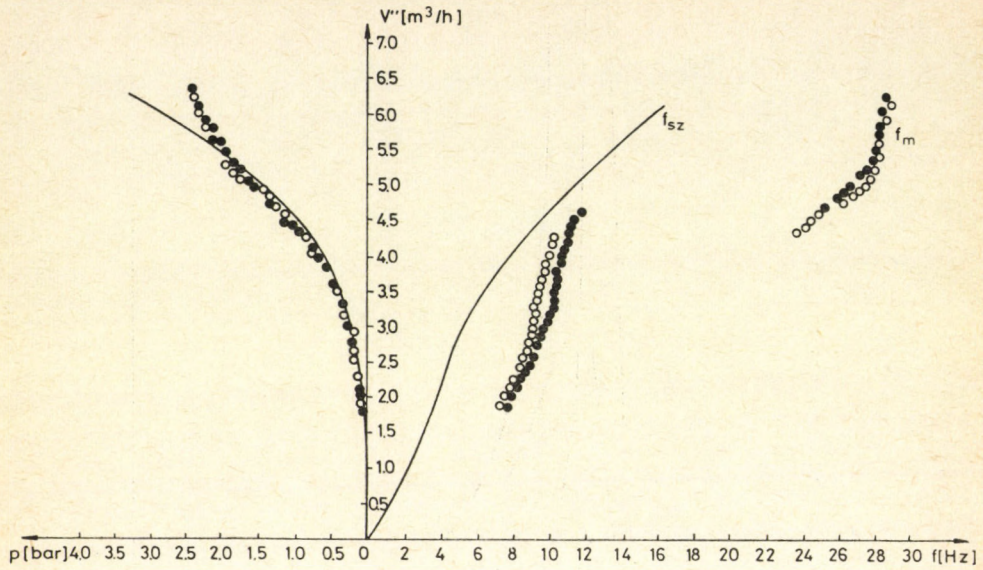

Fig. 6
Relationships between air pressure, air flow rate and the frequency of the vibrating system ($c = 4.34 \times 10^{-5}$ m/N)

6. Summary

The study of the dynamics of a pneumatic ball vibrator led to the following conclusions in respect to the design of the vibrator:

- good agreement between measured $p - V''$ data and those calculated by Eq. (22) indicates that the change of state of gas in the range tested is adiabatic;
- comparison of measured $V'' - f$ data with those calculated by Eq. (18) indicates that Eq. (18) is indeed suitable for the first-approximation-type designing of vibrators;
- detailed explanation of the sudden change in frequency (rotation speed of the ball) requires further theoretical studies;
- analysis of Eq. (18) shows that the frequency range of the vibrator can be increased by increasing the size of the nozzle, d_f and by decreasing the friction coefficient, f_g. It can also be seen that a decrease in the mass of the ball, m_g, or the radius of rotation, R_g, is disadvantageous, because both decrease the excitation force and, what is also important in transportation, the static amplitude, A_{st}.
- analysis of the resonance curves (amplitudes amplification curves) shows that operation below the resonance point is more advantageous for transportation purposes, because in this range the amplification of amplitude increases linearily with the frequency; control is stable, while in the close vicinity of resonance, the operation becomes unstable. Above the resonance point, the amplification of amplitude decreases to such an

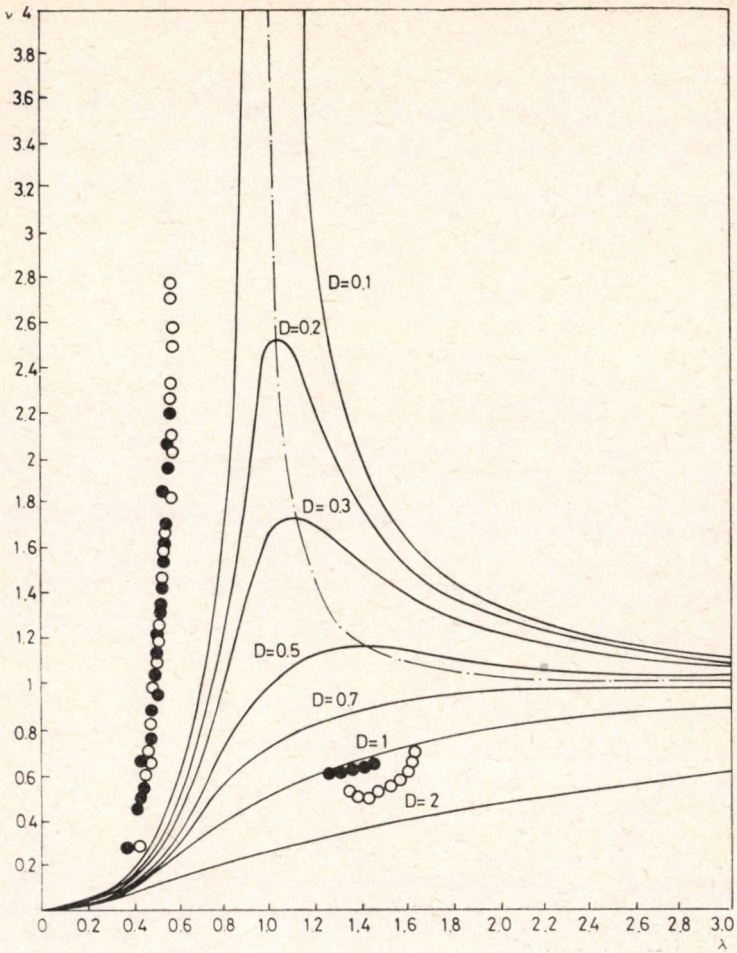

Fig. 7
Comparison of the theoretical and measured resonance curves ($c = 4.34 \times 10^{-5}$ m/N)

extent that it reduces, in fact, to damping and transportation requires excessive energy input;

— since the operation frequency of the ball vibrator is, in general, high, its eigen-frequency, ω_0, should also be high (this ensures that the operation frequency is below the resonance frequency). This can be achieved by decreasing the spring constant (increasing the rigidity of the spring), and the vibrating total mass, M. The latter also leads to increased static amplitude, A_{st}.

Thus, in conclusion, it can be stated that when pneumatic ball vibrators are used in vibrating transporting systems, the transporting elements (through, channel, and tube, etc.) should be rigid and of low mass, so that the operation frequency remains below the resonance frequency.

SYMBOLS

A_{st} — static amplitude, m
C_1 — overall resistance, coefficient, —
c — spring coefficient, m/N
d_f — nozzle diameter, m
d_1 — characteristic diameter of air jet acting upon the ball, m
F_c — centrifugal force, N
F_f — force created by the air jet, N
F_g — excitation force, N
F_i — inertia force, N
F_s — friction force, N
F_t — propulsive force of air jet upon entry, N
f_g — coefficient of rolling friction, —
f_m — measured vibration frequency, Hz
f_{sz} — calculated vibration frequency, Hz
M — constant vibrating mass, kg
M_0 — overall vibrating mass, kg
m_{cs} — mass of bolts, kg
m_g — mass of ball, kg
m_1, m_2, m_3 — additional masses, kg
n — rotation speed of the ball, s^{-1}
p_n — normal pressure, Pa
R — radius of the path of the ball, m
R' — turning radius of the ball vibrator, m
Re — REYNOLDS number, —
S_f — cross section area of nozzle, m^2
S_g — cross section area of ball perpendicular to air jet, m^2
t — time, s
t_1 — pulse time, s
u'' — air velocity in nozzle, m/s
V'' — air flow rate, m^3/h
$\bar{v}_g$ — average circumferential velocity of ball, m/s
η'' — dynamic viscosity of air, Pas
$\varkappa$ — adiabatic exponent, —
λ — frequency ratio, —
ν — coefficient of amplitude amplification, —
ϱ'' — density of air, kg/m^3
ϱ_n'' — normal density of air, kg/m^3
ω — angular velocity, s^{-1}
ω_0 — eigen frequency, s^{-1}

REFERENCES

1. BYKHOVSKI, I. I.: Fundamentals of Vibration Engineering. Mir Publ., Moscow, 1972.
2. Vibracii v tekhnike. Spravochnik No. 4. Edit.: LAVENDEL, E. E., Mashinostroennie, Moscow, 1981.
3. GRUMAG Vibrationstechnik Geräte und Maschinen, Schweiz.
4. NETTER Vibrationstechnik GmBH, FRG.
5. BRAUER, H.: Movement of Single Particles in Various Flow Fields. Advances in Transport Processes. d. by MUJUMDAR, A. S. and MASHELKAR, R. A. Hemisphere Publ. Co. New York, 1981. Vol. II. pp. 353–385.
6. SÁRKÖZI, Z.: Technical Tables and Equations. Műszaki Könyvkiadó, Budapest, 1977. pp. 321–322. (in Hungarian).
7. LUDVIG, GY.: Dynamic of Machines. Műszaki Könyvkiadó, Budapest, 1983. (in Hungarian).

РЕЗЮМЕ

В стати приведены результаты изучения зависимостей между гидродинамическими и кинематическими характеристиками пневматического шарикового вибратора. Проведены измерения для определения динамических характеристик колебательной системы маятниковой подвеской; полученные данные сопоставлены с литературными данными. Авторами установлено, что при использовании пневматического шарикового вибратора у транспортеров маятниковая подвеска является эффективным решением, режим работы которых надо выбрать в дорезонансном интервале параметров, кроме того массу транспортного органа необходимо уменьшать, а жёсткость увеличивать.

HUNGARIAN JOURNAL
OF INDUSTRIAL CHEMISTRY
VESZPRÉM
Vol. 13. pp. 107–119 (1985)

SYNTHESIS OF HEAT EXCHANGER NETWORKS

G. M. Ostrovsky, V. I. Ivakhnenko, S. A. Vinokurov, M. G. Ostrovsky and T. A. Berezhinsky

(L. Ya. Karpov Research Institute, Moscow, USSR)

Received: October 15, 1984

The paper considers a method for the synthesis of a heat exchanger network relying upon the "assignment algorithm" in linear programming and on the decomposition method of optimization. The relationship between the synthesis of a heat exchanger network, and total optimization of the chemical plant into which the network is involved, are also discussed.

SCOPE

Heuristic methods [1, 2], a method based on thermodynamic — combinotarial approach [3, 4], and also purely mathematical methods have been proposed for the synthesis of heat exchanger networks (HEN).

Ref. [5] makes use of both heuristic and mathematical approaches. The advantages and disadvantages of all the approaches are discussed in [6]. Papers of the third group mostly make use of methods built around the "assignment algorithm" in linear programming [7, 8, 9]. Heat load in each heat exchanger is assumed in all of these studies to be equal to some value Q independent of the heat exchanger. Since, generally speaking, heat loads of different heat exchangers are not equal, this assumption is rather restrictive. Moreover, it forbids heat exchange between streams, where it is thermodynamically permissible, but is below Q. Of course, if Q is chosen to be sufficiently small [8], the second disadvantage would not be appreciable, but the number of heat exchangers might grow, thus resulting in greater capital investments.

The majority of studies assume that temperatures of HEN input and output streams are given, and the relationship between the synthesis of HEN and the operation of the chemical plant (CP) to which it belongs is not considered.

The present paper discusses a method enabling the synthesis of the HEN with heat exchangers having different heat loads. It also enables one to regard the problem of synthesizing the HEN as a part of the CP. In its turn,

this would allow one to take into consideration the pressure drops in the HEN, which may sometimes be appreciable [10]. The method is based on a combined application of the "assignment algorithm" and decomposition principle of fixation.

Problem Formulation

Let there be N hot streams $S_h=(S_{h1}, \ldots, S_{hn})$ and M cold ones $S_c=S_{c1}, \ldots, S_{cM})$. The HEN consists of a set of heat exchangers, heaters and coolers. The set of heat exchangers will be referred to as an internal system, and that of the heaters and coolers — an external system [7]. Supply temperatures of hot S_{hi}, $(i=\overline{1, N})$ and cold S_{cj}, $(j=\overline{1, M})$ streams are, respectively:

$$T^0_{ki}, \ (i=\overline{1, N}); \quad T^0_{cj}, \ (j=\overline{1, M}) \tag{1}$$

Target temperatures of hot and cold streams respectively will be:

$$T^t_{hi}, \ (i=\overline{1, N}), \quad T^t_{jc}, \ (j=\overline{1, M}) \tag{2}$$

The HEN often is synthesized so that in each stream there is only one unit of the external system located after all the internal system units. Such a HEN will be called basic if each stream in the internal system may exchange heat only once.

Let us assume that there is only one type of heat exchanger, heater and cooler. No restriction is imposed on the heat exchanger type, but for the sake of convenience it will be assumed below that counter-current heat exchangers are employed whose mathematical models may be found in [12]. Estimate now the number of searched variables: one for heat exchangers (heat transfer area A_{ij}), two for coolers (heat transfer area A_{hi} and water flow rate V_{hi}, where i is the number of the hot stream where the cooler is placed), one for the heater (heat transfer area A_{cj}, where j is the number of the cold stream where the heater is placed). Thus, if there are P heat exchangers in a HEN, the maximal number R of searched variables will be $P+M+2N$.

Denote by M_p the set of p pairs of numbers (p being the number of heat exchangers in a HEN) (i, j) where each pair (q, r) corresponds to the heat exchange between q-th hot and r-th cold streams. Optimization criterion is then as follows:

$$F=\sum_{(i, j)\in M_p} F^{(1)}_{i, j}+\sum_{k=1}^{N} F^{(2)}_k \sum_{l=1}^{M} F^{(3)}_l \tag{3}$$

where $F^{(1)}_{i, j}$, $F^{(2)}_k$, $F^{(3)}_l$ are, respectively, expenditures on the heat exchanger, cooler and heater:

$$F^{(1)}_{i, j}=\delta a A^{b}_{i, j}; \qquad F^{(2)}_k=\delta a A^{b}_{hk}+\alpha_1 V_{hk}$$

$$F^{(3)}_l=\delta a A^{b}_{cl}+\alpha_2 V_{cl} \tag{3a}$$

The problem of the HEN synthesis is posed as follows: it is desired to find a HEN structure and to determine values of the searched variables so as to make the temperatures of hot and cold streams before and after the HEN equal to (1) and (2), and to minimize criterion (3).

Arbitrary HEN constructed for sets of hot, S_h and cold, S_c streams will be denoted below as $(S_h \times S_c)$-HEN. The problem of designing basic $(S_h \times S_c)$-HEN will be referred to as the basic synthesis problem of the $N \times M$ dimensionality.

Basic HEN Optimization

Assume at first that $N = M$ and that the number of heat exchangers $p = N$.

Introduce Boolean variables $x_{i,j}$ as follows:

$$x_{ij} = \begin{cases} 1 \text{ if there is a match of a hot stream } S_{hi} \text{ and cold one } S_{cj}, \\ 0 \text{ otherwise} \end{cases} \tag{4}$$

Matrix $X = \|x_{ij}\|$ is called assignment matrix. By definition, in basic HEN only one heat exchanger may be in each hot or cold stream, hence:

$$\sum_{i=1}^{N} x_{ij} = 1, \quad \sum_{j=1}^{N} x_{ij} = 1 \tag{5}$$

Since coolers/heaters of only one type are used in the HEN, there is no need in enumeration to synthesize an external system and any cooler/heater may be assigned to a given hot/cold stream. Therefore, let us assign to the heat exchanger, where streams S_{hi} and S_{cj} exchange heat, one cooler reducing hot stream S_{hi} temperature to T^t_{hi} and one heater heating cold stream S_{cj} to temperature T^t_{cj}. The set of heat exchanger and related cooler and heater will be referred to as i, j-elementary unit *(Fig. 1)* 13. A basic HEN consists of N such i, j-elementary units. Rewrite, therefore, criterion (3) as:

$$F = \sum_{(i,j) \in M_N} F_{ij}$$

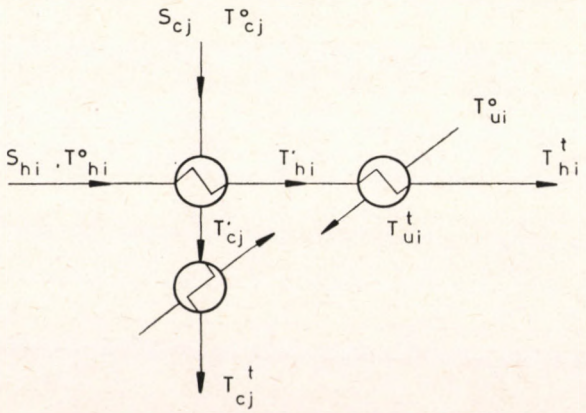

Fig. 1
i,j-elementary unit

where $F_{i,j} = F^{(1)}_{i,j} + F^{(2)}_{i} + F^{(3)}_{j}$ is that part of (3) which refers to the i, j-elementary unit. The problem of i, j-elementary unit optimization with respect to criterion $F_{i,j}$ may be written as follows:

$$\min F_{i,j}$$

$$A_{c,j},\ A_{c,j}; \qquad A_{hi},\ V_{hi} \tag{6}$$

provided that:

$$T'_{cj} = T^{t}_{cj}; \qquad T'_{hi} = T^{t}_{hi} \tag{7}$$

Since in a basic HEN there is only one heat exchanger in each stream, there is no interrelationship between the elementary units, and each unit may be optimized separately resulting in an optimal regime for HEN as a whole.

Denote by f_{ij} the optimal value of criterion $F_{i,j}$ obtained through (6) and (7). The $N \times N$-matrix $\Phi = \|f_{ij}\|$ will be referred to as an estimate matrix. Let us introduce the objective function:

$$F = \sum_{i=1}^{N} \sum_{j=1}^{M} f_{ij} x_{ij} \tag{8}$$

Due to conditions (4) and (5), in any case, F involves only N of f_{ij} values. Now, the problem of synthesis may be formulated as that of assignment:

$$\min \sum_{i} \sum_{j} f_{ij} x_{ij}$$

$$\sum_{i=1}^{N} x_{ij} = 1; \qquad \sum_{j=1}^{N} x_{ij} = 1 \tag{9}$$

Consider now the case where $N > M$ and the number of heat exchangers is M. There evidently will be a heat exchanger in each cold stream. At the same time, M hot streams will have heat exchangers, and the rest of them, $N - M$ will not. Boolean variables x_{ij} satisfy in the case under consideration the following relationships:

$$\sum_{j=1}^{M} x_{ij} \leq 1 (i = \overline{1, N}), \qquad \sum_{i=1}^{N} x_{ij} = 1, \qquad (j = \overline{1, M}). \tag{10}$$

If there is no heat exchanger in p-th hot stream, it will be cooled only by a cooler. Denote by f_i minimal expenditures on a cooler of i-th hot stream, when there is no heat exchange between this stream and cold ones. Introduce variables:

$$\varphi_i = \sum_{j=1}^{M} f_{ij} x_{ij} + \left(1 - \sum_{j=1}^{M} x_{ij}\right) f_i$$

The following relationship holds:

$$\varphi_i = \begin{cases} f_{ij} \text{ if } i\text{-th hot stream is matched with } j\text{-th cold one,} \\ f_i \text{ if } i\text{-th hot stream is not matched with any cold one.} \end{cases}$$

Indeed, if i-th hot stream exchanges heat with j-th cold one, then allowing for (4) and (10), $x_{ij} = 1$, $x_{ip} = 0$ $(p \neq j)$, whence the second term in the expression for φ_i is zero and $\varphi_i = f_{ij}$; if i-th hot stream does not exchange heat with cold streams, $x_{ij} = 0$ $(j = 1, M)$ and the first term in φ_i is zero and the second one is f_i. Thus, φ_i is the cost of cooling i-th hot stream by any cooling techni-

que, and $\varphi_1 + \ldots + \varphi_N$ under constraints (10) would represent the cost of one of the possible HEN's. In this case, the HEN synthesis problem may be written as follows:

$$\min_{x_{ij}} \sum_{i=1}^{N} \sum_{j=1}^{M} \left(f_{ij} x_{ij} + \left(1 - \sum_{j=1}^{M} x_{ij} \right) f_i \right)$$

provided that (10) is met. Having reduced similar terms in the expression for criterion, we obtain the asymmetrical assignment problem.

Synthesis of a HEN when Each Stream May Exchange Heat More than Once

Consider two approaches to this problem. In the first one [13] as well as in [7, 8, 9], each hot S_{hi} (cold S_{cj}) stream is decomposed into n_i (m_j) pseudo-streams *(PS)* as follows:

1. The supply temperature $T^0_{hi,l+1}$ of $(l+1)$-st *PS* is equal to the target temperature $T^t_{hi,l}$ of l-th *PS*.

2. The supply temperature of the first *PS* is equal to the supply temperature of the initial stream, and the output temperature of the last *PS* is equal to that of the target one.

Similar to [7, 8, 9], we assume that each *PS* may exchange heat only once. But in contrast to these studies, we shall not assume that the same amount Q of heat is extracted from each hot *PS* or added to each cold one.

Let us make a new, continuous enumeration to all the hot *PS*'n and regard them as a new set of hot streams $\overline{S}_h$. Similarly, all the cold *PS*'s are regarded as a new set of cold streams $\overline{S}_c$. Numbers $\overline{N}$, $\overline{M}$ of streams in sets $\overline{S}_h$, $\overline{S}_c$ are, respectively: $\overline{N} = n_i + \ldots + n_N$ and $\overline{M} = m_1 + \ldots + m_M$.

Let us employ the decomposition principle of fixation [10] and fix supply and output temperatures of all the *PS*'s. Construct an optimal basic $\overline{S}_h \times \overline{S}_c$-HEN for new sets of hot, $\overline{S}_h$ and cold, $\overline{S}_c$ streams. To this end, one has to solve the basic synthesis problem of dimensionality $\overline{N} \times \overline{M}$. Of course, a solution to this problem would not give an exact solution to the original HEN synthesis problem, because *PS* supply and target temperatures were given arbitrarily. Therefore, the following two-level procedure is proposed. At the first level, the basic HEN synthesis $\overline{N} \times \overline{M}$ problem is solved under given *PS* supply and target temperatures. Next, at the second level the obtained fixed network is optimized, all the technological variables A_{ij}, A_{hi}, A_{cj}, V_{hi} being used as searched variables. Here well developed nonlinear programming methods [14] may be applied. A solution of this problem gives updated values of *PS* supply and target temperatures. And again the basic synthesis $\overline{N} \times \overline{M}$ problem is solved under new values of *PS* supply and target temperatures, etc.

Estimate the number of operations required at each iteration of this method. Let $N = M$ and each initial stream be decomposed into n *PS*'s, i.e. $\overline{N} = nN$.

1. Determination of the matrix Φ at the lower level requires solving $\overline{N}^2 = n^2 N^2$ problems of optimization of i, j-elementary units, and solving the assignment problem withf $nN \times nN$-matrix Φ.

2. At the upper level, it will be necessary to solve the optimization problem of fixed-structure HEN with nN heat exchangers. In doing so, the maximal amount of searched variables will be $4nN$ ($3nN$ are areas of heat exchangers, heaters and coolers, and nN are water flow rates).

Determination of elements f_{ij} of the matrix Φ may be appreciably simplified if areas $A_{i,j}$ in heat eschangers and coolers were chosen so as to make the temperatures maximally close to each other:

$$T^0_{hi} - T'_{cj} = \Delta T_{min} \tag{13}$$

where ΔT_{min} is the given value. This technique is, of course, approximate, because it is not known in advance how to select ΔT_{min}.

Practical application of this approach has revealed that solving the assignment problem at the first level often gives overcomplicated networks, because the HEN may turn out to be cyclic, while the optimal HEN is cyclic. Therefore, it seemed expedient to simplify the HEN determined through solving the assignment problem by means of some heuristic rules.

If there are two interconnected elementary units in the HEN *(see Fig. 2)*, they are substituted by a single one [9]. It is also reasonable to change the position of the heater with nearest heat exchanger as it is done in the ED-method of LINHOFF nad FLOWER [15]. Sometimes we were able to combine heaters located in the same cold stream. Similar operations are also performed with coolers.

Consider now another approach. At first, represent HEN as m-stage *(Fig. 3)* network where each stage is basic $S_h \times S_c$-HEN. Hot and cold streams go through all the stages from the first till m-th. Clearly, the resulting HEN is global, because under sufficiently great m any acyclic HEN (without stream splitting) may be obtained.

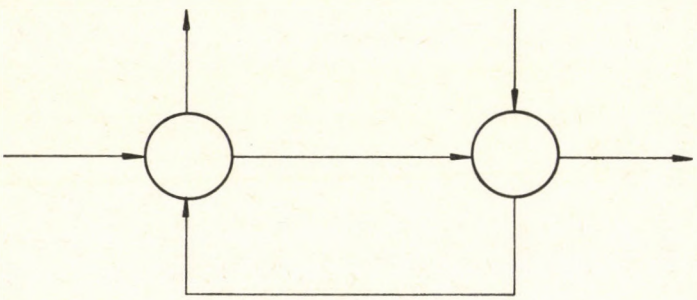

Fig. 2
Example of disposition of elementary units substituted by one unit

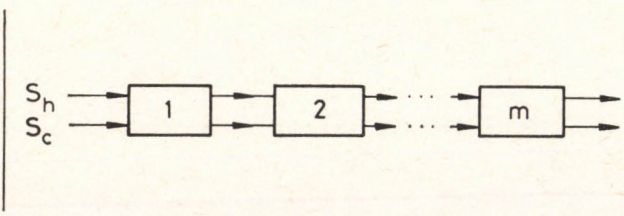

Fig. 3
Representation of HEN as m-stage network

Again make use of the fixation principle, which reduces the HEN synthesis to a two-level optimization procedure. According to this principle, fix temperatures of all the intermediate hot and cold streams. As mutual influence of all the stages is in this case eliminated, one can define optimal HEN structures independently for each stage. Consider the k-th stage. Since each stage is basic $S_h \times S_c$ HEN, the problem of HEN synthesis at each stage is reduced to the basic problem of synthesis of dimensionality $N \times M$. In order to solve it, one has to solve the asymmetrical assignment problem.

Having solved this problem for all the stages of the global system, we will determine some HEN and thus complete the first-level procedure. At the second level, temperatures of all the intermediate streams are set free and the whole of the HEN is optimized, all the design variables being used as searched ones.

Since all the variables are continuous, at this level one of the nonlinear programming methods is used. Optimization determines new temperatures of intermediate streams. Fix them again and proceed to the first-level problem, etc.

Therefore, the procedure of the HEN synthesis is cyclic, with each cycle reduced to the above two-level procedure. Denote the values of criterion (I) obtained as a result of the first and second level procedures by $F^{1,i}$, $F^{2,i}$. Since during optimization at the second level we take the values of design variables obtained at the I-st level as the initial point, then the following inequality is valid:

$$F^{2,i} < F^{1,i} \tag{11}$$

Futhermore, since on the I-st level of the i-th cycle solving the assignment problem at each is performed under fixed values of input and output temperatures, found as a result of the 2nd level procedure of the $i-1$-th cycle, then the following inequality holds:

$$F^{1,i} \leq F^{2,i-1} \tag{12}$$

Iteration terminate if one of the following inequalies is satisfied:

$$\|F^{1,i} - F^{2,i}\| < \varepsilon$$

$$\|F^{2,i-1} - F^{1,i}\| < \varepsilon$$

Inequalies (11), (12) ensure a reduction of the criterion at each iteration.

Let us compare both approaches. Assume that $N = M$ and the number of stages m in the 2nd approach is equal to the number of pseudostreams into which the initial stream is decomposed in the first approach. Each iteration of the Ist approach requires solving m^2N^2 optimization problems (for determination of the estimate matrix Φ) and one optimization problem of the dimensionality $4mN$. Each iteration of the 2nd approach requires solving mN^2 optimization problems of the dimensionality 4 (for determination of m estimate matrices for m stages) and one optimization problem of the dimensionality $4mN$. Thus, with respect to the amount of computations, the 2nd approach is better. Moreover, solving the assignment problem by the 2nd approach gives more simple acyclic networks, which also simplifies the solving procedure. However, a cyclic HEN cannot be obtained through the 2nd approach.

Synthesis of a HEN with Stream Splitting

Both of the above approaches are easily generalized to the case where a HEN with split streams is desired. For the sake of example, consider the first approach. Let *PS*'s be introduced as above called pseudo-streams of the first kind. Consider 1-th *PS* obtained from hot stream S_{hi} (Fig. 4). Decompose by means of stream divider (Fig. 4b) this 1st-kind *PS* into m_{il} 2nd-kind *PS*'s. Denote the resulting set by $\bar{S}^{l}_{hi}$. Each q-th 2nd-kind *PS* will be characterized by flow rate $\alpha^{il}_{q} V_{ki}$ $\left(\text{where } \sum_{q=1}^{mil} \alpha^{il}_{q} = 1\right)$, its supply and target temperatures will coincide with those of the 1st-kind *PS*, i.e. will be $T^{0}_{h,l}$ and $T^{t}_{hi,l}$, respectively.

Perform such an operation over all the 1st-kind *PS*'s. We suggest that hot 2nd-kind *PS* may exchange heat with any 2nd-kind *PS* only once, and vice versa.

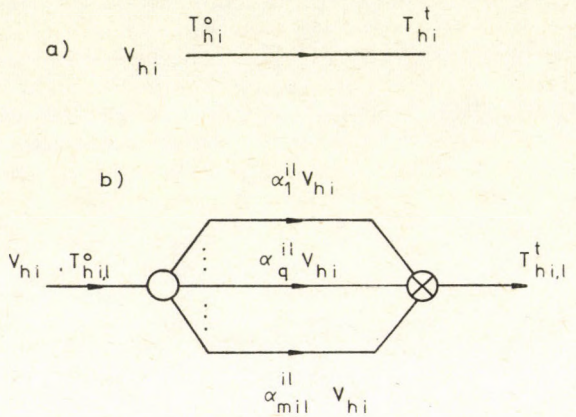

Fig. 4
Splitting of pseudo-stream

After heat exchange, all the 2nd-kind *PS*'s belonging to the same set S^{i}_{hl} (or S^{l}_{cj}) are mixed in the mixer. Unite all the 2nd-kind hot *PS*'s into a new set $\bar{\bar{S}}_{h}$, and cold ones into set $\bar{\bar{S}}_{c}$. Again the two-level procedure of the first approach may be used, the only difference being that along with supply and target *PS* temperatures, structural parameters α^{il}_{q} will also be used as searched variables. Of course, the dimensionality of optimization problems at both levels might grow dramatically.

Synthesis of a HEN as a Part of Chemical Plant

All the HEN synthesis studies assume that stream temperatures (1), (2) at HEN input and output are given. At the same time, an important problem arises of selecting these values from the viewpoint of a *CP* as a whole. Moreover, the majority of studies disregard power consumption for pressure drops

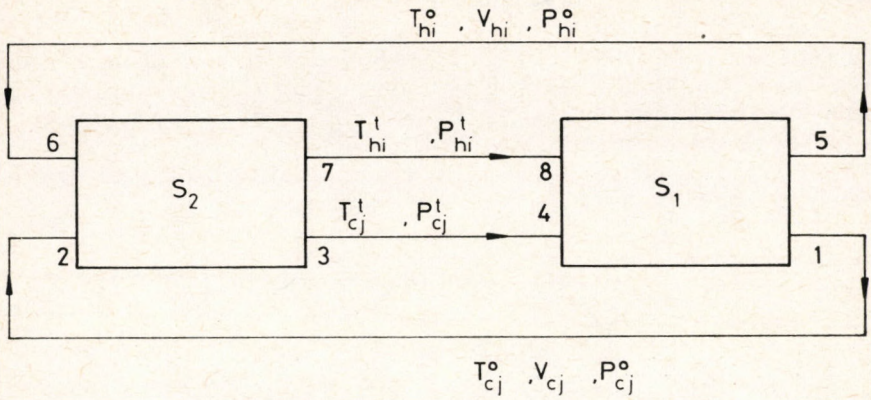

Fig. 5
Chemical plant involving HEN as its part

required for streams transportation. Both of these problems may be solved if a HEN is synthesized as a part of a *CP*. Let a *CP* consist of a general part S_1 (with given structure) and HEN S_2 *(Fig. 5)*. Subsystems S_1 and S_2 are related by cold (1–2), (3–4) and hot (5–6), (7–8) streams. As above, denote by (1), (2) temperatures of hot and cold streams at input and output of HEN S_2, by V_{hi}, V_{cj} flow rates of hot and cold streams, and by ΔP_{hi}, ΔP_{cj} pressure drops in hot and cold streams of the HEN.

Consider the following problem: determine the optimal HEN structure provided that all the network S operates optimally.

Assume for the sake of simplicity that a HEN should be basic.

This problem will again be solved by means of the decomposition principle of fixation.

At first, assume that some structure of S_2 is given. Optimize *CP* S as a whole and determine supply (1) and target (2) temperatures and drops ΔP^{0}_{hi} and ΔP^{0}_{cj} in each HEN stream. Find optimal structure of a basic HEN for given temperatures (1), (2) and fixed pressure drops ΔP^{0}_{hi}, ΔP^{0}_{cj}. Basic HEN synthesis procedure will be as above, the only difference being as follows. Optimization of i, j-elementary unit would require 1). more complicated mathematical models of heat exchanger, heater and cooler, where output temperatures and pressure drops may be represented as functions of pipe diameter, number and length, 2). constraints on pressure drop in addition to those on temperature (7), and 3). use of pipe diameters, number and length as searched variables.

This is again followed by optimization of the whole network S giving new temperatures and pressures at the input and output of HEN S_2. Now synthesis of S_2 may be repeated with new temperatures (1), (2) and pressure drop, etc.

Computer Experiment

Tasks 4SP1 and 6SP1 were executed on a computer. In both of them, estimate matrices were computed under the assumption that the minimal temperature difference reached in each heat exchanger $\Delta T_{min} = 20$ °C. Optimization was done by the method of the augmented Lagrangian [16].

At first, consider the results of 4SP1. Each initial technological stream was decomposed into three pseudo-streams of equal heat content.

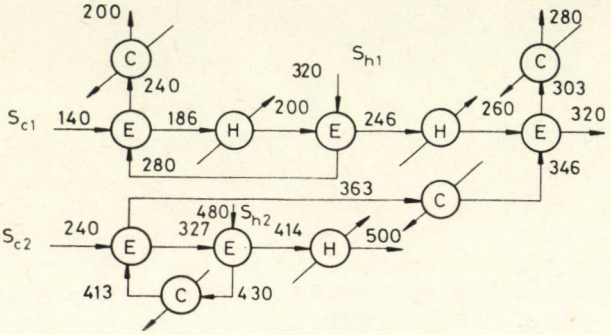

Fig. 6
HEN resulting after the first solution of the "assignment problem" (task 4SP1)

The first solution of the assignment problem resulted in network shown in *Fig. 6*. Optimization criterion was \$ 31,034. Uniting some i, j-elements and shifting some heaters and coolers of the network *(Fig. 6)* resulted in a HEN shown in *Fig. 7* with criterion \$ 30,600. Optimization of this network gave the network of *Fig. 8* criterion \$ 10,627. In [1] a HEN was constructed with criterion 13,590.

Improved criterion was obtained, because in optimization of the network of *Fig. 7* condition $\Delta T_{min} = 20$ °C was disregarded. As a result, one of the heat exchangers had $\Delta T_{min} = 1.3$ °C.

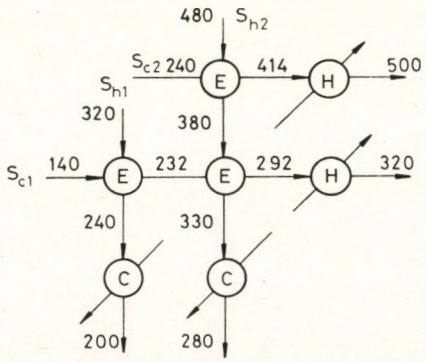

Fig. 7
HEN resulting after matching elementary units and shifting heaters and coolers (task 4SP1)

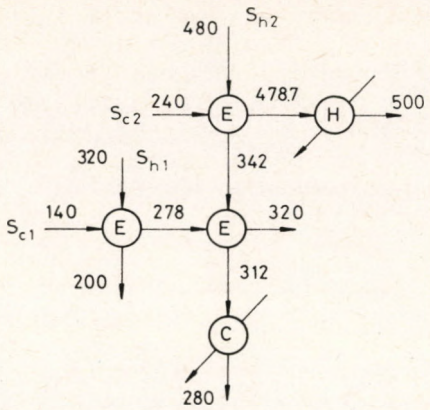

Fig. 8
HEN obtained after optimization of the network of *Fig. 7* (task 4SP1)

Consider now the results of 6SP1. Each initial technological stream was decomposed into two pseudo-streams with equal heat contents.

The first solution of the assignment problem gave a HEN with criterion \$ 44,660. Uniting of some i, j-elements and shifting some heaters and coolers of the HEN, resulted in the HEN with criterion \$ 42,890. Its optimization resulted in the HEN *(Fig. 9)* with criterion \$ 35,017. In [1], a HEN was constructed with criterion 35,010. It is of interest that the HEN obtained through the assignment problem, and its transformation, both contained feedbacks. Therefore, calculation of the final HEN required iteration procedure. The final HEN has no feedback.

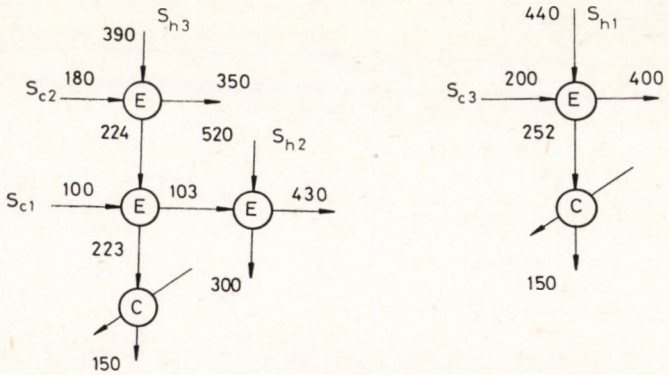

Fig. 9
HEN obtained after solution of the assignment problem and optimization (task 6SP1)

Conclusion

This paper suggests a rather general approach to HEN synthesis. In contrast to heuristic methods, it does not require numerous assumptions, such as use of only countercurrent heat exchangers, equality of the effective heat trans-

fer coefficients in all the heat exchangers, and the absence of phase changes in streams [1]. Moreover, ΔT_{min} should not be given an advance; it results automatically after the second-level optimization and may differ in different heat exchangers. This is especially important with HEN's where the maximal degree of energy recovery is sensitive to ΔT_{min} and the capital investments are not small compared to current expenses (as it is the case in literature).

If it is technologically expedient to meet the following condition in heat exchangers:

$$\Delta T_{min} \geq a$$

where a is some given value, this condition may be allowed for both in the optimization problem and generation of matrix Φ as a constraint of the inequality type imposed on the searched variables.

However, we are not going to oppose our approach to the heuristic ones, because they may be applied jointly. For example, by means of any heuristic approaches one may synthesize a HEN to be used later as the first approximation for the procedure described in this paper. Heuristic techniques may be also used in between the assignment and optimization stages. As distinct from [7, 8, 9] which make use of the "assignment algorithm", heat loads in all the heat exchangers are not assumed to be equal.

The method under consideration enables one to easily take into account the constraints occurring in realistic problems, such as those on the upper value of the heat transfer area.

SYMBOLS

$A_{i,j}$ — heat transfer area in the exchanger for i-th hot and j-th cold streams;
A_{hi} — heat transfer area of the cooler of i-th hot stream;
A_{cj} — heat transfer area of the heater of j-th cold stream;
V_{hi} — water flow rate in cooler;
V_{cj} — steam flow rate in heater;
$F^{(1)}_{i,j}$ — cost of heat exchanger for i-th hot and j-th cold streams;
$F^{(2)}_{k}$ — cost of cooler for k-th hot stream;
$F^{(3)}_{l}$ — cost of heater for l-th cold stream;
δ — pay-back coefficient;
a, b — coefficients ($b=0.6$);
α_1 — cost of cooling water;
α_2 — cost of steam;
$S_h=(S_{h1}, \ldots, S_{hk})$ — set of hot streams;
$S_c=(S_{c1}, \ldots, S_{cM})$ — set of cold streams;
$(S_h \times S_c)$HEN — basic heat exchange network for sets of hot, and cold, S_1 streams;
T'_{hi} — temperature of hot stream S'_{hi} at heat exchanger output;
T'_{cj} — temperature of cold stream S'_{cj} at heat exchanger output.

REFERENCES

1. NISHIDA, N., LIN, Y. A. and LAPIDUS, L.: AIChE Journal; *1977*, 23 (1), 77.
2. PONTON, J. W. and DONALDSEN, R. A. B.: Chem. Eng. Sci., *1974*, 29, 2375.
3. FLOWER, J. R. and LINHOFF, D.: AIChE Journal, *1980*, 26 (1), 1.
4. LINHOFF, B.: Thermodynamic analysis in the design of process networks, Ph. D. Thesis, University of Leeds, England (1979).
5. GROSSMAN, I. E. and SARGENT, R. W. H.: Computers and Chemical Engineering, *1978*, 1.
6. NISHIDA, N., STEPHANOPOULOS, G. and WESTERBERG, A. W.: AIChE Journal, *1982*, 27 (3), 321.

7. Kobayashi, S., Umeda, T. and Ichikawa, A.: Chem. Eng. Sci., *1971*, 26, 1367.
8. Rockstroh, L. and Hartmann, K.: Chem. Techn., *1975*, 27 (8) 439.
9. Cena, V., Mustacchi, C. and Natali, F.: Chem. Eng. Sci., *1977*, 32, 1227.
10. Rathore, R. N. S. and Powers, J.: Ind. and Eng. Chem. Process Des. and Develop., *1975*, 14 (2), 175.
11. Ostrovski, G. M. and Volin, J. M.: Chem. Eng. Sci., *1974*, 29, 2355.
12. Hwa, C. S.: A.I. Ch.E. — I. Chem.E. Symp. Ser. *1965*, 4, 101.
13. Ivakhnenko, V. I. Ostrovsky, G. M. and Berezhinsky, T. A.: Teoreticheskie osnovy khimicheskoi tekhnologii, *1982*, XVI (3), 348 (in Russian).
14. Himmelblau, D. M.: Applied nonlinear programming, McGrow Hill, 1972.
15. Linhoff, B. and Flower, J. R.: AIChE Journal, *1978*, 24 (4), 642.
16. Pierre, D. A. and Lowe, M. J.: Mathematical programming via augmented Lagrangian. Addison-Wesley Publishing Company, London, 1975.

РЕЗЮМЕ

В стати описана методика проектирования сети теплообменников которая основана на алгоритме распределения линейного програмирования и разложения оптимизации. Приведен также анализ зависимости между синтезом сети теплообменников и польной оптимизацией химического завода работающего теплообменниками.

HUNGARIAN JOURNAL
OF INDUSTRIAL CHEMISTRY
VESZPRÉM
Vol. 13. 121–134 (1985)

PINCH ORIENTED SYNTHESIS STRATEGY FOR MULTICOMPONENT SEPARATION SYSTEMS WITH ENERGY INTEGRATION

Z. FONYÓ, I. MÉSZÁROS, E. RÉV, and M. KASZÁS

(Technical University of Budapest, Department of Chemical Engineering, Budapest H 1521, Hungary)

Received: November 27, 1984

A new two-level strategy for synthesizing multicomponent separation systems with energy integration was developed. At the first level, beside the optimized separation sequences, the economical energy matches between the reboiling and condensing streams are designated. At the second level a heat exchanger network synthesis is attached including sensible heat too. The main feature of both levels is the utilization of the pinch principle. With the help of this new synthesis strategy, the computation load could be reduced by 60% compared to former methods.

1. Introduction

Ordinary distillation systems are widely employed in industrial plants for separating various kinds of mixtures into their components. The creation of even a simple separation sequence of multicomponent mixtures involves the generation (or synthesis) of a process flowsheet. The number of alternate, feasible separator sequences increases rapidly as the number of components to be separated increases. In order to reduce the magnitude of the combinatorial problem, several systematic procedures for synthesis of the most economical separation sequences were developed.

The synthesis of distillation systems is also very important from the viewpoint of energy conservation. In the synthesis of an energy integrated distillation system, two key subproblems are: (1) the selection of the operating conditions and sequence of the separation and (2) the determination of a heat exchanger network for energy recovery. Unfortunately, the heat exchanger network cannot be determined until the distillation sequence has been selected, and the optimum design of the separators is greatly influenced by the energy integration. Because of this information feedback between the distillation sequence and heat exchanger network, several combined methods are suggested for synthesizing an optimal (or small number of nearly optimal) multicomponent distillation system(s) with heat integration. A bounding strategy

combined with dynamic programming [10, 11], an enumeration algorithm for screening the feasible subproblems [7], and an extensively state optimized method [8] are some of the examples for determining the optimal sequence and operating conditions of distillation systems with heat integration. None of these algorithmic synthesis techniques involved the new energy targeting techniques and the Pinch Principle, which led in many practical applications to considerable savings over the past five years [4, 5, 12]. Only a thermodynamic approach suggested by NAKA et al. [9] utilizes the recent advances in process integration for systematic multicomponent distillation synthesis, but their method cannot explicitly evaluate the capital cost.

Because neither heuristic nor evolutionary synthesis procedures are guaranteed to create the optimal sequence, this paper proposes a new algorithmic strategy, the pinch oriented synthesis for multicomponent distillation systems with energy integration. By excluding the forbidden energy matches through the pinch temperature, the calculation load may be considerably decreased, moreover optimal heat recovery networks of integrated chemical plants, based on both energy and capital cost, can be constructed.

2. Synthesis Strategy

The general problem to synthesize an optimal separation process with energy integration involves decisions concerning separation methods, type of separators (a single or complex), arrangement and operating conditions of separators, energy matches, and heat recovery network, etc. Its objective function is the total annual cost, which is a combination of capital and operating expenses. To reduce the complexity of the synthesis algorithm and simplify the solution space for the synthesis procedure, in this study the following assumptions are made:

1. Only straight distillation is considered with simple sequence (single feed, two-product columns).
2. Each column operates at high recovery, sloppy splits of key components are not allowed.
3. The cost of changing temperature and pressure of liquid streams between columns is negligible.
4. Saturated liquid feeds and products are present in each distillation column.
5. Energy matches are considered only between the reboiling and condensing streams in the course of the first part of the synthesis procedure. The heat recovery network design for other streams, including sensible heat too, is performed sequentially.
6. No vapour recompression is considered.
7. Mixtures are assumed to be ideal solutions.
8. The volatility order does not change.

The basic strategy was to decompose the original problem into a number of subproblems, each of which involves two distillation columns. For the sake of synthesizing more realistic flowsheets, in this work higher order energy maches are not considered. Although our ultimate aim is to synthesize the process network after an extensively state optimized distillation sequence, for comparison with previous works, in this study only the pressure and the reflux

Table 1.

Design equations and data

1. Minimum theoretical number of stages (FENSKE equation):

$$\frac{d_{LK}}{w_{LK}} = (\alpha_{LK,T}\alpha_{LK,B})^{\frac{1}{2}S_m} \cdot \frac{d_{HK}}{w_{HK}}$$

2. Minimum reflux ratio (UNDERWOOD equation):

$$\sum_{i=1}^{N} \frac{\alpha_i z_i}{\alpha_i - \Theta} = 1 - \varphi$$

$$R_m = \left(\sum_{i=1}^{N} \frac{\alpha_i d_i}{\alpha_i - \Theta} - 1 \right) \Big/ D$$

3. Number of stages (GILLILAND correlation):

for $\frac{R-R_m}{R+1} < 0.05$; $\quad \lg \frac{S-S_m}{S+1} = -0.3397 - 0.0906 \lg \frac{R-R_m}{R+1}$

for $0.05 < \frac{R-R_m}{R+1} < 0.15$; $\quad \frac{S-S_m}{S+1} = 4.166 \left(\frac{R-R_m}{R+1}\right)^2 - 1.75 \left(\frac{R-R_m}{R+1}\right) + 0.673$

for $0.15 < \frac{R-R_m}{R+1}$; $\quad \frac{S-S_m}{S+1} = 0.25 \left(\frac{R-R_m}{R+1}\right)^2 - 0.85 \left(\frac{R-R_m}{R+1}\right) + 0.6$

4. Diameter of the distillation column:

$$L = (2.9 \cdot 10^{-5} V D (R+1) T_T / P)^{1/2}$$

Where: $V = 0.761(1/P)^{1/2}$

5. Height of distillation column:

$$H = 0.61 \frac{S}{\eta} + 4.27$$

6. Latent heat:

$$r = 45T \left(\frac{P}{T}\right)^{-0.119}$$

7. Vapour pressure (ANTOINE equation):

$$\lg P = A - \frac{B}{C+T}$$

8. Assumed values:
overall heat transfer coefficient:

hydrocarbon—water:	2520 kJ/m²h°C
hydrocarbon—ammonia:	2520 kJ/m²h°C
steam—hydrocarbon:	2100 kJ/m²h°C
hydrocarbon—hydrocarbon:	1680 kJ/m²h°C

overall tray efficiency: 0.8
minimum allowable temperature difference: 8.5 °C.

Table 2.

Cost data and equations

1. Total annual cost = annual operating cost + $\frac{\text{total installed equipment cost}}{\text{project life}}$

2. Installed column cost (\$) = $4.34[762(H/12.2)^{0.68}]$
   for $P > 3.4$ bar: $(1 + 0.015(P - 3.4))$ is applied.

3. Installed tray cost (\$): $70 \frac{S}{\eta} \left(\frac{L}{1.22}\right)^{1.9}$

4. Column instrumentation cost (\$): 4000

5. Installed heat exchanger cost (\$):

$$3.39 \left[9000 \left(\frac{F}{92.1}\right)^{0.65}\right]$$

   for $P > 10.2$ bar $(1 + 0.015(P - 10.5))$ is applied.

6. Maintenance cost: 2.0% of installed equipment cost

7. Utility cost (\$/year): $8500\ UQ/10^6$

ammonia for $-50 < t < 32$;	$U = (4.36 - 0.131t)/4.2$
water for $t = 32$;	$U = 0.0477$
steam for $32 < t < 300$;	$U = (-0.12 + 0.01t)/4.2$

8. Assumed values: project life 10 years
   operation hours 8,500 h/yr.

ratio for each distillation column are selected as design variables and the fraction vaporization of the feeds was fixed to zero. This study uses almost the same assumptions and design/cost equations and data as did RATHORE et al. [11]. *Table 1* and *2* summarize the design equations and the cost basis used for the calculation and optimization.

We had to decide between two ways of generating all subproblems. One is to generate directly only feasible subproblems, the other is to generate all subproblems and to screen the feasible ones. In our case, the former was more convenient to select, because it could avoid the troublesome checking of the feasibility, moreover a top down approach, the pinch oriented enumeration algorithm could be used, instead of the dynamic programming. This method is capable of reducing the calculation load considerably and theoretically can be extended for evaluating complex columns and vapour recompression.

The main idea of the pinch oriented enumeration is the utilization of the heat cascade principle. According to this theory, the pinch divides the heat exchange system: the subsystem below the pinch is a heat source, the other subsystem above the pinch is a heat sink. A system of maximum energy recovery (or minimum utility) can be designed if (1) heat is not transfered across the pinch, (2) cold utilities are not used above, and (3) hot utilities are not used below. After generating all feasible subproblems, the candidate energy matches to be evaluated can be considerably reduced by excluding the uneconomical subproblems transfering heat across the pinch. The steps of the pinch oriented synthesis strategy are given in *Fig. 1.*

1. Identify the mixture to be separated and other process streams available for heat integration.
2. Generate the ordered list and all separation tasks using list splitting.
3. Generate all feasible separation sequences.
4. Generate all feasible two-column subproblems using the feasibility matrix of energy matches.
5. Calculate and optimize the separation tasks without energy integration for reflux ratio and pressure.
6. Select a feasible separation sequence determined in step 3.
7. Identify a column as heat source.
8. Calculate the heat recovery pinch temperature and heat cascade of the remaining columns.
9. Identify a subproblem: assign the column selected in step 7 to the nearest heat sink above the pinch temperature in the heat cascade.
10. Repeat steps 7, 8 and 9 for each column in the separation sequence considered.
11. Repeat steps 6, 7, 8, 9 and 10 for each separation sequence generated in step 3.
12. Change pressures and reflux ratios by optimizing each allowable two-column subproblem in step 9 in order to assign economic heat integrations.
13. Select the optimal separation process and synthesize optimal heat exchanger system.

Fig. 1
The synthesis strategy for distillation systems with energy integration

3. Synthesis Procedure

The first step is to identify the mixture to be separated, the available utilities and the other process streams available for energy integration. The second step is to generate the ordered list calculated from relative volatilities. This list is split into sublists representing streams which could be present in the separation process. In our case, high recoveries are assumed so the effect of nonkey-components from the incomplete separation can be neglected. The list splitting procedure was adapted from HENDRY and HUGHES [2].

Step 3 and 4 are the generation of all feasible separation sequences and all feasible two-column subproblems following the same rules and procedures as used by RATHORE et al. [11], MURAKI and HAYAKAWA [7], and will not be detailed here. *Table 3* and *4* show the separation tasks and the separation sequences for 5-component mixtures. *Fig. 2* summarizes the $2 * 63$ feasible energy integrated subproblems (pair of energy integrated columns) for the same example.

Step 5 is to calculate and optimize the separation tasks for reflux ratio and pressure without integration. The objective function of the tasks is the annual cost, based on both operating and capital expenses. The design and cost equations are given in *Tables 1* and *2*. After calculating temperatures and heat

Table 3.

Separation tasks for 5-component mixtures

Separation task number	Separation task	Separation task number	Separation task
1	A/B	11	A/BCD
2	B/C	12	AB/CD
3	C/D	13	ABC/D
4	D/E	14	B/CDE
5	A/BC	15	BC/DE
6	AB/C	16	BCD/E
7	B/CD	17	A/BCDE
8	BC/D	18	AB/CDE
9	C/DE	19	ABC/DE
10	CD/E	20	ABCD/E

Table 4.

Separation sequences for 5-component mixtures

Sequence number	Separation sequence	Sequence number	Separation sequence
1	17-14-9-4	8	19-5-4-2
2	17-14-10-3	9	19-6-4-1
3	17-15-4-2	10	20-11-7-3
4	17-16-7-3	11	20-11-8-2
5	17-16-8-2	12	20-12-3-1
6	18-9-4-1	13	20-13-5-2
7	18-10-3-1	14	20-13-6-1

SEPARATION TASK (SOURCE)	SEPARATION TASK (SINK)																			
	1	2	3	4	5	6	7	8	9	10	11	12	13	14	15	16	17	18	19	20
1			F	F		F			F	F		F	F					F	F	F
2				F	F			F			F		F		F	F	F		F	F
3	F						F			F	F	F		F		F	F	F		F
4	F	F			F	F			F					F	F		F	F	F	
5		F		F									F						F	F
6	F			F									F						F	F
7			F								F					F	F			F
8		F									F					F	F			F
9	F			F										F			F	F		
10	F		F											F			F	F		
11		F	F				F	F												F
12	F		F																	F
13	F	F			F	F														F
14			F	F					F	F							F			
15		F		F													F			
16		F	F				F	F									F			
17		F	F	F			F	F	F	F				F	F	F				
18	F		F	F					F	F										
19	F	F		F	F	F														
20	F	F	F		F	F	F	F			F	F	F							

Fig. 2

loads in reboiler and condensers for all separation tasks, in Step 6, a feasible separation sequence is selected. Step 7 is to identify a column as the heat source and thereafter, in step 8, the calculation of the heat recovery pinch temperature and the heat cascade of the remaining subsystems is performed.

Step 9 is to identify the subproblems appropriate to the Pinch Principle, i.e. in this sequence the selected column is paired with the nearest heat sink above the pinch temperature determined previously. In this study, we assumed that once the column has been integrated into the cascade, the position of the pinch will not change. After all columns are selected and paired (Step 10), furthermore all separation sequences are surveyed (Step 11), the allowable energy integrated subproblems (pairs of columns) can be optimized (Step 12). With the nomination of the allowable matches, based on the Pinch Principle, the energetically irrational (uneconomical) subproblems can be excluded in order to reduce the calculation load.

For optimization, the multivariable simultaneous logical search plan of HOOKE and JEEVES [3] was adapted.

After obtaining the optimal solution for each subproblem in the optimization phase, it is easy to directly enumerate the feasible and economical combinations for each separation sequence from the list of distillation sequences (step 13). At the end of the synthesis, the optimal separation process is selected, and the optimal heat exchanger network is synthesized according to the guide on process integration by LINNHOFF et al. [5].

This method was programmed for a PDP—10 (TPA—1140) computer at the Computer Center of our Department and several test problems were successfully solved.

4. Separation of light paraffins- an example

In order to illustrate the procedure outlined above, the example of HEAVEN [1] was selected. The feed stream contains five light ideal hydrocarbons at the following composition:

Component	Mole Fraction
Propane (A)	0.05
i-Butane (B)	0.15
n-Butane (C)	0.25
i-Pentane (D)	0.20
n-Pentane (E)	0.35

The feed rate is 907 Kmol/h and a purity specification of 1% is assumed for the adjacent non-key components. To evaluate the effect of energy integration, first the distillation system without energy integration is solved. The two best separation sequences are shown in *Fig. 3*. The sequences correspond to flowsheets developed from heuristic rules. The total annual cost of the optimal sequence is 3.37×10^5 \$/yr; which is about 5.3% smaller than RATHORE's solution. The source of the difference is that the models of physical properties. such as heat transfer coefficients, latent heats, and ANTOINE coefficients were different, i.e. these data were not mentioned in their paper.

Thereafter the synthesis problem with energy integration is solved according to the strategy given in *Fig. 1*. The five best separation sequences with energy

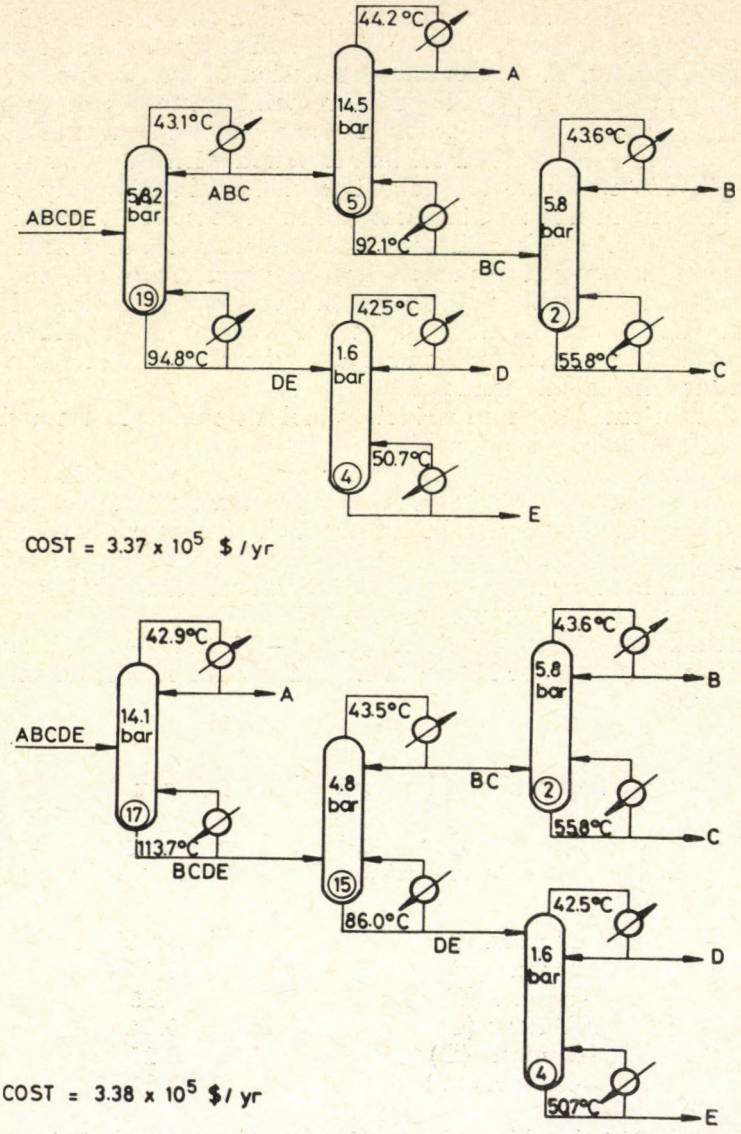

Fig. 3

integration ignoring sensible heat are shown in *Fig. 4*. For comparison, the three best sequences synthesized by RATHORE et al. [11] are shown in *Fig. 5*. The total annual cost of our optimal sequence is 3.09×10^5 \$/yr; it is about 12.9% smaller than that of the optimal process without energy integration. *Fig. 6* shows the optimal flowsheet with energy integration after the sequential synthesis of heat exchanger network.

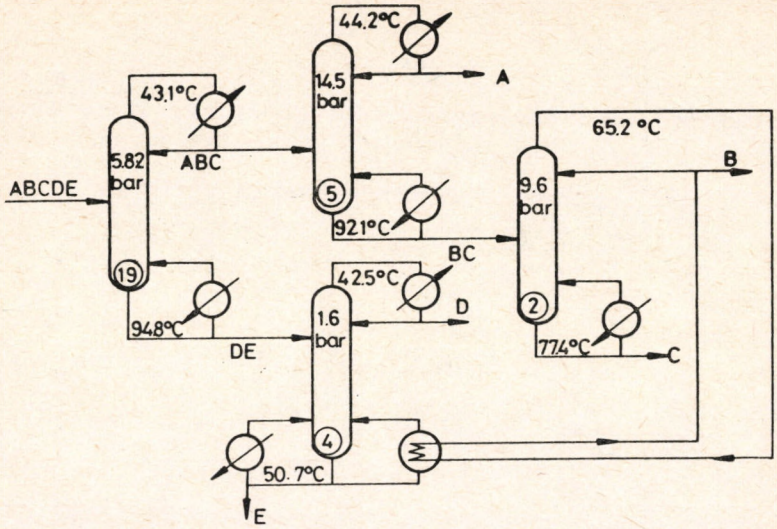

COST = 3.090×10^5 $/yr

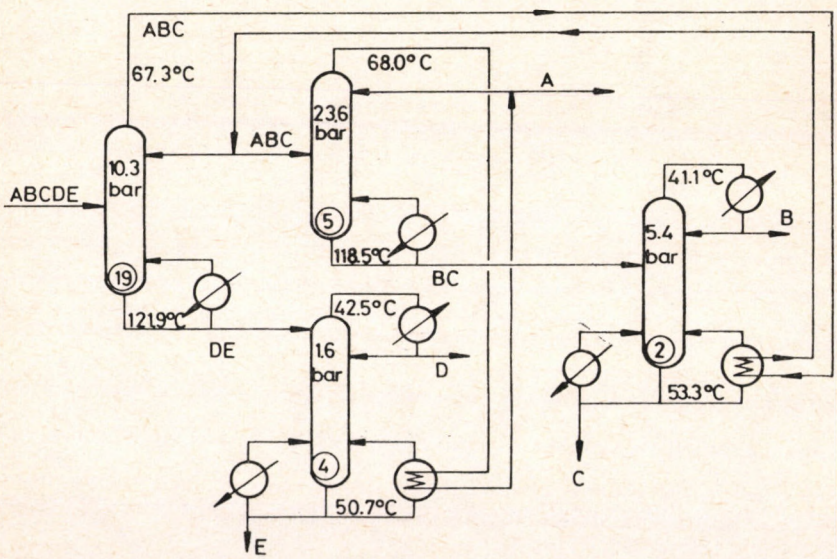

COST = 3.098×10^5 $/yr

Fig. 4/a

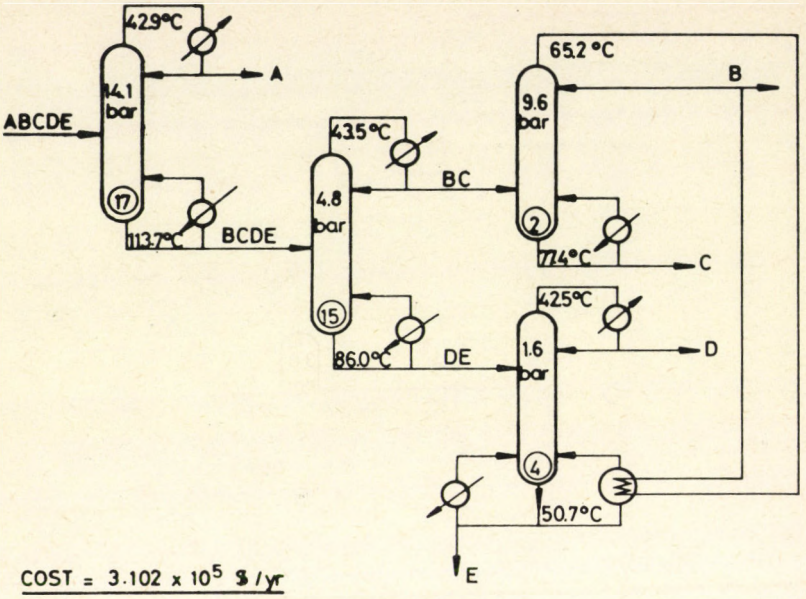

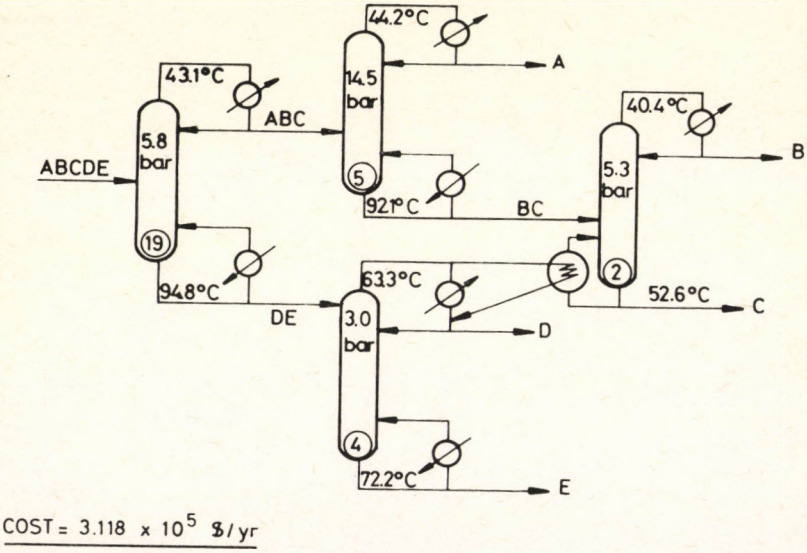

Fig. 4/a—b

5. Discussion and conclusions

An efficient, useful method is developed for synthesizing a small number of nearly optimal distillation separation flowsheets with an energy integration and heat exchanger network. By utilizing the Pinch Principle, the main cal-

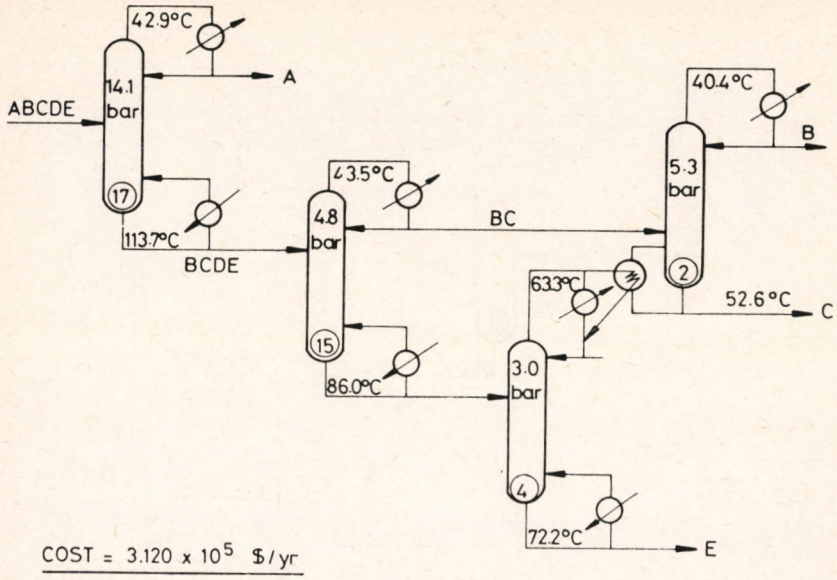

Fig. 4/c

Table 5.

The most economical energy matches

Energy match		Cost without match (bar) ($/yr)	Pressure without match (bar)		Cost with match ($/yr)	Pressure with match (bar)		Match profit ($/yr)
sink column	source column		1.	2.		1.	2.	
4	2	216,296	1.63	5.77	188,613	1.63	9.63	27,682
4	18	259,743	1.63	7.56	233,389	1.52	11.60	26,353
4	14	240,909	1.63	5.52	215,006	1.60	9.2	25,902
2	4	216,296	5.77	1.63	190,439	5.32	3.02	25,857
4	6	230,764	1.63	7.75	205,023	1.61	12.8	25,741
2	19	287,633	5.77	5.82	274,408	5.41	10.3	24,174
2	15	160,868	5.77	4.75	137,457	5.50	8.9	23,411
2	13	156,291	5.77	5.94	135,047	5.48	10.5	21,243
2	8	147,813	5.77	4.91	127,353	5.54	9.05	20,459
4	19	227,827	1.63	5.82	207,871	1.63	9.75	19,955
4	6	230,764	1.63	7.75	210,860	1.61	12.8	19,904
4	15	218,466	1.63	4.75	198,840	1.63	8.2	19,625

culation load, and the optimization of the two-column subproblems, could be considerably reduced, moreover optimal heat recovery networks of integrated chemical plants could be constructed.

For the 5-component example outlined above, the calculated subproblems were 43, instead of the complete enumeration survening 126 matches, therefore the CPU-time could be reduced approximately by 60%.

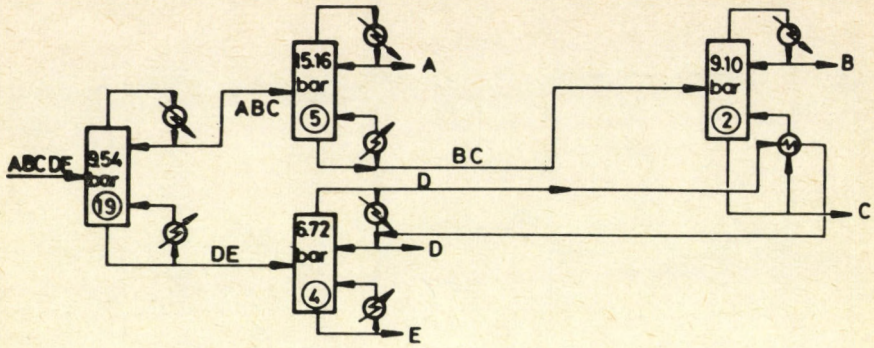

COST = 3.4906×10^5 $/yr

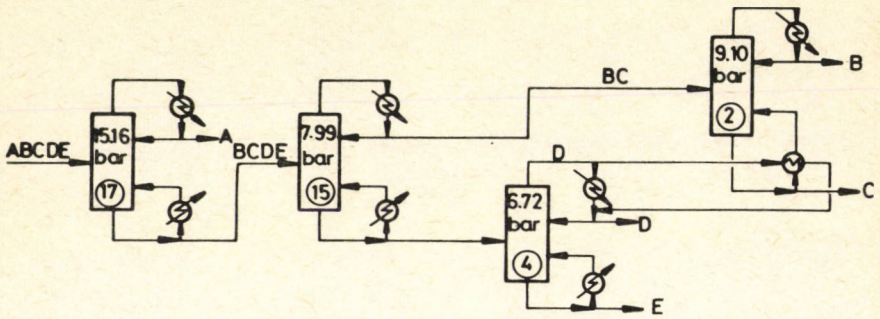

COST = 3.5317×10^5 $/yr

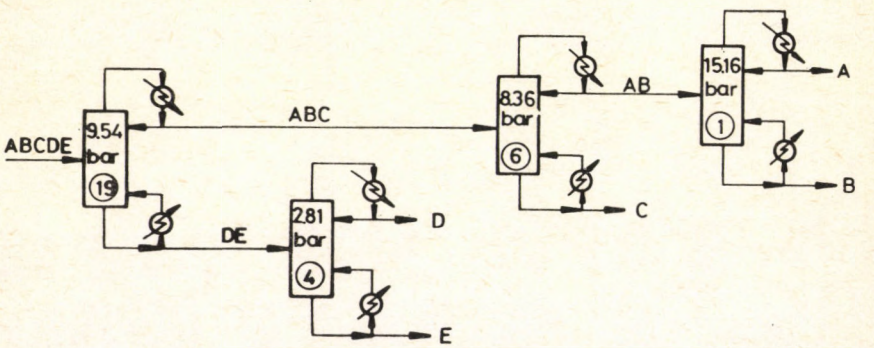

COST = 3.5577×10^5 $/yr

Fig. 5

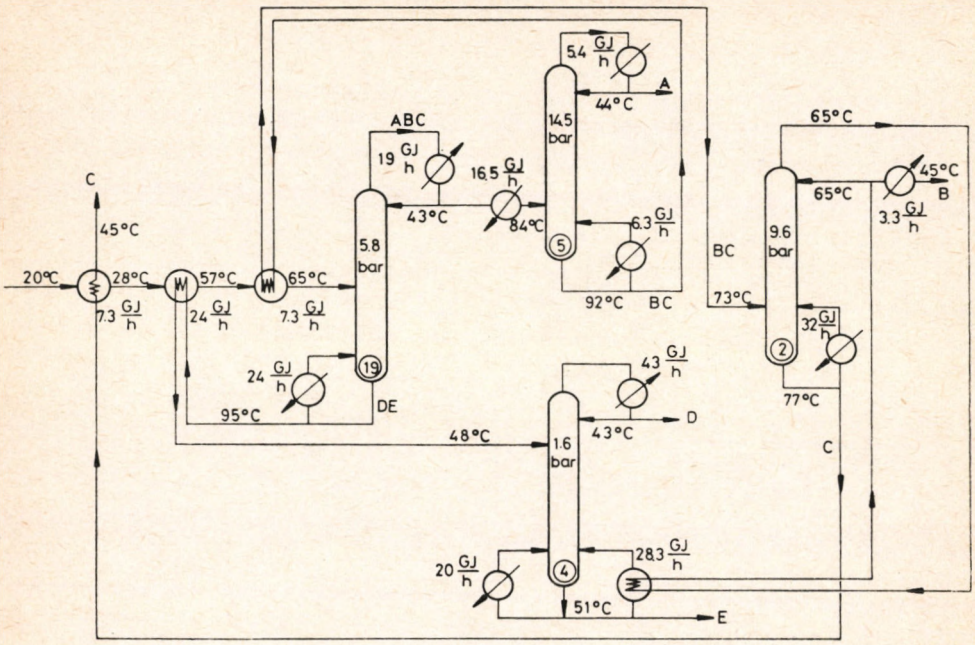

Fig. 6

In this study, 33 subproblems (matches) proved to be economical, i.e. the separation cost decreased, instead of 5 subproblems reported by RATHORE [11]. The twelve best economic matches and costs of the participating separation tasks with and without integration and the pressures and match profits are listed in Table 5.

The best match profit in our study is 2.77×10^4 \$/yr and this is about 55% larger than that of RATHORE's solution. The resulting profit gain is a consequence of our more extensive, simultaneous optimization strategy.

A few observations about our solutions are in order. The condenser temperature of the columns at the optimal solutions proved to be condensable by cooling water, unless the column is selected for heat integration as a heat source. This result confirms the reality of the objective function used. It was also found for the examples that the optimum reflux ratio for a separation task increases, by about 10%, when the energy match is available to drive that separation.

Since some of the assumptions of this study reduce the applicability of the method, additional efforts are needed to consider the fraction vaporization of the feed as design variables, to include vapour recompression and bottom flash distillation and higher order energy matches. Further investigations are necessary to study the sensitivity of the synthesis method to the objective function, the optimization technique, physical properties, and the feed disturbances.

SYMBOLS

A, B, C	ANTOINE constants
d	component mole rate in distillate, kmol/h
D	flow rate of distillate, kmol/h
F	area of heat exchanger, m^2
H	height of distillation column, m
L	diameter of distillation column, m
N	number of components in the feed mixture
P	pressure, bar
Q	heat duty, kJ/h
r	latent heat, kJ/kmol
R	reflux ratio
S	number of stages
t	utility temperature, °C
T	temperature, K
U	cost of utilities, $/GJ
V	average vapour velocity, m/s
w	component mole rate in bottom product, kmol/h
z	component mole rate in feed, kmol/h
α	relative volatility
φ	fraction of liquid in column feed
η	column efficiency
Θ	variable in UNDERWOOD equation to be calculated by trial and error

Subscripts

LK	light key component
HK	heavy key component
m	minimum
i	component
T	column top
B	column bottom

REFERENCES

1. HEAVEN, D. L.: "Optimum Sequencing of Distillation Columns in Multicomponent Fractionation", MS Thesis, University of California, Berkeley, 1969.
2. HENDRY, J. E. and HUGHES, R. R.: Chem. Engng. Progr., *1972*, 68 (6), 71.
3. HOOKE, R. and JEEVES, T. A.: J. Assoc. Comp. Mach., *1961*, 8 (2).
4. LINNHOFF, B. and TURNER, J. A.: Chem. Engng., *1981*, 88 (Nov. 2), 56.
5. LINNHOFF, B. et al.: "User Guide and Process Integration for Efficient Use of Energy", Pergamon Press, Oxford, *1982*.
6. LINNHOFF, B., DUNFORD, H. and SMITH, R.: Chem. Engng. Sci., *1983*, 38 (8), 1175.
7. MURAKI, M. and HAYAKAWA, T.: J. Chem. Engng. Japan, *1981*, 14 (3), 233.
8. MINDERMAN, P. A. and TEDDER, D. W.: AIChE Symp. Ser., *1982*, 78 (214), 69.
9. NAKA, Y., TERASHITA, M. and TAKAMATSU, T.: AIChE J., *1982*, 28 (5), 812.
10. RATHORE, R. N. S., VAN WORMER, K. A. and POWERS, G. J.: AIChE J., *1974*, 20 (3), 491.
11. RATHORE, R. N. S., VAN WORMER, K. A. and POWERS, G. J.: AIChE J., *1974*, 20 (5), 940.
12. UMEDA, T., NIIDA, K. and SHIROKO, K.: AIChE J., *1979*, 25 (3), 423.

РЕЗЮМЕ

Авторы занимались разработкой двухэтапной стратегии многокомпонентной системы сепарации имеющей интеграцию энергии. На первом этапе кроме оптимализации процессов сепарации учитывали вопросы экономичности. Синтез сети теплообменников осуществляется на втором этапе. С помощью описанной в стати новой стратегии синтеза время расчёта снижается на 60%.

Guide for authors

The "Hungarian Journal of Industrial Chemistry" is a joint publication of the Veszprém scientific institutions of the chemical industry that deals with the results of applied and fundamental research in the field of chemical processes, unit operations and chemical engineering in the form of original articles written in the English, Russian, German and French languages.

In addition to the scientific workers of the institutions at Veszprém, the Editorial Board of this publication also welcomes articles for inclusion in this periodical, which are written by authors who are engaged in the above mentioned fields.

1. Manuscripts should be sent—in duplicate—to the Editor-in-Chief:

Dr. Endre Bodor
Veszprém University of Chemical Engineering (VVE), P.O.B. 158
H—8201 Veszprém, Hungary

2. In a brief letter attached to the manuscripts, authors should declare that:
   a) their works is original and has not previously been published elsewhere in its present format, and
   b) for the purposes of correspondence, they can be contacted at the address and telephone number which they give.
3. Manuscripts should be typed on paper of A/4 size.

The first page should give the title, the author's name, place of work and a brief summary of the article (maximum of 15 lines).

If possible the article should be presented with an introduction, experiments carried out, conclusions and discussion. Tables and Figures must be presented on separate sheets and their position in the text should be noted on the margin. A summary of the symbols used, and captions of the Figures should be attached separately to the manuscripts.

It is regretted that photographs cannot be included in the periodical.

The Tables and Figures should not exceed an A/4 size. If diagrams are presented, only the explanation and dimensions of the ordinate and abscissa, and marking numbers are required, while further explanatory texts can be given in the captions of the Figures. The equations used should be numbered, and Tables and Figures should be numbered and noted on the margin.

With regard to units, it is essential that an SI (Système International d'Unités) should be used.

4. References should be prepared in the following manner:
   a) Publications which have appeared in periodicals; e. g.

WAKAO, N. and SCHWARTZ, J. M. Chem.: .Eng. Sci. *1962*, 17 (3), 825—827.

   b) Books; e. g.

SATTERFIELD, C. N.: Mass Transfer in Heterogeneous Catalysis. MTI Press, Cambridge, Mass., 1951, pp. 26—32.

   c) Patents; e. g.

U.S. Pat. 3,425,442 Brit. Pat. 997,665 Hung. Pat. 553,243

   d) Published lectures; e. g.

HIH, S., HHU, C. and LEECH, W. J.: A Discrete Method to Heat Conduction Problems. 5th International. Heat Transfer Conference, Tokyo, 1975. Co. 2.4.

5. Authors receive 50 complimentary copies of the edition in which their article appears.

Editorial Board
Hungarian Journal of Industrial Chemistry

Ára: 300 Ft

CONTENTS

VASSÁNYI, I., SZABÓ, S., MRS. CSIKÓS, ZS. and JELINKÓ, R.: Examination of Changes in Phase and Chemical Composition of Pyrophyllite-lTc on Chlorination 1

KOVÁCS, B., MÉSZÁROS, P. and ORSZÁG, I.: Electrochemical Treatment of Sulphur Compounds and Organics Containing Waste Waters 11

TIMÁR, L. and SIKLÓS, J.: An Effective Flash Algorithm for Process Simulators Using Cubic Equations of State 19

ARANYI, A., BAKOS, M., KREIDL, J. and STEFKO, B.: Residence Time Distribution in a Baffle Plate Type Tubular Liquid-Liquid Two-Phase Reactor 39

FÁY, GY. and TŐRÖS, R.: On the Determination of Thermostatic Equations of State. II. 47

LAZAROV, J.: Heuristic Procedures for Structural Analysis of Chemical Industrial Systems. I. Heuristic Approach for Analysis of Topologic Models 69

LAZAROV, J.: Heuristic Procedures for Structural Analysis of Chemical Industrial Systems. II. A New Approach for Partitioning of Flowsheets 81

SZALAY, A. and ERDÉSZ, K.: Studies on Vibrational Transport. I. Dynamic Studies on a Pneumatic Ball Vibrator 93

OSTROVSKY, G. M., IVAKHNENKO, V. I., VINOKUROV, S. A., OSTROVSKY, M. G. and BEREZHINSKY, T. A.: Synthesis of Heat Exchanger Networks 107

FONYÓ, Z., MÉSZÁROS, I., RÉV, E. and KASZÁS, M.: Pinch Oriented Synthesis Strategy for Multicomponent Separation Systems with Energy Integration 121

Egyetemi Nyomda — 85.3149 Budapest, 1985. Felelős vezető: Sümeghi Zoltán igazgató